INVESTIGATING THE ROLE OF ER STRESS SENSOR IRE1α IN POSTNATAL TOOTH DEVELOPMENT

by

Yuqiao Zhou

Bachelor of Dental Surgery, Sichuan University, 2013

Master of Science, University of Pittsburgh, 2016

Submitted to the Graduate Faculty of

THE SCHOOL OF DENTAL MEDICINE in partial fulfillment

of the requirements for the degree of

Doctor of Philosophy

University of Pittsburgh

2018

UNIVERSITY OF PITTSBURGH

SCHOOL OF DENTAL MEDICINE

This dissertation was presented

by

Yuqiao Zhou

It was defended on

November 13, 2018

and approved by

Hongjiao Ouyang, DMD, PhD, Associate Professor,
Departments of Endodontics, College of Dentistry, Texas A&M University,
Department of Internal Medicine, The Charles and Jane Pak Center of Mineral Metabolism
and Clinical Research, University of Texas Southwestern Medical Center

Mary L. Marazita, Ph.D., Director, Center for Craniofacial and Dental Genetics
Professor, Dept. of Oral Biology, School of Dental Medicine
Professor, Dept. of Human Genetics, Graduate School of Public Health
Professor, Dept. of Psychiatry and Dept. of Clinical and Translational Science,
School of Medicine

Mark P. Mooney, Ph.D., Professor, Department of Oral Biology,
School of Dental Medicine

Elia Beniash, Ph.D., Professor, Department of Oral Biology,
School of Dental Medicine

Dissertation Director: John R. Shaffer, Ph.D., Assistant Professor,
Department of Human Genetics, Graduate School of Public Health
Department of Oral Biology, School of Dental Medicine

University of Pittsburgh

Copyright © by Yuqiao Zhou

2018

INVESTIGATING THE ROLE OF ER STRESS SENSOR IRE1α IN POSTNATAL TOOTH DEVELOPMENT

Yuqiao Zhou, B.D.S, M.S, PhD

University of Pittsburgh, 2018

The IRE1α/XBP1 pathway is an endoplasmic reticulum (ER) stress branch required for the development of multiple secretory cells. Whether IRE1α/XBP1 pathway regulates postnatal tooth development is unknown. Thus, my central hypothesis is that the IRE1α/XBP1 signaling pathway is an essential physiological regulator for postnatal tooth development. I used two approaches to investigate this hypothesis: (1) characterization of a mouse model and *in vitro* experimental follow-up, and (2) observational genetics studies in human. Firstly, I participated in generating and charactering a novel genetic mouse model carrying an *Ern1* (encoding Ire1α) deletion in the odontoblastic and osteoblastic lineage cells. It was observed that the deletion of IRE1α in odontoblast lineage cells led totwo co-existing changes including (1) loss of XBP1 signaling, and (2) heightened ER stress. At the tissue level, odontoblast deficiency of IRE1α leads to compromised dentinogenesis, and at the cellular level, IRE1α-deficiency resulted in decreased odontoblast differentiation and proliferation. In addition, I found that *Ire1a* deficient mice displayed delayed tooth eruption of incisors and molars.

Having observed that the IRE1α /Xbp1 signaling axis is important for mineralized tissues in the mouse model, I then investigated whether human genetic variants in *ERN1* and *XBP1* influence dental and bone phenotypes. I employed an *in silico* candidate gene approach testing the genetic association of variants in *ERN1* and *XBP1*, with tooth eruption, dental caries and bone

mass phenotypes. Three different categories of genetic variants were investigated, common coding variants, common possible cis-acting regulatory variants, and low-frequency coding variants. I found a missense SNP in the *ERN1* gene was significantly ($p<0.05$) associated with dental caries in the primary dentition. I also observed locus-wide significant associations between common possible cis-acting regulatory variants near *ERN1* and *XBP1* for tooth eruption, caries, and bone phenotypes ($p<0.00022$). The associated SNPs are in known promoter and enhancer regions in relevant cells, e.g. osteoblasts. In addition, I observed low-frequency coding variants in *XBP1* were significantly associated with dental caries in the primary dentition ($p<0.05$). These findings provided both genetic and *in vivo* mouse functional evidence for the role of IRE1α/XBP1 in regulating dentinogenesis, tooth eruption and bone mass.

TABLE OF CONTENTS

LIST OF FIGURES

LIST OF TABLES

PREFACE

I would like to express my gratitude for Dr. Hongjiao Ouyang, my PhD dissertation committee member, and Dr. John Shaffer, my dissertation advisor. Dr. Hongjiao Ouyang guided me throughout the mouse genetic studies performed in the first and half years of my PhD training, which led to the conceptualization of this dissertation work. The PhD dissertation would not be possible without her scientific contribution, funding resources, mouse model created by her lab, and her mentorship throughout the time I work in her lab. I would like to express my gratitude for Dr. John Shaffer, my dissertation advisor. He has been a great mentor to me during my time at the Center for Craniofacial and Dental Genetics (CCDG). I admired his knowledge in human genetics, passion about teaching and caring about students. Without his guidance, completion of the thesis work would not be possible. I would like to thank Dr. Mary Marazita, who has been kindly supporting me since I joined CCDG. She has been a role model to me. I thank her for her guidance and leading an awesome team at CCDG. I am grateful to Dr. Mark Mooney and Dr. Elia Beniash, for their mentorship, full support and encouragement throughout my study and research, and to make each committee meeting a rewarding experience.

I acknowledge the faculties, staff and students of the Center for Craniofacial Regeneration (CCR) for their generosity in reagent/equipment and knowledge sharing, especially during my time in the wet lab. I thank the CCDG team, including faculties, staff and students, for providing me with the resources that I needed to complete this dissertation, and for their help with my research. I also thank the faculty member and resident in the Department of Endodontics, such as Dr. Herb Ray and Dr. Hsiao-Ling Shen for assisting in characterizing the tooth phenotypes of the *Ern1*-deficient mice.

DISCLAIMER

Chapters 1 and 2 of this dissertation are reproduced with modifications from "Zhou, Yuqiao. **Inactivation of ire1α in osterix-cre expressing dental mesenchyme disrupts dentin formation.** Diss. University of Pittsburgh, 2016."

1.0 INTRODUCTION

The endoplasmic reticulum (ER) is a multifunctional organelle essential for the folding and maturation of newly synthesized secretory and transmembrane proteins (Hetz, 2012). Osteoblasts, odontoblasts and ameloblasts are professional secretory cells responsible for synthesizing and secreting the extracellular matrix (ECM) proteins necessary for bone and tooth formation. ECM proteins need to be properly folded in the endoplasmic reticulum before being secreted into the ECM (Kim et al., 2014). Events that disturb protein folding lead to the accumulation of misfolded and/or malformed proteins in the ER lumen, resulting in the cellular stress condition termed ER stress (Hetz, 2012). To cope with ER stress, cells activate three signal transduction pathways, which are mediated by PKR-like ER kinase (PERK), activating transcription factor 6 (ATF6), and inositol requiring enzyme 1α (IRE1α), respectively. Activation of these transduction pathways lead cells to shut down global protein synthesis and up-regulate the overall cellular protein folding capacity in an attempt to ensure cell survival and appropriate cellular function during periods of ER stress (Rutkowski and Kaufman, 2004). Collectively, these signaling transduction pathways are designated as the ER stress signaling or unfolded protein responses (UPR). Upon ER stress, binding immunoglobulin protein (BiP) dissociates from three ER-transmembrane transducers leading to their activation. ATF6α translocates from the ER to the Golgi compartment where it is cleaved by intramembrane proteolysis to generate a soluble active transcription factor, which induces the transcription of target genes whose functions are to increase ER content, degrading

misfolded proteins, and reducing the load of new proteins entering the ER. Activated PERK phosphorylates eukaryotic initiation factor 2 alpha (eIF2α) resulting in mRNA translation attenuation to relieve the burden of ER (Rutkowski and Kaufman, 2004).

IRE1α is an ER membrane-resident protein that has both kinase and endoribonuclease (RNase) activities (Zhang et al., 2011). Upon its activation, IRE1α executes unconventional splicing of XBP1 mRNA to produce a spliced form of Xbp1 (Xbp1s). XBP1s derived from s Xbp1s mRNA translocates to the nucleus and drives the expression of many proteins required for ER biogenesis, protein folding, and the clearance of misfolded and malformed proteins (Yoshida et al., 2001). Schematic representation of the ER stress signaling pathways is shown in Figure 1.

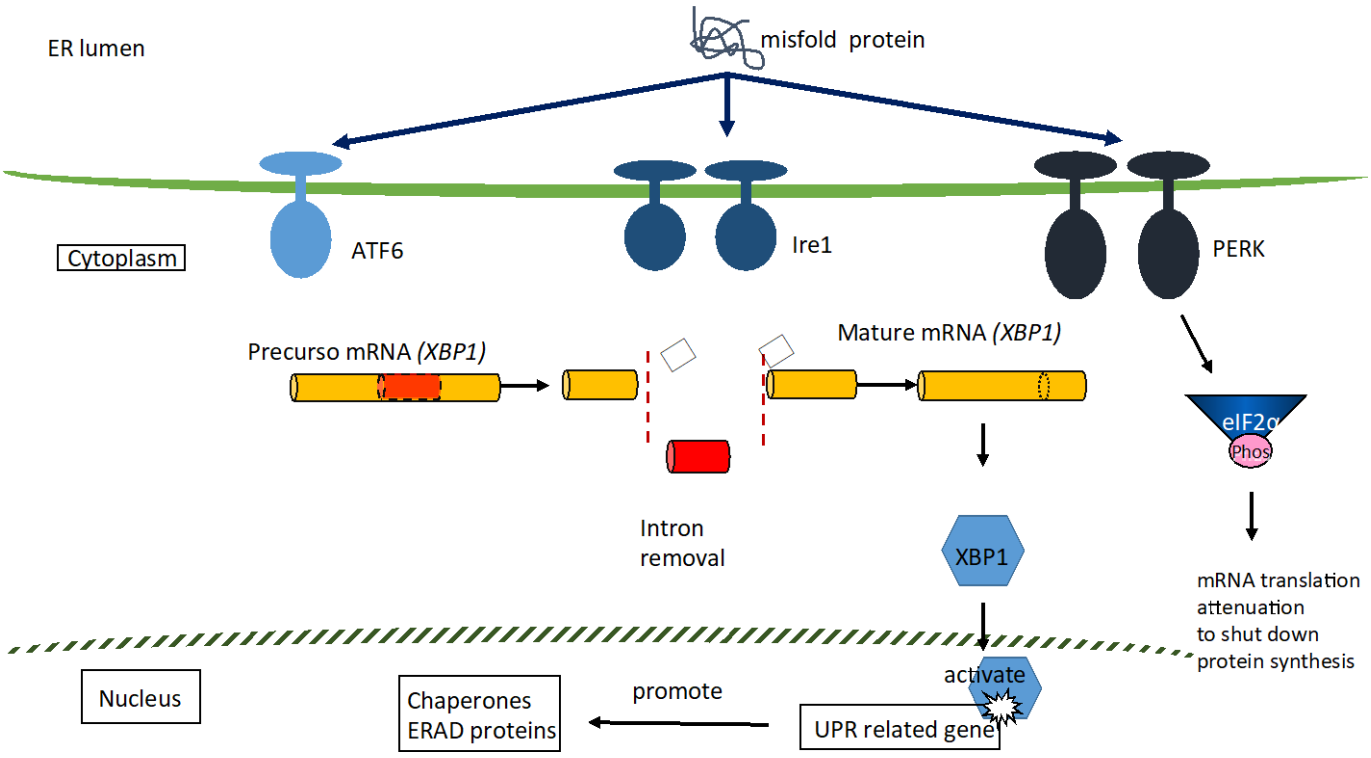

Figure 1. A schematic illustration of IRE1α / XBP1 signaling pathway and p-PERK/p-eIF2α signaling pathway.

To cope with ER stress, IRE1α executes unconventional splicing of XBP1 mRNA to produce a spliced form of Xbp1 (Xbp1s). XBP1s derived from s Xbp1s mRNA translocates to the nucleus and drives the transcription of a variety of drives gene expression of many proteins required for ER biogenesis, protein folding, and the clearance of misfolded and malformed proteins; Activated PERK phosphorylates eukaryotic initiation factor 2 alpha (eIF2α) resulting in mRNA translation attenuation to relieve the burden of ER.

IRE1α/XBP1s pathway is especially important in organs specialized to secrete proteins including endocrine and exocrine organs, e.g., the liver, pancreas, and salivary glands (Reimold et al., 2000; Zhang et al., 2005; Zhang et al., 2011). The following sections focus on the implications of ER stress signaling pathways for mineralized tissue development, including that of bone and tooth.

1.1 ER STRESS PATHWAY: IRE1α/XBP1 AND MINERALIZED TISSUE DEVELOPMENT

1.1.1 ER stress pathway: IRE1α/XBP1 and bone development

During bone development, osteoblasts are responsible for synthesizing and secreting a large amount of bone extracellular matrix, such as collagen, and, therefore, undergo a certain level of ER stress. The physiological amount of ER stress induces the adaptive program of cells to handle the stress, and maintain the physiological state of cells (Tohmonda et al., 2011). *In vitro* analysis has revealed that the IRE1α/XBP1 pathway is essential for BMP2-induced osteoblast differentiation (Tohmonda et al., 2011). In addition, *Osterix* (*Osx*)—an essential transcription factor for osteoblast differentiation – has been identified as a target gene for XBP1s (Tohmonda

et al., 2011). Although published studies investigating the role of IRE1α in osteogenic differentiation are restricted to *in vitro* studies, these results provide sufficient evidence that IRE1α plays vital role in bone formation and homeostasis, thereby opening up avenues for *in vivo* studies. In addition to studies of osteoblast development, studies on other types of bone cells have also demonstrated a regulatory role of ER stress signaling IRE1α/XBP1s in bone formation/resorption and bone marrow homeostasis. Xu et al. reported that the osteoblastic IRE1α/XBP1s pathway controls osteoclastogenesis, and that XBP1s in bone marrow stromal cells is critical for myeloma cell growth (Xu et al., 2012). Tohmonda et al. found that the conditional deletion of IRE1α in mouse bone marrow cells increases bone mass as the result of defective osteoclastic bone resorption (Tohmonda et al., 2015b). *In vitro* analysis showed that suppression of the IRE1α/XBP1 pathway in osteoclast precursors substantially inhibited the formation of multinucleated osteoclasts. Recently, an *in vivo* study showed cartilage-specific ablation of XBP1 signaling in mouse resulted in a chondrodysplasia, characterized by dysregulated chondrocyte proliferation and delayed cartilage and mineralization (Cameron et al., 2015b).

1.1.2 ER stress pathway: IRE1α/XBP1 and tooth development

ER stress has been found to be involved in the biological process of enamel secretion (Brookes et al., 2017) . The IRE1α/XBP1 pathway has been indicated to play a role in ameloblast development and enamel secretion, evidenced by IRE1 activation in secretory stage ameloblasts, *in vitro* (Kubota et al., 2005). Xbp1 mRNA was expressed five times greater in secretory enamel organ cells compared to maturation stage enamel organ, suggesting that IRE1α/XBP1 activation and the triggering of the ER stress response are important events in the secretory ameloblasts (Tsuchiya et

al., 2008). The activation of ER stress accompanied by an increase in ER stress markers, including xbp1, has been implicated in Amelogensis Imperfecta (AI), a genetic condition characterized by enamel biomineralization defects, and dental fluorosis, a condition characterized by enamel hypomineralization (Brookes et al., 2017; Liu et al., 2015) . ER stress is recognized as a mechanism of AI pathogenesis (Brookes et al., 2014Brookes et al., 2017) and represents a possible therapeutic target through use of protein chaperoning/anti-apoptotic drugs such as 4-phenylbutyrate (Brookes et al., 2014).

1.2 OVERALL RESEARCH GOAL AND SPECIFIC AIMS

To address my central hypothesis that IRE1α/XBP1 signaling pathway is an essential physiological regulator for postnatal tooth development, three specific aims were pursued. In Aim 1 and 2 , I participated in breeding and characterizing a novel genetic mouse model created by Dr. Hongjiao Ouyang's lab. This mouse model carried an *Ern1* deletion in cells that express *Osterix*, an essential transcription factor of both osteoblast and odontoblast lineage cells. In Aim 3, I performed observational genetic studies in humans.

Specific aim 1: Define the tissue specific role of IRE1α/XBP1 in dentinogenesis *in vivo*.

> **Hypothesis:** IRE1α/XBP1 regulates dentinogenesis through promoting the proliferation and differentiation of dental mesenchymal cells.

Specific aim 2: Define the tissue specific role of IRE1α/XBP1 in tooth eruption *in vivo*.

Hypothesis: The IRE1α/XBP1 signaling pathway regulates tooth eruption by regulating bone remodeling necessary for eruption pathway formation, through both bone formation and bone resorption.

Specific aim3: Investigate the association between *ERN1* and *XBP1* polymorphisms and tooth eruption, caries and bone phenotype in human cohorts.

Hypothesis: Genetic variants at the *ERN1 and XBP1* loci are associated tooth eruption, dental caries and bone phenotypes.

2.0 DEFINING THE TISSUE SPECIFIC ROLE OF IRE1α/XBP1 IN DENTINOGENESIS *IN VIVO*.

2.1 INTRODUCTION

Odontoblasts are professional secretory cells that have highly developed ER to manage a physiological level of ER stress during synthesis and secretion of dentin extracellular matrix proteins required for proper dentinogenesis (Kim et al., 2014). However, the role of ER stress signaling, especially the most evolutionarily conserved IRE1α /XBP1 branch, in regulating odontoblast differentiation and dentinogenesis has remained essentially unknown.

In *dentinogenesis imperfecta* and AI, abnormal ER stress in respective dentin/enamel and bone forming cells overwhelms the ER stress regulatory mechanisms and drives cells to undergo apoptosis (Brookes et al., 2013) (von Marschall et al., 2012), underscoring the important role of ER stress signaling in tooth development under pathological conditions. Targeted interventions aiming at rescuing dental phenotypes by relieving ER stress has been promising in AI animal models (Brookes et al., 2013). The development of targeted interventions required a profound understanding of ER stress signaling during normal tooth development. However, there is a general lack of knowledge on how ER stress molecules regulate ER stress during postnatal tooth development. The ER stress signaling pathways consists of three branches, mediated by three ER transmenbrane proteins, ATF6α, PERK and IRE1α. Among them, overexpression of ATF6 in human dental pulp cells induced odontoblastic differentiation and matrix mineralization. Despite the *in vitro* evidence that IRE1α /XBP1s is involved in enamel secretion, the role of IRE1α /XBP1s has not been reported in regulating dentin formation.

The IRE1α/XBP1s pathway is especially important in organs specialized to secrete proteins including endocrine and exocrine organs, e.g., the liver, pancreas, and salivary glands (Reimold et al., 2000; Zhang et al., 2005; Zhang et al., 2011). Recently, accumulating evidence suggests that IRE1α/XBP1s is involved in bone formation and remodeling, e.g., osteoblasts, osteoclast and chondrocytes (Cameron et al., 2015b; Tohmonda et al., 2011; Tohmonda et al., 2015b). Given the similar nature of odontoblasts and the above secretory cells, it is conceivable that IRE1a/XBP1s is involved in dentinogenesis by odontoblasts.

Recently, Dr. Ouyang lab generated transgenic mice that carry genetic deletion of *Ern1* in cells that express *Osterix*, an essential transcription factor of both osteoblast and odontoblast lineage cells (Revu et al., 2014). These mice displayed reduced bone mass, dentin defects and delayed tooth eruption. These observations guided me to further investigate the role of IRE1α/XBP1 signaling in dentin formation, as described in this chapter. I expect the outcome of this study to improve understanding of molecular and cellular requirements for proper dentin formation, and in the long term, to provide the biological basis for designing targeted intervention for dental anomalies.

2.2 MATERIALS AND METHODS

2.2.1 Generation of Ire1α conditional knock out (Ire1α CKO) mice

Generation of the Ire1α conditional knock out (Ire1α CKO) mice. Osterix-Cre mice were purchased from The Jackson Laboratory (cat# 006361), and $Ire1\alpha^{F/+}$ mice were generated as

previously described (Wang et al., 2012; Zhang et al., 2011). *Osterix-Cre* mice and *Ire1α*$^{F/F}$ mice were bred to create genotypically appropriate mice. Mice genotyped *Ire1α*$^{F/F}$*; Cre*$^{+}$ were designated as *Ire1α* conditional knockout *(Ire1α* CKO). Mice genotyped *Ire1α*$^{F/F}$ and *Ire1α*$^{+/+}$*; Cre*$^{+}$ were used as controls. Genotyping was performed by PCR and resolved by 2% agarose DNA gel electrophoresis. Mice were of same genetic background (C57BL/6). All animal experimental procedures were approved by the University of Pittsburgh Institutional Animal Care and Use Committee.

2.2.2 Isolation of teeth and quantitative real time PCR (qRT-PCR)

Control and *Ire1α* CKO mice pups were sacrificed at post-natal day 14, and their maxillae were removed. Mandibular molars were surgically isolated by means of micro-dissection and crushed into powder in liquid nitrogen. Total RNA was isolated from mice mandibular molars using the Trizol-Chloroform isolation method (Invitrogen). cDNA was obtained by reverse-transcribing 1µg of total RNA, using the cDNA synthesis kit (Promega Life Sciences), according to the manufacturer's protocols. qRT-PCR was performed using SYBR Green Select Master Mix (Applied Biosystems). qRT-PCR analyses were performed to determine the mRNA expression of odontoblast markers, including alpha1(I) collagen *(Col-1),* alkaline phosphatase *(Alp),* dentin matrix protein 1 *(Dmp1),* and dentin sialophosphoprotein *(Dspp)* in the molars (Magne et al., 2004). Xbp1 mRNA splicing (*Xbp1s/Xbp1t*) and the mRNA levels of XBP1s target genes, such as *ERdj4* and *Edem1*, were examined to assess the functional consequences of IRE1α deficiency in odontoblasts *in vivo*. mRNA levels of β-catenin downstream targets, e.g., *Lef1, cyclin D1, cmyc*

and *Col6a1* were also investigated. The amplification conditions used for all genes were set to be 10 min at 95°C, followed by a two-step cycling PCR used for 40 cycles at 95°C for 15s and 60°C for 1min (Step One plus Applied Biosystem). The Ct values were normalized to the reference gene GAPDH and expressed as fold-changes over the experimental controls.

2.2.3 H&E and immunohistochemical (IHC) staining

Mandibles were isolated and fixed overnight in 10% normal formalin buffer. Tissues were then demineralized using 10% EDTA, and subjected to standard H&E and IHC staining. IHC staining was performed using the standard ABC and DAB detection kits (Vector Labs), as previously described (Chen et al., 2013). The primary antibodies were rabbit polyclonal antibodies to IRE1α (cat#sc-20790, Santa Cruz Biotechnology), XBP1 (cat#sc-7160, Santa Cruz Biotechnology), BiP/Grp78 (cat#ab21685, Abcam), β-catenin (cat#ab16051, Abcam), p-eIF2α (cat#SAB4504388, Sigma Life Sciences), and p-PERK (cat#orb6693, Biorbyt), respectively. A normal rabbit immunoglobulin fraction was used as a negative control (cat#X0903, DakoCytomation).

2.2.4 Microcomputed Tomography (Micro-CT)

For Micro-CT analysis, non-demineralized tissues were kept in 70% ethanol. Micro-CT densitometry and 3D morphometry analysis of mouse mandibular bone was performed using a VivaCT 40 (SCANCO Medical, Brüttisellen, Switzerland) *in vivo* Micro-CT scanner with a

10.5µm voxel size, following standard techniques as recommended by the American Society for Bone and Mineral Research, as previously described (Verdelis et al., 2011).

2.2.5 *In vivo* dynamic dentin formation analysis

5-day-old mice received intraperitoneal (IP) injections twice with calcein at a concentration of 0.01mg/per 1g of body weight. The two injections were performed 6 days apart. Two days after the second calcein injection, the mandibular bones with the first mandibular molars were harvested, frozen in the liquid nitrogen and embedded in OCT gel (Thermo Scientific™). The frozen tissue sections were prepared using Cryostat Microtom (Micron) at a thickness of 7µm with analysis performed using a fluorescent microscope at a 20X magnification. The dentin matrix deposition rate (µm/day) was defined as the mean distance between the two calcein labels, as measured by Adobe photoshop CS6 software, divided by the number of days between the injections.

2.2.6 BrdU in vivo labeling

BrdU in vivo labeling. BrdU (BD Biosciences) injections were performed through IP at the level of 100µl for 10g of body weight, one day prior to the harvesting of bone tissue. To determine cell proliferation, BrdU staining was performed, according to manufacturer's instructions, using the BrdU In-Situ detection kit II (cat# 551321, BD Pharmingen).

2.2.7 TUNEL staining

Mandible samples were isolated and fixed in 10% neutral buffered formalin, decalcified in10% EDTA@pH 7.0, and embedded in paraffin molds. Serial sections of paraffin tissues (7μm) were subjected to deparaffinization, followed by histological analysis. Sections were cut along the sagittal plane of mandibular molars. Sections were then deparaffinized and rehydrated in decreasing concentrations of ethanol. The TUNEL assay was performed with TACS TBL kit (R&D Systems, Minneapolis, MN) according to the manufacturer's instructions. Positive and negative control included nuclease treatment or exclusion of TdT enzyme, respectively. Apoptotic cells were defined as condensed, blue-stained nuclei under light microscopy exam. Quantification of apoptotic cells was as percentage of total cell counted.

2.2.8 Statistical analysis

Statistical analyses were performed using Student's t-test. Two tailed distributions, assuming 2 samples of equal variances, were used when appropriate. Sample number of at least $n = 3$, with a P-value < 0.05, were considered statistically significant.

2.3 RESULTS

2.3.1 Odontoblasts express BIP, IRE1α and XBP1s during dentinogenesis *in vivo*

Odontoblasts express IRE1α,XBP1s and ER stress markers BIP, pPERK and peIF2α, during dentinogenesis. To assess the potential involvement of the IRE1α/XBP1 pathway in dentinogenesis, I determined the protein expression of IRE1α, XBP1, and an XBP1s target, Immunoglobulin Binding Protein (BIP). The latter is also an ER chaperone protein and ER stress marker (Bertolotti et al., 2000). IHC staining on both molar and incisors of wild-type (WT) animals revealed that IRE1α was expressed in the murine odontoblast lineage cells, such as pulp cells and mature odontoblasts during postnatal tooth development, such as on postnatal day 5 (Figure 2A-a) and day 30 (Figure 2A-c). The XBP1 protein was also expressed in odontoblast lineage cells at several stages tooth development, such as the day 14 (Figure 2B-a) and 30 (Figure 2B-b). It is worth noting that while IRE1α and XBP1 are expressed in odontoblast lineage cells, they are more prevalently expressed in mature odontoblasts that actively produce predentin. Similar to these observations, it was observed that BIP, an XBP1s target gene and ER stress marker, is also predominantly expressed in extracellular matrix-producing mature odontoblasts, at various postnatal tooth developmental stages, such as day 5 and day 30 (Figure 1A-b,c,f,g). A strong BIP expression was also observed in mature ameloblasts in the developing tooth as well (Figure 2A-b,c). Consistently, pPERK and peIF2α, two widely used ER stress markers were also expressed in odontoblasts in day 14 molars and incisors (Figure 2B-c,d). Collectively, these observations demonstrated that ER stress is a physiological phenomenon intrinsic to dentinogenesis, and that IRE1α/XBP1 signaling is activated in odontoblasts during dentinogenesis.

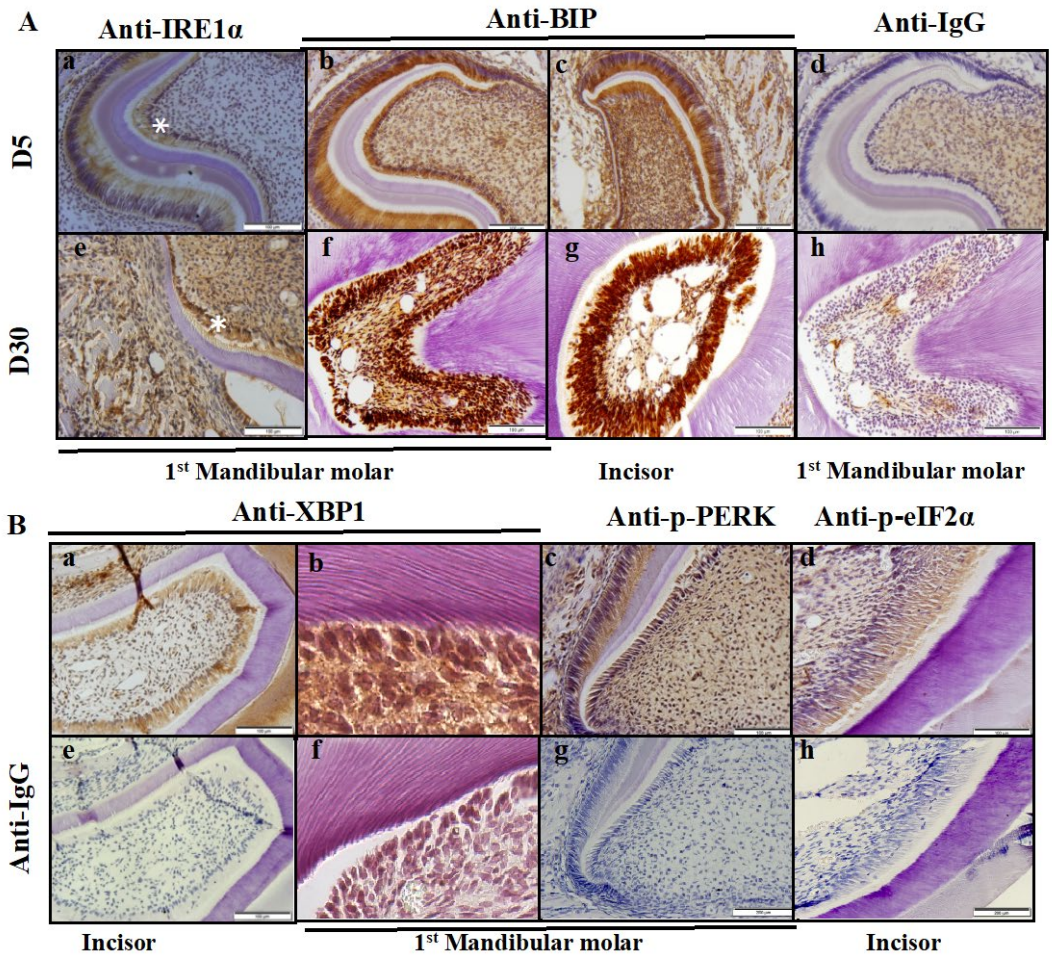

Figure 2. Odontoblasts express IRE1α,XBP1s and ER stress markers BIP, pPERK and peIF2a, during dentinogenesis.

(A) Immunohistochemical (IHC) staining showing that odontoblasts strongly express IRE1α, and BIP, an ER chaperone protein and ER stress indicator, at various developmental stages of the mandibular molars and incisors, such as day 5 and day 30, indicating that odontoblasts experience physiological ER stress during dentinogenesis. A negative control (NC) was stained with the relevant isotype (d,h). Scale bars: 100μm.(B) IHC staining showing that odontoblasts strongly express XBP1 in molars and incisors of wildtype mice at postnatal day 14 (a) and day 30 (b). (c,d) phosphorylated p-PERK and p-eIF2a are strongly expressed in odontoblasts of molars and incisors of WT mice. A negative control (NC) was stained with the relevant isotype (e,f,g,h). Scale bars: 100μm.

2.3.2 Generation of odontoblast-specific *Ire1α* conditional knockout mice

To determine the biological role of IRE1α in dentinogenesis, an IRE1α conditional knockout (*Ire1a* CKO) mouse model was generated as previously described (Zhang et al., 2011) through a series of breedings using homozygous mice harboring a *loxP* site-flanked *Ire1a* allele ($Ire1\alpha^{F/F}$) with *Osterix* -Cre transgenic mice, which over-express Cre under the control of the promoter of Osterix, a transcription factor predominantly expressed in odontoblasts and osteoblasts(Wang et al., 2012; Zhang et al., 2011). Consequently, *Ire1a* is conditionally knocked out in *Osterix* expressing cells, including odontoblast and osteoblast lineage cells (Chen et al., 2009). The current study aims at understanding the function of IRE1α in regulating odontogenesis. $Ire1\alpha^{F/F}$; Cre^{+} mice were odontoblast-specific *Ire1a* conditional knockout mice (*Ire1a* CKO) (Figure 3). Control littermates include both $Ire1\alpha^{F/F}$ and $Ire1\alpha^{+/+}$; Cre^{+} mice to exclude the possible impact of Cre gene on dentin, if any. (Figure 3). Age- and gender-matched control and CKO littermates were used (Figure 3B).

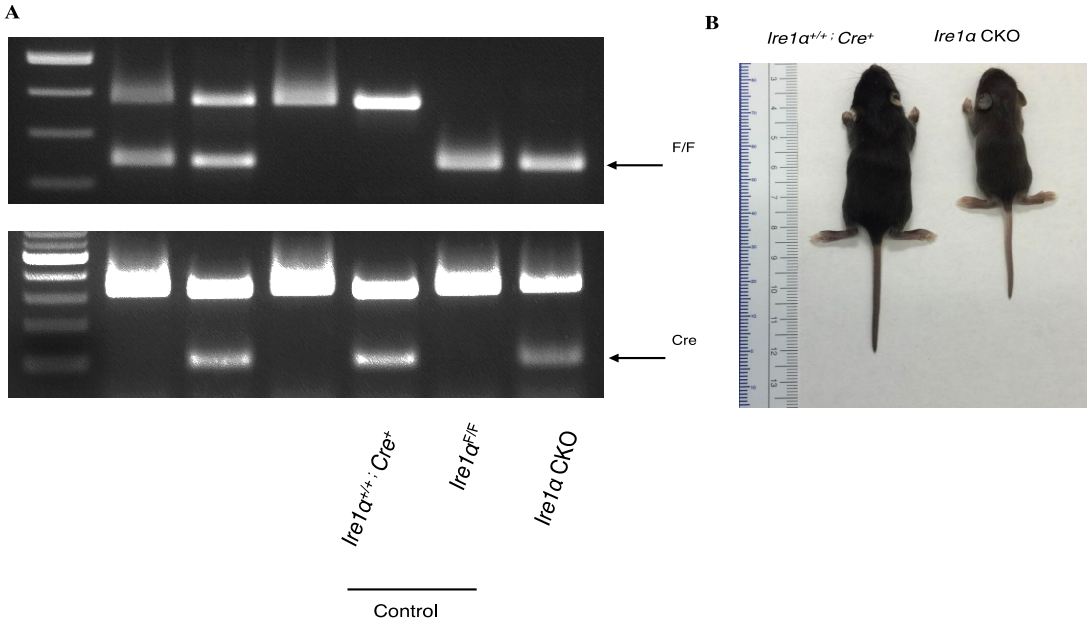

Figure 3. Generation of odontoblast-specific Ire1α conditional knockout mice.

(A) Genotypes of mice. Pups were identified by genotyping and designated *Ire1α*$^{F/F}$; *Cre*$^{+}$ mice as odontoblast-specific IRE1α conditional knockout mice (*Ire1a* CKO). Control mice include both *Ire1α*$^{+/+}$; *Cre*$^{+}$ and *Ire1α*$^{F/F}$ mice. (B) Clinical photo showing a 14-day-old *Ire1α* CKO mouse displaying reduced body size compared with a *Ire1α*$^{+/+}$; *Cre*$^{+}$ littermate.

2.3.3 *Ire1α* CKO mice displayed compromised IRE1α/XBP1 signaling activity and a heightened ER stress level in odontoblasts and mandible osteoblasts

IHC analysis of the mandibular first molars revealed that *Ire1α* CKO mice had reduced IRE1α protein expression in odontoblasts compared with corresponding control counterparts, including both *Ire1α*$^{+/+}$; *Cre*$^{+}$ (Figure 4A-a,b) and *Ire1α*$^{F/F}$ mice (Figure 4A-c,d). Such reduction is observed in the osteoblasts of alveolar bone as well (Figure 4A-e,f). As IRE1α protein is required for generating mRNAs of XBP1s, *Ire1α* CKO mice displayed significant reductions in both the mRNA levels of the spliced form of *Xbp1* (*Xbp1s*) ($p < 0.0001$), as well as the ratio between the mRNA level of spliced *Xbp1* vs. total *Xbp1* (*Xbp1s*/*t*) ($p < 0.0001$), reflecting a compromised responsiveness of IRE1α-deficient odontoblasts in response to endogenous ER stress in odontoblasts (Figure 4C). Consequently, *Ire1a* CKO mice exhibited reduced XBP1 protein expression in odontoblasts compared with control littermates (Figure 4A-g,h).

IRE1α acts through XBP1s to induce the mRNA expression of many genes involved in protein quality control, e.g., ER degradation-enhancing alpha-mannosidase-like protein 1 (*Edem1*) and endoplasmic reticulum–localized DnaJ 4 (*ERdj4*). qRT-PCR analysis of the mandibular molars revealed significant reduced mRNA levels of *ERdj4* ($p < 0.05$) and *Edem1* ($p = 0.0725$) (Figure 4C), indicating a loss-of-function of XBP1s signaling in IRE1α-deficient odontoblasts. Taken together, these data indicate that *Ire1a* CKO mice displayed a compromised IRE1α/ XBP1s signaling activity in the odontoblasts *in vivo*.

As intact IRE1α/XBP1s signaling is indispensible for ER homeostasis (Yoshida et al., 2001), I hypothesized that the odontoblast-specific disruption of the IRE1α/XBP1s signaling

transduction pathway would exacerbate endogenous ER stress and activate other branches of ER stress signaling transduction pathways, e.g., the phosphorylated PERK (p-PERK) and eIF2α (p-eIF2α) pathways. Supporting this notion, the IHC staining demonstrated that IRE1α-deficient mice displayed the increased protein expression of both phosphorylated p-PERK and p-eIF2α in odontoblasts, compared with control counterparts (Figure 4B- a,b,e,f, asterisks). The enhanced protein expression of the two molecules was also observed in the osteoblasts of mandibular bones, compared with control counterparts (Figure 4B-c,d,g,h arrows). The latter observation echoes my recent finding indicating the increased p-PERK and eIF2α protein levels in IRE1α-deficient skeletal osteoblasts as well (data not shown). These observations suggest that deficiency of IRE1α in dental mesenchyme leads to heightened ER stress and compensatory activation of the p-PERK/p-eIF2α pathway. These results demonstrated that an intact IRE1α/XBP1s pathway is essential for the proper maintenance of the ER homeostasis in odontoblasts and osteoblasts. In addition, these findings also demonstrated that the successful odontoblast deletion of *Ire1α* was achieved and such deletion is of physiological consequence at the molecular level.

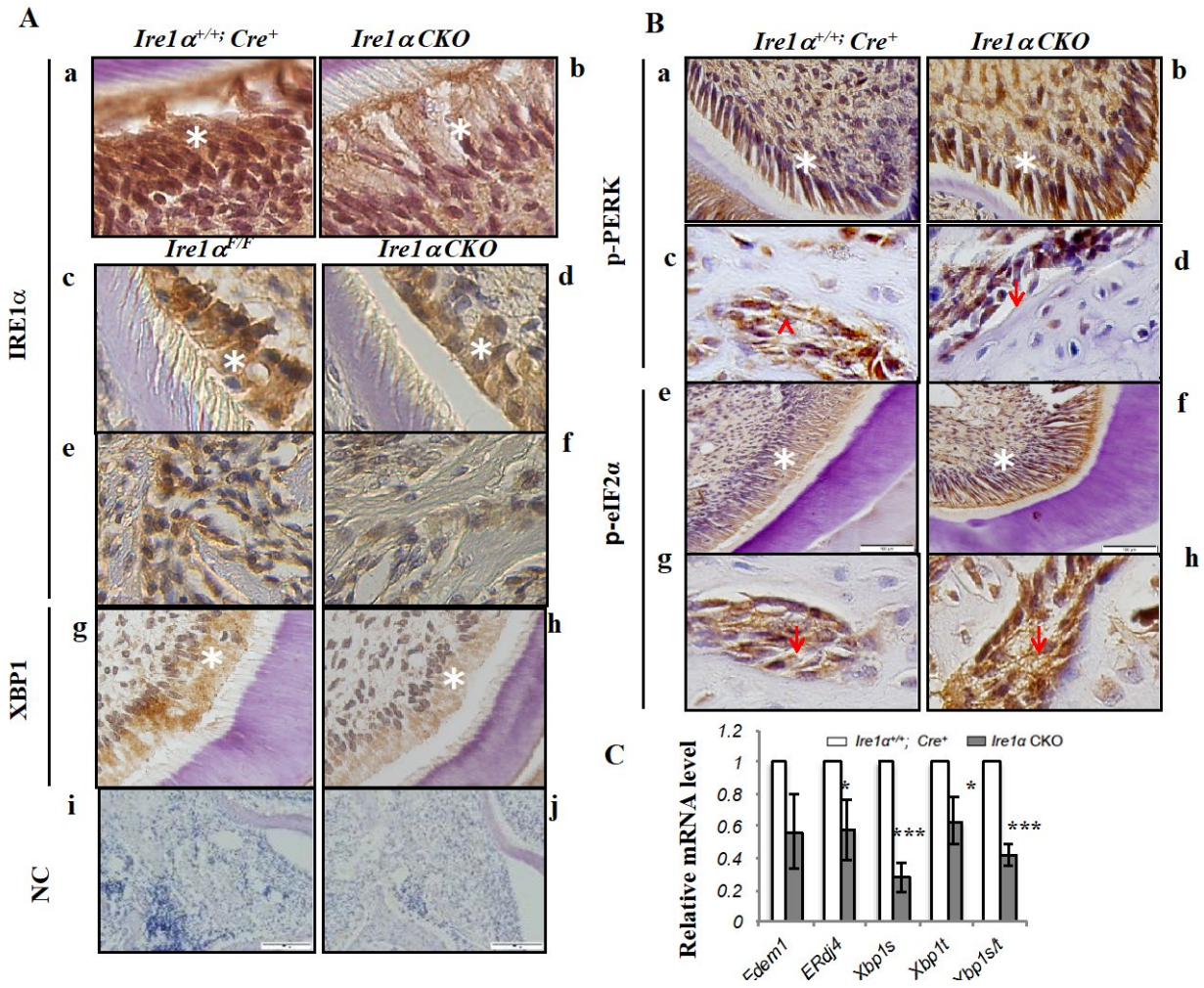

Figure 4. Ire1a CKO mice displayed compromised IRE1α/XBP1 signaling activity and a heightened ER stress level in odontoblasts and mandibles.

(A) IHC staining showing that 14-day-old Ire1α CKO mice displayed a reduction in IRE1α (a,b,c,d) and XBP1 protein expression (g,h) in odontoblasts (asterisks) of the first mandibular molar and incisor, compared with control littermates (Ire1α+/+; Cre+ and Ire1αF/F). (e,f): IHC staining showing 30-day-old Ire1α CKO mice displayed reduced IRE1α protein expression in osteoblasts of the mandibles compared with control littermates. Scale bars: 100μm. A negative control (NC) was stained with the relevant isotype (i,j). (B) IHC staining showing increased protein expression of p-PERK (a,b,c,d) and p-eIF2α (e,f,g,h) in the odontoblast (asterisks) and osteoblasts (arrows) of 14-day old Ire1α CKO mice mandibular tooth and bone, compared with control (Ire1α+/+; Cre+) counterparts. A negative control (NC) was also stained with

the relevant isotype. Scale bars: 100μm. (C) qRT-PCR analyses showing that 14-day-old Ire1α CKO mice displayed reductions in both the IRE1α endoribonuclease activity, as evidenced by the decreased ratio between Xbp1s vs. total Xbp1 (Xbp1t) mRNA (Xbp1s/t), and mRNA levels of XBP1s downstream target genes Edem1 and ERdj4 in the isolated mandibular molars, compared with those of control (Ire1α+/+; Cre+) counterparts (n = 3). Error bars represent SE of the mean. * $p < 0.05$, ** $p < 0.01$, and *** $p < 0.001$.

2.3.4 Odontoblast deficiency of IRE1a leads to delayed tooth eruption and defects in dentin formation

Ire1a CKO mice displayed delayed tooth eruption of both the maxillary (Figure 5A, arrows) and mandibular (Figure 5A, arrow heads) incisors, as compared to control littermates. Micro-CT of 30-day-old *Ire1a* CKO mice and control mice was performed to evaluate the mineralization of dentin. Micro-CT analyses showed that *Ire1a* CKO mice displayed a significantly reduced root dentin volume, compared with control counterparts (Figure 5B). Furthermore, histogram of different mineral density frequencies showed that 30-day-old *Ire1α* CKO mice experienced delayed mineralization of root dentin of both first and second mandibular molars, compared with control counterparts (Figure 5C). Thus it was concluded that IRE1α is an important regulator for timely tooth eruption, proper dentin volume and dentin biomineralization**.**

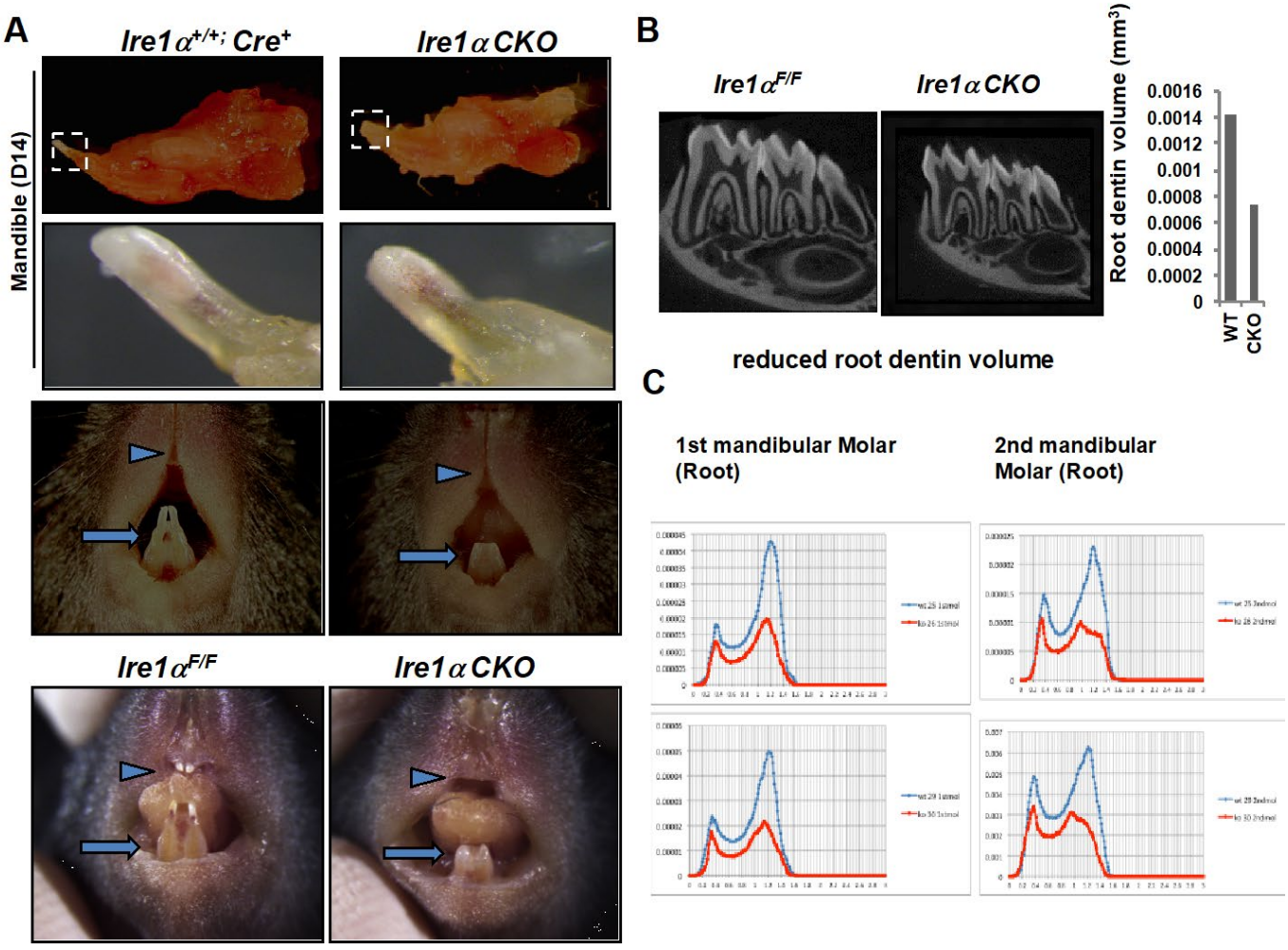

Figure 5. IRE1α deficiency in odontoblast leads to defects in dentin and tooth eruption.

(A) Clinical photos showing that 14-day-old male *Ire1α* CKO mice displayed delayed tooth eruption of both the maxillary (arrows) and mandibular (arrow heads) incisors, as compared to control (*Ire1α*$^{+/+}$; *Cre*$^{+}$ (upper panel) or *Ire1α*$^{F/F}$ (lower panel)) littermates. (B) The sagittal views of Micro-CT analyses of the mandibles of 30-day-old mice demonstrating that *Ire1α* CKO mice displayed a significantly reduced root dentin volume, compared with control counterparts (n = 2). (C) Histogram of different mineral density frequencies showing that 30-day-old male *Ire1α* CKO mice experienced the delayed mineralization of root dentin of both first and second mandibular molars, compared with control littermates (n = 2).

2.3.5 Odontoblast deficiency of IRE1α leads to compromised *in vivo* dentin matrix deposition, contributing to the reduced thickness of dentin

The effects of IRE1α odontoblastic deficiency on dentin formation and predentin maturation were further verified by histological analysis. The thickness of the dentin and predentin of the incisor and first molar were assessed by histology, and quantitative analysis was performed (Figure 6A-B). Dentin thickness in HE stained sections was decreased significantly in the first molars of Ire1a CKO mice compared with their control littermates ($p < 0.005$), while the ratio of predentin to dentin thickness was increased significantly ($p < 0.05$) (Figure 6A-B). At the morphological level, HE sections revealed abnormal odontoblast organization in *Ire1α* CKO mice incisors and molars, compared with controls (Figure 6, A).

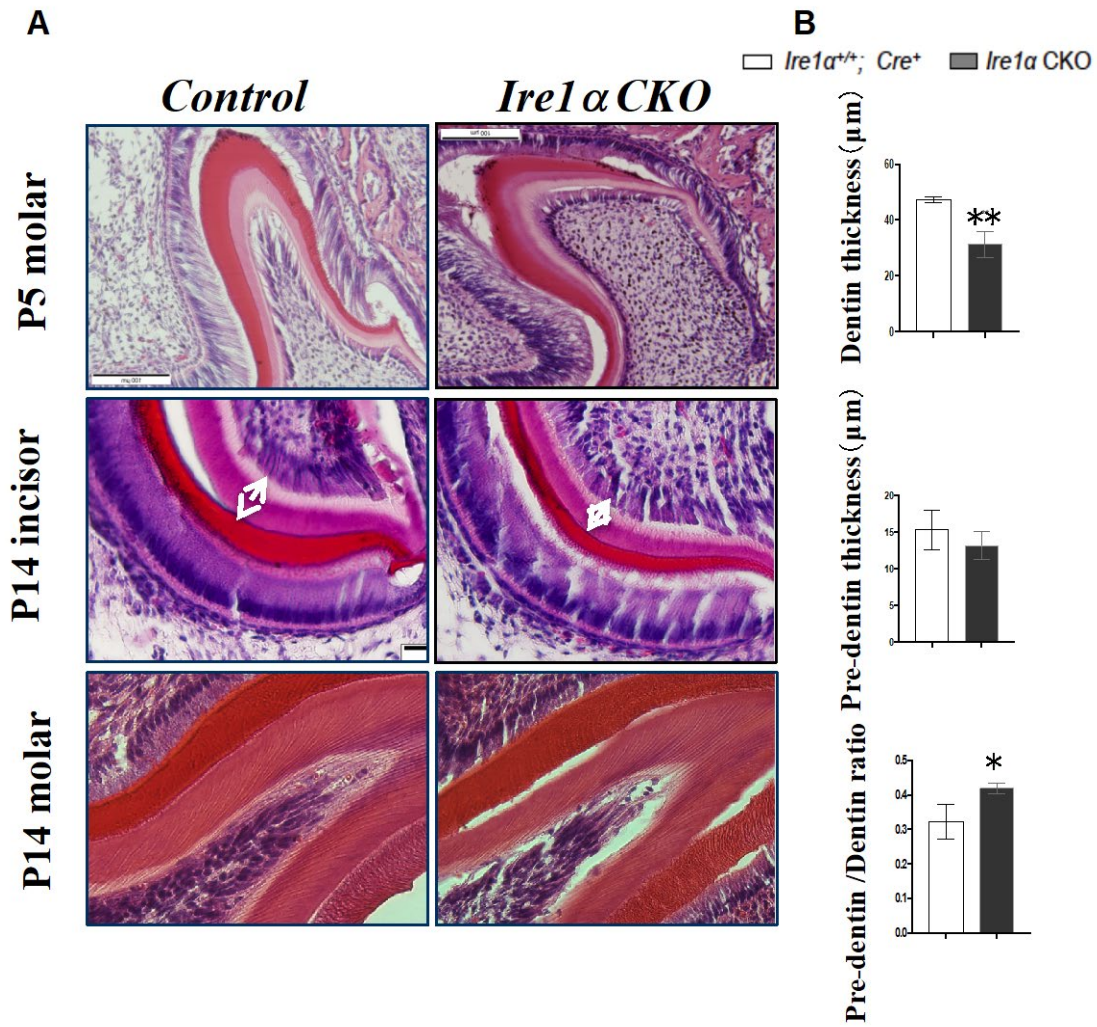

Figure 6. IRE1α deficiency in odontoblast leads to defects in dentin.

(A) H&E-stained coronal histological sections of mandibular incisors and molars of 5-day-old (upper panel) and 14-day-old (lower panel) mice showing that *Ire1α* CKO mice had the reduced thickness of both dentin and predentin layers (arrows), compared with corresponding control littermates ($Ire1\alpha^{+/+}$; Cre^{+}). Scale bars: 100μm. (B) Quantitative analysis showing reduced dentin thickness and increased ratio of predentin to dentin in the first molars (n = 3; *$p < 0.05$.). The thickness (μm) is presented as the mean ± S.E.M of 3 animals of each group. *$p < 0.05$.

Histomorphometric analysis of dentinogenesis was performed via double calcein labeling, which revealed a significant decreased dentin mineral apposition rate in molars of Ire1a CKO mice, compared with control ($p < 0.05$) (Figure 7). These data indicated that odontoblastic deficiency of IRE1α caused reduced dentinogenesis and abnormalities in the morphology of odontoblast *in vivo*.

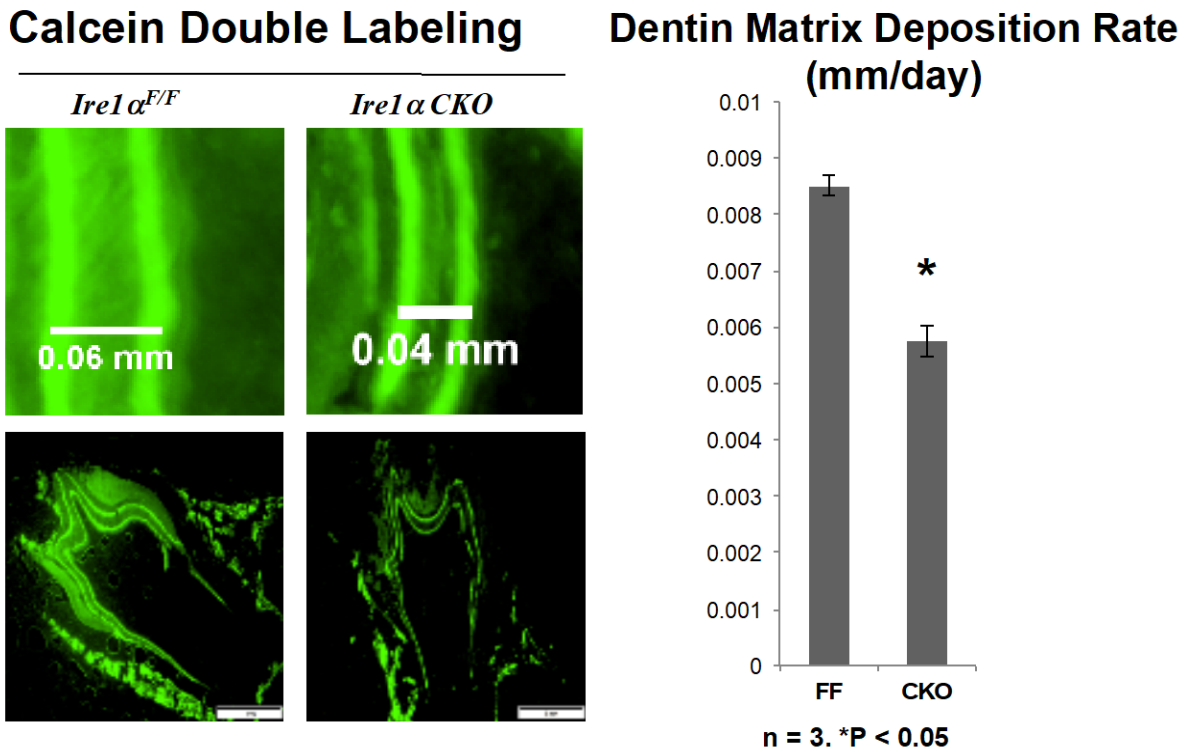

Figure 7. IRE1α deficiency in odontoblast leads to reduced dentin matrix deposition rate

Calcein double labeling showing that 14-day-old female *Ire1α* CKO mice displayed a significantly reduced dentin matrix deposition rate, compared with *Ire1α*$^{F/F}$ littermates (n = 3; *$p < 0.05$.)

2.3.6 Odontoblast deficiency of IRE1α leads to reduced gene and protein expression of odontoblast markers, indicating disrupted odontoblast differentiation in the absence of IRE1α

Disrupted dentinogenesis and odontoblasts organization in *Ire1α* CKO mice led me to evaluate the expression levels of the dentin extracellular matrix proteins in the odontoblasts, including two important markers for odontoblast differentiation, DSPP and DMP1. IHC demonstrated that the odontoblasts in control mice demonstrated strong DSPP and DMP1 protein expression, whereas *Ire1α* CKO odontoblasts exhibited a decreased level of DSPP and DMP1 protein expression (Figure 8, A and B).

Total RNA was extracted from isolated molars of 14-day-old control and *Ire1α* CKO mice and qRT-PCR analysis was performed to determine the relative levels of *Dspp*, *Dmp1* and other odontoblast markers including alpha1 (I) collagen (*Col-1*), alkaline phosphatase (*Alp*), and osteocalcin (*Ocn*) (Magne et al., 2004). A significant decrease in *Dspp* and *Dmp1* mRNA expression in *Ire1α* CKO, compared with those of control molars, was observed ($p < 0.05$), suggesting that loss of IRE1α in the dental mesenchyme disrupts odontoblast differentiation (Figure 8C). The mRNA levels of Alpha1(I) collagen(*Col-1*), a major extracellular matrix protein of dentin, and osteocalcin (*Ocn*), a marker of mature mineralized tissue, were also significantly down-regulated ($p < 0.05$) (Figure 8C). These results suggest that the reduced dentinogenesis exhibited in *Ire1α* CKO mice may be attributed to impaired odontoblasts differentiation and function.

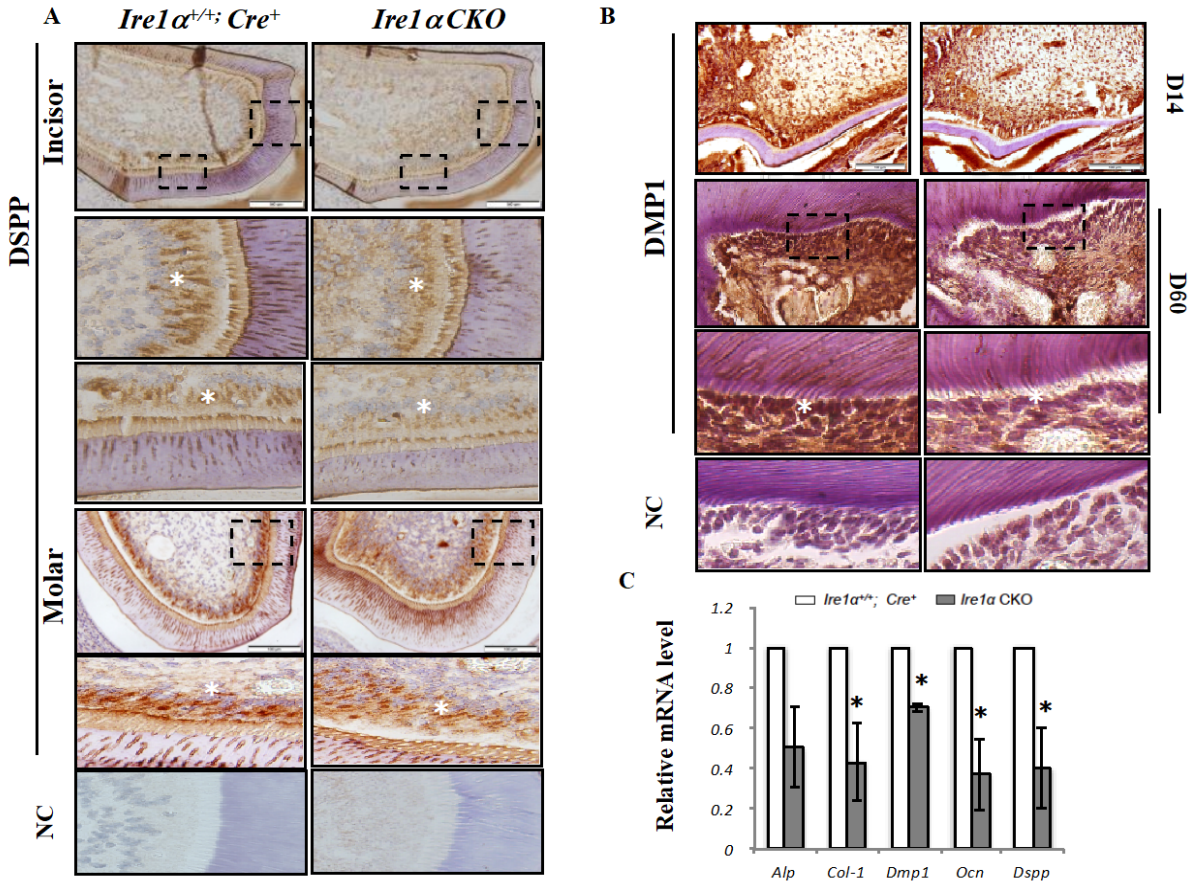

Figure 8. Odontoblastic deficiency of IRE1α leads to altered expression of Odontoblast Markers, indicating disrupted odontoblast differentiation.

(A and B) IHC staining showing reduced DMP1 and DSPP proteins in odontoblasts (asterisks) of 14-day-old male *Ire1α* CKO mice as compared with control (*Ire1α*$^{+/+}$; *Cre*$^{+}$) counterparts. Scale bars: 100µm. (C) qRT-PCR analyses showing that 14-day *Ire1α* CKO mice had reduced mRNA expression of odontoblast markers, such as, *Dmp1, Dspp, Col-1,* and *Ocn,* in mandibular molars, compared with control (*Ire1α*$^{+/+}$; *Cre*$^{+}$) littermates (n = 3; *$p < 0.05$.). Error bars represent SE of the mean.

2.3.7 Odontoblastic deficiency of IRE1α leads to disrupted dental mesenchyme proliferation, but not apoptosis

Reduced dentinogenesis in *Ire1α* CKO mice promoted me to investigate the role of IRE1α in regulating odontoblasts proliferation. The cell proliferation assay by 5-bromo-2'-deoxyuridine (BrdU) labeling and staining was performed on post-natal day 9 *Ire1α* CKO and *Ire1α*$^{+/+}$; *Cre*$^{+}$ mice. I observed cells positive for BrdU in the dental epithelium and in the mesenchyme (pulp cells, pre-odontoblasts, and odontoblasts) compartments of these mice. *Ire1α* CKO mice displayed a significant reduction in the number of Brdu-positive cells in dental papilla, indicating decreased proliferation of odontoblast-lineage cells in the area, compared with *Ire1α*$^{+/+}$; *Cre*$^{+}$ mice (Figure 9A-C, quantification of Brdu-positive dental papilla cells in both molar and incisors are shown in Figure 9C). The data demonstrated that odontoblast IRE1α is an important regulator for odontoblast proliferation *in vivo*.

I further examined apoptosis and found that IRE1α deficiency did not cause altered apoptosis of odontoblasts *in vivo*, as shown by terminal deoxynucleotidyl transferase dUTP nick end labeling (TUNEL) assays (Fig 10).

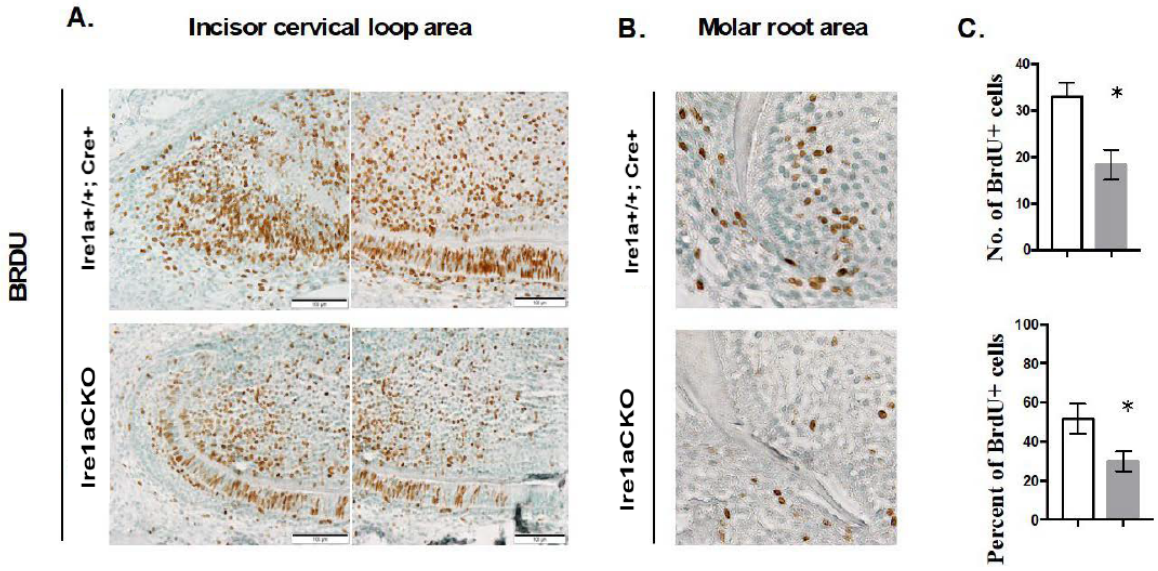

Figure 9. Odontoblastic deficiency of IRE1α leads to disrupted odontoblast proliferation.

(A and B) BrdU staining showing reduced odontoblasts proliferation in 9-day-old Ire1α CKO mice incisors and molar root area, compared with Ire1α+/+; Cre+ littermates. Proliferating cells incorporating BrdU are stained brown. (C) Quantification of BrdU+ cells in dental papilla of 9-day-old mice molars and incisors cervical loop area (right). The latter is represented as the percent of BrdU+ cells (n = 3; *p < 0.05). Error bars represent the SE of mean.

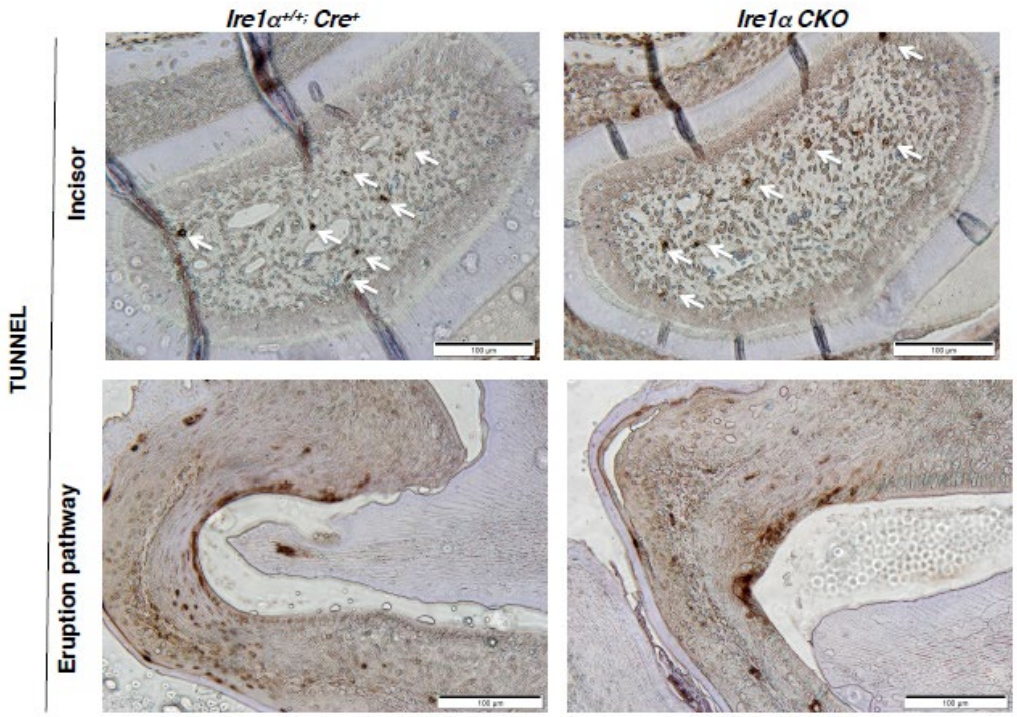

Figure 10. Odontoblastic deficiency of IRE1α does not affect dental mesenchyme apoptosis.
Representative images of TUNEL assay of 9-day-old Ire1α CKO mice incisors and molars, compared with Ire1α+/+; Cre+ littermates. Scale bars: 100μm. Brown color reaction indicates cells that underwent apoptosis.

In summary, these data support that odontoblastic deficiency of IRE1α compromised odontoblast differentiation and proliferation *in vivo*, which are the major driving forces underlying repressed dentinogenesis in *Ire1α* CKO mice *in vivo*.

2.3.8 Odontoblast deficiency of IRE1α leads to decreased β-catenin protein expression in mandibular tooth and bone

The molecular mechanism(s) underlying compromised dentinogenesis in *Ire1a* CKO mice were determined. Wnt/β-catenin signaling is a key signaling transduction pathway that promotes odontoblast differentiation and proliferation (Han et al., 2014; Kim et al., 2013; Liu et al., 2008; Zhang et al., 2013). Dr. Hongjiao Ouyang's lab's previous studies on bone reported that an intact IRE1α function is required for maintaining the steady-state protein expression of β-catenin in osteoblasts (Shankar et al, 2016 ASBMR). Thus I determined β-catenin protein expression in mandibles via IHC staining and found that *Ire1a* CKO mice displayed reduced β-catenin protein levels in odontoblasts (Figure 11A, arrows) and osteoblasts (Figure 11B), compared with control littermates. Consistently, mRNA expression of *Axin2* and *cmyc*, two β-catenin target genes, was significantly reduced in *Ire1a* CKO mice compared with control mice ($p < 0.05$) (Figure 11C). This observation suggests a possible molecular mechanism by which IRE1α regulates odontoblast differentiation and dentinogenesis, that is through WNT/β-catenin signaling.

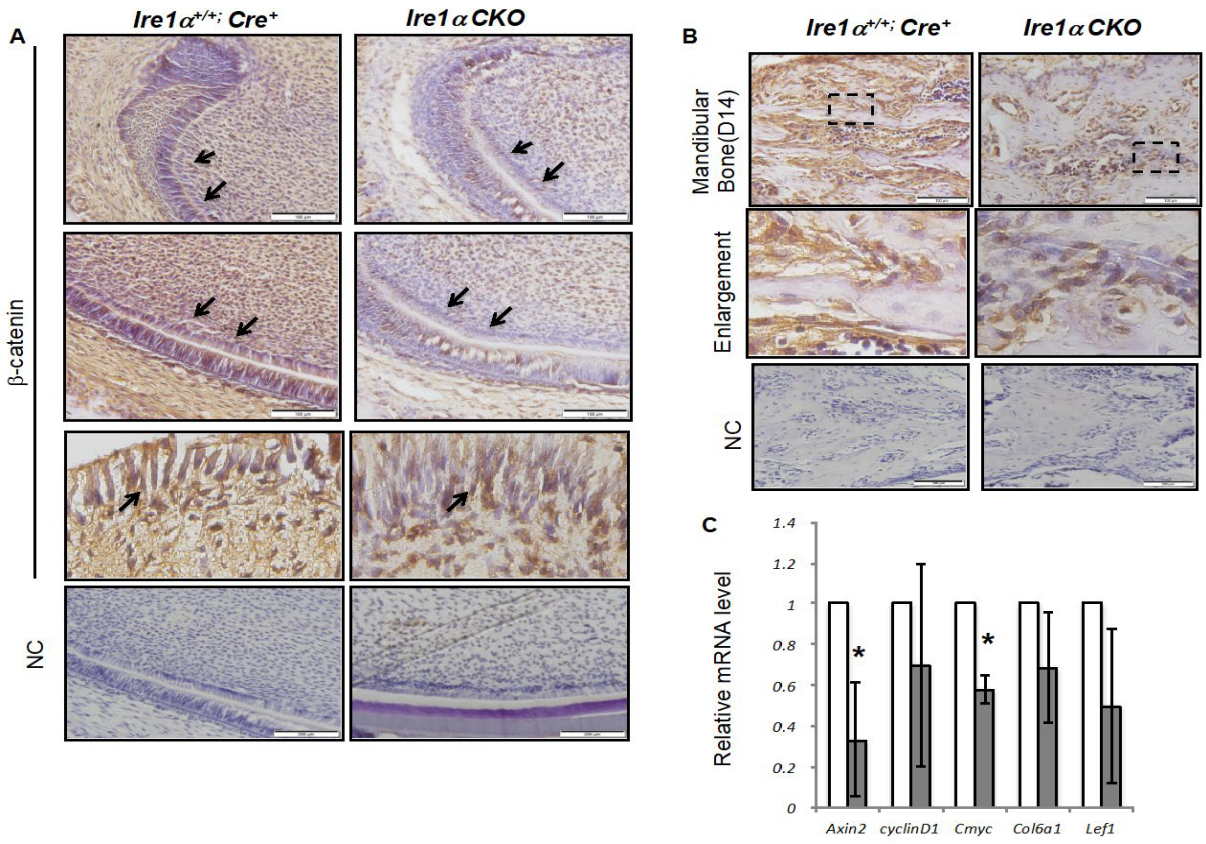

Figure 11. Odontoblastic deficiency of IRE1α leads to decreased β-catenin protein expression in tooth and mandibular bone.

(A) IHC staining showing reduced β-catenin protein expression in the odontoblast of 14-day-old *Ire1α* CKO mice, compared with *Ire1α*$^{+/+}$*; Cre*$^{+}$ littermates. (B) IHC staining showing reduced β-catenin protein expression in osteoblast of 14-day-old *Ire1α* CKO mice mandibular bone, compared with *Ire1α*$^{+/+}$*; Cre*$^{+}$ littermates. A negative control (NC) was also stained with the relevant isotype. Scale bars: 100μm. (C) qRT-PCR analyses showing reduced mRNA expression of β-catenin downstream target genes, such as *Axin2* and *Cmyc* in molars of 14-day-old *Ire1α* CKO mice, compared to *Ire1α*$^{+/+}$*; Cre*$^{+}$ littermates. ($n = 3$). *$P < 0.05$. Error bars represent SE of the mean.

2.4 DISCUSSION

Employing a novel odontoblast-specific IRE1α knockout mouse model created by Dr. Hongjiao Ouyang's lab, I demonstrated for the first time that the ER stress transducer IRE1α is an essential regulator for dentinogenesis, indicating its critical biological significance in tooth development.

Our studies demonstrated that the ER stress indicators BIP, p-PERK and p-eIF2α were highly expressed in odontoblasts of mouse mandibular incisors and molars of WT mice in different stages of postnatal development. These observations revealed that ER stress is a biological phenomenon intrinsic to odontoblasts during postnatal tooth development. Moreover, IRE1α and XBP1 were found to be highly expressed in odontoblasts of WT mice, suggesting the involvement of IRE1α /XBP1 signaling in odontoblast differentiation and/or function. Further characterization of the IRE1α-defocoent mice demonstrated that the deletion of IRE1α in odontoblast lineage cells led to two co-existing changes in these cells, including 1) loss of function of XBP1s signaling, and 2) heightened ER stress level and compensatory activation of p-PERK/p-eIF2α signaling. The latter observation indicates that IRE1α is important for the odontoblast ER homeostasis. Accompanying the heightened ER stress observed in IRE1α-deficient odontoblasts, odontoblast deficiency of IRE1α leads to compromised dentinogenesis, which is supported by the reduced matrix deposition as shown by calcein double labeling (Figure 7) and delayed dentin matrix biomineralization as shown by HE staining (Figure 6) and micro-CT (Figure 5B). As odontoblasts are the key cell type that produce dentin matrix protein and induce its biomineralization, I further determined the impact of lack of IRE1α on odontoblasts. I found that odontoblasts in *Ire1a* CKO mice displayed poor organization and a smaller cell body compared with control counterparts (Figure 6A). Further, these cells were less differentiated, as revealed by reduction of dentin matrix protein expression, such as DSPP and DMP1 at both mRNA and protein levels, compared with

cells from control counterparts (Figure 8A-C). These results suggest that IRE1α might be involved in odontoblast differentiation.

I further determined the role of IRE1α in regulating odontoblasts proliferation and apoptosis. The cell proliferation assay by BrdU labeling and staining revealed significantly reduced number of Brdu-positive cells in the dental papilla cells of both molar and incisors. However, IRE1α deficiency did not cause increased apoptosis of odontoblasts *in vivo*, as shown by TUNEL assays. These results taken together suggest the role of IRE1α in regulating odontoblast differentiation and proliferation. Furthermore, I observed that Wnt/β-catenin signaling, a key signaling transduction pathway that promotes odontoblast differentiation and proliferation, were compromised in odontoblasts in the absence of IRE1α. The latter finding is consistent with previous studies reporting that an intact IRE1α function is required for maintaining the steady-state protein expression of β-catenin in osteoblasts (Revu et al., 2014). Importantly, it suggests a possible molecular mechanism by which IRE1α regulates odontoblast differentiation and dentinogenesis.

Finally, I examined the molecular mechanism underlying compromised odontoblast differentiation in *Ire1α* CKO mice. Both loss- and gain-of-function strategies provided compelling evidence that β-catenin is an essential regulator for dentinogenesis and odontoblast differentiation (Han et al., 2014; Kim et al., 2013; Liu et al., 2008; Zhang et al., 2013). Consistent with this notion, I found β-catenin signaling is compromised in IRE1α-deficient dentin and odontoblasts both *in vivo* and *in vitro*, as shown by 1) reduced β-catenin protein expression and 2) reduced mRNA level of down-stream target genes in isolated mice molars. It is worth noting that odontoblast β-catenin mRNA level remains similar between the WT and *Ire1a* CKO mice, suggesting that the downregulation of β-catenin protein expression occurs at the post-transcriptional level (data not

shown). Dr. Ouyang's lab recently discovered that osteoblast-deficiency of IRE1α leads to the secondary activation of p-PERK/p-eIF2α pathway, resulting in reduced β-catenin protein in the face of ER stress in osteoblasts (Revu et al., 2014). Here, I also found increased ER stress and the gain of function of the p-PERK/p-eIF2α pathway activity in IRE1α-deficient odontoblasts. Thus, it is conceivable that IRE1α plays a similar role in maintaining ER homeostasis and proper β-catenin protein synthesis in odontoblast as well as it does in osteoblasts. Further investigation is needed to determine the impact of lack of IRE1α in regulating β-catenin protein stability in dental mesenchyme.

2.5 CONCLUSION

Our studies demonstrated that ER stress is a physiological event during odontoblast differentiation. I showed for the first time, that IRE1α/XBP1 is an important regulator for dentinogenesis and tooth eruption during postnatal tooth development. The lack of IRE1α/XBP1 signaling leads to multiple pathological consequences involving both possible transcriptional and translational mechanisms. This study also demonstrates that heightened ER stress has pathological impacts on tooth development. Further investigation is needed to determine the molecular mechanisms by which the IRE1α/XBP1s pathway controls odontoblast differentiation and tooth eruption and elucidate even broader biological functions of this pathway in regulating the development, homeostasis and regeneration of other mineralized tissues of tooth, such as enamel and cementum.

2.6 ACKNOWLEDGEMENTS

The work in this chapter was supervised and supported by my dissertation committee member, Dr. Hongjiao Ouyang, to whom I owe a great deal of gratitude, for her critical role in conceiving and supervising the project, providing funding resources, mouse model and preliminary data for the project, and for being such a great mentor during my time in her lab. I gratefully acknowledge my colleagues Drs. Shankar Revu, Kai Liu, Qi Han and Risheng Chen, who provided tremendous support during my time at Dr. Ouyang's lab.

This study was supported by NIH/NCI (RO1DE017439, RO1CA182418 and R21CA161150 to H.J.O.), start-up funds from the University of Pittsburgh School of Dental Medicine, School of Medicine, and the Office of Senior Vice Chancellor for the Health Sciences (H.J.O.). I am thankful for Dr. Kostas Verdelis for the Micro-CT analysis, Drs. Shankar Revu and Hsiao-Ling Shen, and Herbert Ray for contributing the project, regarding study design and initial data collecting. I thank Dr. Randal J. Kaufman for generously providing Ire1αF/+ animals for my studies. The authors are grateful for the Graduate Student Research Award (GSRA) from the Department of Oral Biology, School of Dental Medicine at the University of Pittsburgh. I thank Drs. Elia Beniash, Thottala Jayaraman and Heather Szabo-Rogers for graciously sharing the antibodies of DSPP and DMP1 as well as the DSPP primers, respectively.

3.0 DEFINING THE TISSUE SPECIFIC ROLE OF IRE1α/XBP1 IN TOOTH ERUPTION *IN VIVO*.

3.1 INTRODUCTION

Previously we found *Ire1a* CKO mice displayed delayed tooth eruption of both the maxillary (Figure 3A-a,b, arrows) and mandibular (Figure 3A-a,b, arrow heads) incisors and molars (Figure 3A-c,d) as compared to control littermates. In this chapter, I determined the mechanism behind delayed tooth eruption.

Several theories of tooth eruption has been proposed and later refuted. The most compelling mechanism is explained by *dental follicle theory*, evidenced by the classical experiment where removal of dental follicle in dogs leads to failure of molar eruption (Marks and Cahill, 1984). According to this theory, dental follicle cells secret cytokines into the periodontium to recruit and activate osteoclast precursors (Heinrich et al., 2005). Differentiation of osteoclast precursors into active osteoclasts is necessary for resorption of bone coronal to the tooth, resulting in the formation of eruption pathway (Wise and King, 2008). Another widely accepted tooth eruption theory is *bone remodeling theory*, which is compatible with dental follicle theory. This theory contends that in addition to coronal bone resorption, alveolar bone formation at the base of the tooth socket is required for eruption. Thus, in this aim, I examined whether IRE1α/XBP1 signaling controls tooth eruption through regulating bone remodeling, e.g., osteoclast and osteoblast activity. Our hypothesis is that *Ire1α*CKO mice displayed delayed tooth eruption due to a deregulated metabolic process of the bone. To test this hypothesis, osteoclast activity was examined by TRAP staining on mandibular bones containing erupting molars, and osteoblast

activity was determined via histology, qRT-PCR and bone histomorphometric analysis. Supporting this theory, my preliminary data showed that *Ire1α*CKO mice have a low bone mass phenotype, and that both bone formation and bone resorption are compromised in the mandibles of *Ire1αCKO* mice, suggesting slow bone turn over.

3.2 MATERIALS AND METHODS

3.2.1 Osteoclast activity analysis

Tartrate-resistant acid phosphatase (TRAP) staining was performed to compare osteoclast activity in Ire1αCKO mice with that of control mice, using consecutive sections of mandibles at P7 and P14 when bone resorption and tooth eruption is relatively active. Enzyme histochemistry for TRAP was performed using a modification of the manufacturer's protocol (387A-1KT; Sigma-Aldrich). Images of the mandibular alveolar bone surface surrounding the first molar and incisor were obtained, and the number of TRAP-positive cells lining the bone surface was analyzed using ImageJ software. Bone parameters of the alveolar bone surface were measured at 40X. Next, the number of TRAP stained osteoclasts was manually counted in the same field. Results from multiple pairs of mice were pooled for statistical analysis. *Statistical analysis* was performed as described in Chapter 2 using Student's t-test. Sample number of at least $n = 3$, with a P-value < 0.05, was considered statistically significant.

3.2.2 Osteoblast differentiation analysis.

3.2.2.1 qRT-PCR analyses

I determined the impact of IRE1α deficiency on the maturation of preosteobalsts via **qRT-PCR analyses** using skull and mandibular bones of 8-week-old *Ire1α* CKO mice detecting mRNA expression of osteoblast genes, e.g., *Alp,* bone sialoprotein (*Bsp*)*,* type I collagen (*COL-1*)*, Ocn*, *Osx*, and runt-related transcription factor 2 (*Runx2*)*,* compared with *Ire1α*$^{+/+}$*; Cre*$^{+}$ counterparts. qRT-PCR analysis was described in Chapter 2.

3.2.2.2 Double calcein labeling

Histomorphometric analysis of bone formation was performed via double calcein labeling as described in Chapter 2.

3.3 RESULTS

3.3.1 Odontoblastic deficiency of IRE1a leads to delayed tooth eruption

Ire1a CKO mice displayed delayed tooth eruption of both the maxillary (Figure 12 uppder panel, arrows) and mandibular (Figure 12 upper panel, arrow heads) incisors and molars (Figure 12 lower panel) as compared to control littermates. On day 14, while the mandibular incisors of control littermates have reached their full eruption, the IRE1α-deficient mandibular incisors had just partially erupted. At the same time point, while the maxillary incisors of control littermates had emerged from alveolar sockets, the IRE1α-deficient mandibular incisors were still missing from the oral cavity. Similarly, at postnatal day 14, molars of *Ire1αCKO* mice displayed partial eruption compared with that of control mice and were covered by a dental sac (Figure 12 lower panel).

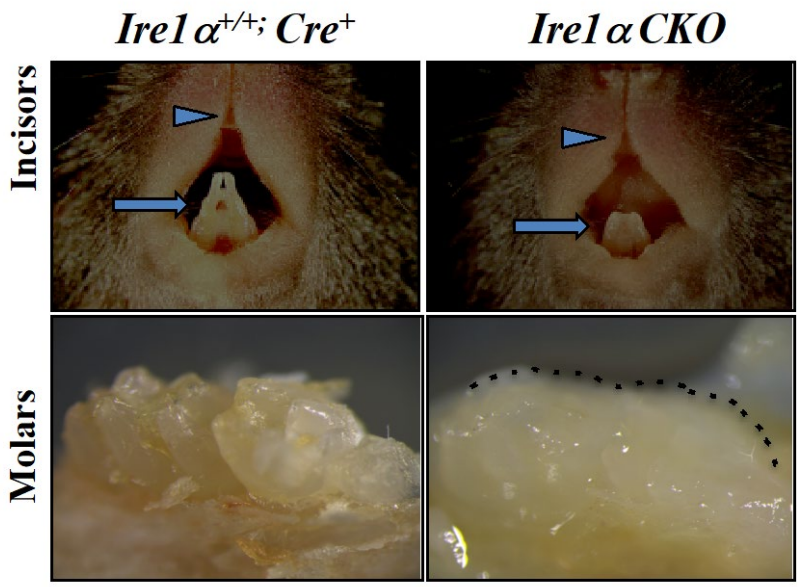

Figure 12. *Ire1α* CKO mice displayed delayed tooth eruption.

Clinical photos showing that 14-day-old male Ire1α CKO mice displayed delayed tooth eruption of both the maxillary and mandibular incisors (upper panel) and molars (lower panel) as compared to control (Ire1α+/+; Cre+) littermates.

3.3.2 Delayed tooth eruption was accompanied by low bone density

It is known that metabolic bone diseases, such as osteopetrosis, a high bone mineral density condition, often are accompanied by delayed tooth eruption due to compromised bone resorption (Luzzi et al., 2006; Suri et al., 2004). However in *Ire1α* CKO mice, I found low bone mineral density in their long bones via Micro-computed tomography (μCT) analyses (Figure 13A), compared with *Ire1α*$^{+/+}$*; Cre*$^{+}$ littermates. H&E staining confirmed the reduced bone mass in long bones and thinner skull in *Ire1α* CKO mice when compared with *Ire1α*$^{+/+}$*; Cre*$^{+}$ littermates (Figure 13B).

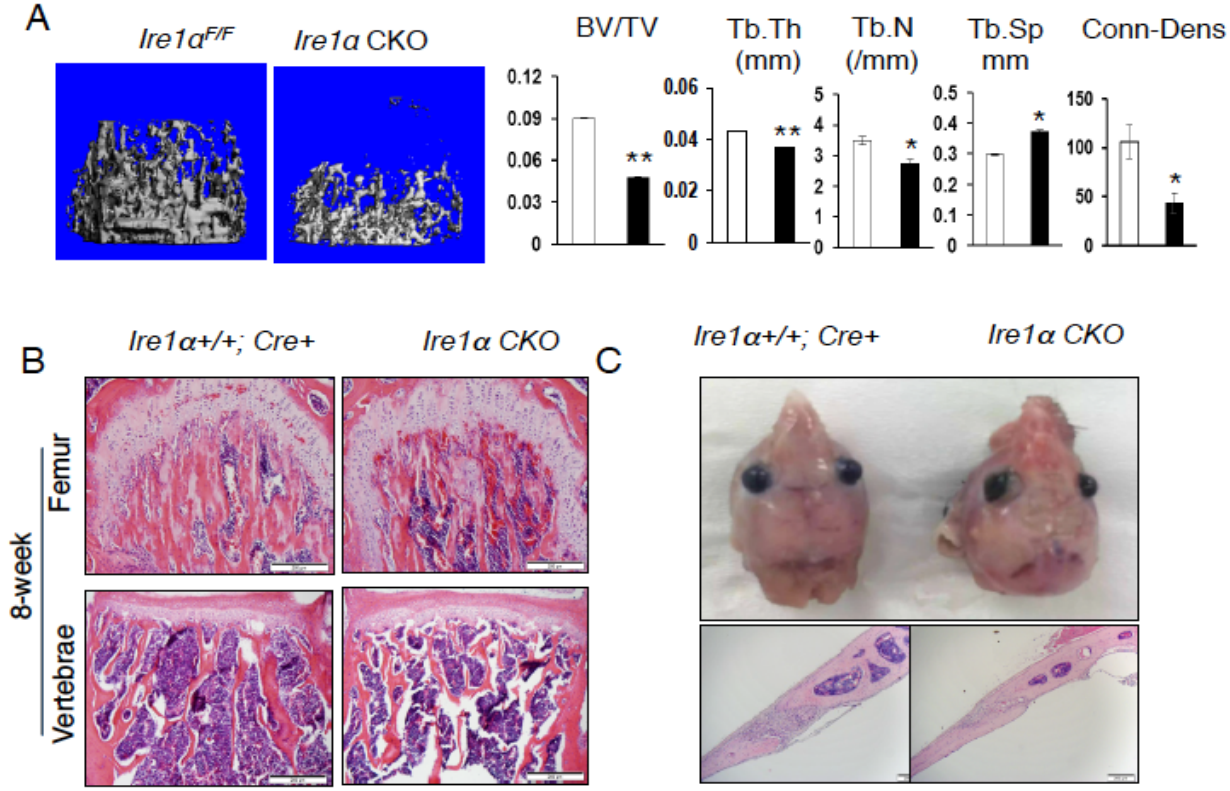

Figure 13. *Ire1a* CKO mice displayed a low bone density phenotype in long bone and skull.
(A) Femurs of 4-week-old female mice demonstrated that *Ire1α* CKO mice displayed significantly reduced three dimensional (3D) trabecular bone volume fraction (BV/TV), thickness (Tb. Th.), number (Tb. N.), and connectivity density (Conn-Dens), but significantly increased trabecular separation (Tb. Sp.), compared with corresponding control counterparts, i.e., $Ire1\alpha^{F/F}$ and $Ire1\alpha^{+/+}$; Cre^{+} littermates (B, C) H&E staining of femur, vertebrae and skull.

3.3.3 Delayed tooth eruption is due to slow bone remodeling

Having observed low bone density in *Ire1α* CKO mice, it was hypothesized that bone formation and bone resorption were affected in *Ire1α* CKO mice, which could possibly lead to delayed tooth eruption. According to bone remodeling theory for tooth eruption, the coordination of two opposing biological processes – bone formation/osteoblastogenesis and bone resorption/osteoclastogenesis contribute to tooth eruption. Thus I investigated the effects of osteoblastic deletion of IRE1α on both bone formation and resorption. *Calcein double labeling* revealed that Ire1α CKO mice had significantly reduced percentages of calcein double and total labeling/field, as well as significantly decreased distances between the double labeling in the skull (Figure 14A) and mandible (data not shown), compared with control animals. This demonstrates that osteoblast deficiency of IRE1α results in compromised dynamic bone formation *in vivo*. Further, qRT-PCR analyses showed that the mandibular bones (Figure 14B) of 8-week-old female Ire1α CKO mice had significantly reduced mRNA expression of osteoblast genes, e.g., *Alp*, bone

sialoprotein *(Bsp), type I collagen (COL-1), Ocn, Opn* and *Dmp1,* compared with *Ire1α*$^{+/+}$*; Cre*$^{+}$ counterparts (Figure 14B). Taken together, the results demonstrate that the major driving force underlying reduced osteoblastogenesis in *Ire1α* CKO mice *in vivo* is compromised osteoblast differentiation in bones formed by intramembranous ossification (skull and mandible).

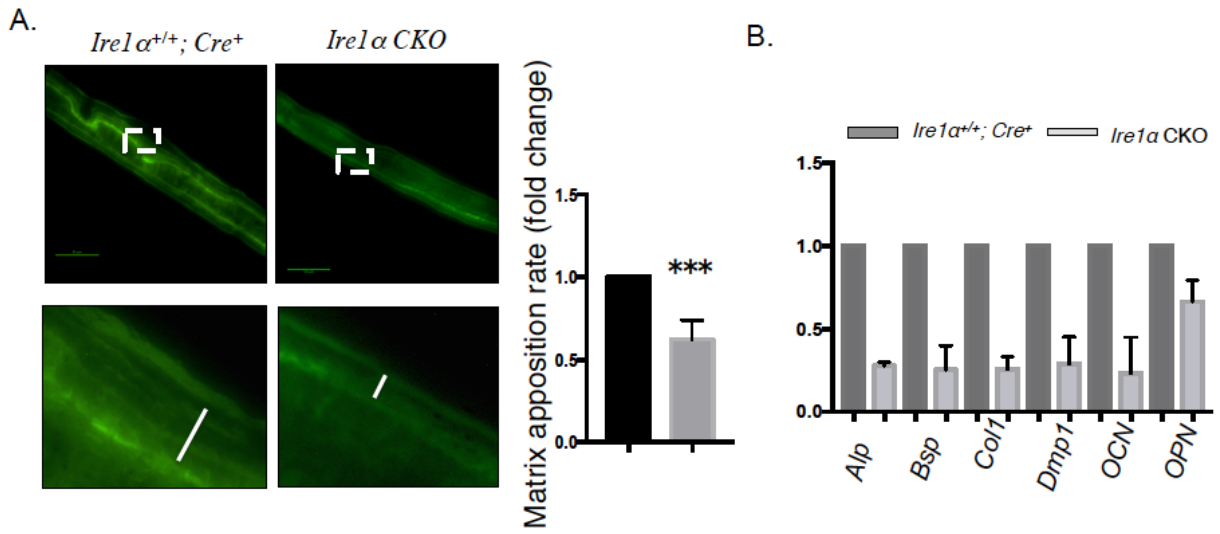

Figure 14. *Ire1a* CKO mice displayed reduced dynamic bone formation rate and osteoblast differentiation in skull and mandibles

(A) Calcein double labeling of the skull of 2-week-old female *Ire1α*$^{+/+}$*; Cre*$^{+}$ and *Ire1α* CKO mice (left panel). Statistical analysis of the relative fold change in matrix deposition rate were performed using five pairs of *Ire1α* CKO mice and control littermates (***$P < 0.001$), with the latter including both *Ire1α*$^{+/+}$*; Cre*$^{+}$ littermates ($n = 3$). The error bar represents ##### (B) qRT-PCR analyses showing mRNA expression of osteoblast markers in mandibular bone (without teeth) lysates of 8-week-old female *Ire1α*$^{+/+}$; *Cre*$^{+}$ and *Ire1α* CKO mice ($n = 3$; *$P < 0.05$). Error bars represent SE of the mean.

Osteoclastogenesis was determined via Tartrate-resistant acid phosphatase (TRAP) staining. TRAP staining revealed that *Ire1α* CKO mice had significantly fewer TRAP-positive osteoclasts on the bone surface compared with *Ire1α*$^{+/+}$; *Cre*$^{+}$ littermates (Figure 15A and B), demonstrating that osteoblast deficiency in IRE1α results in reduced osteoclastogenesis *in vivo*. The observation is consistent with the previous report that disrupting the IRE1α/XBP1s pathway in human osteoblast lineage compromised their capacity to direct osteoclast formation in vitro (Xu et al., 2012).

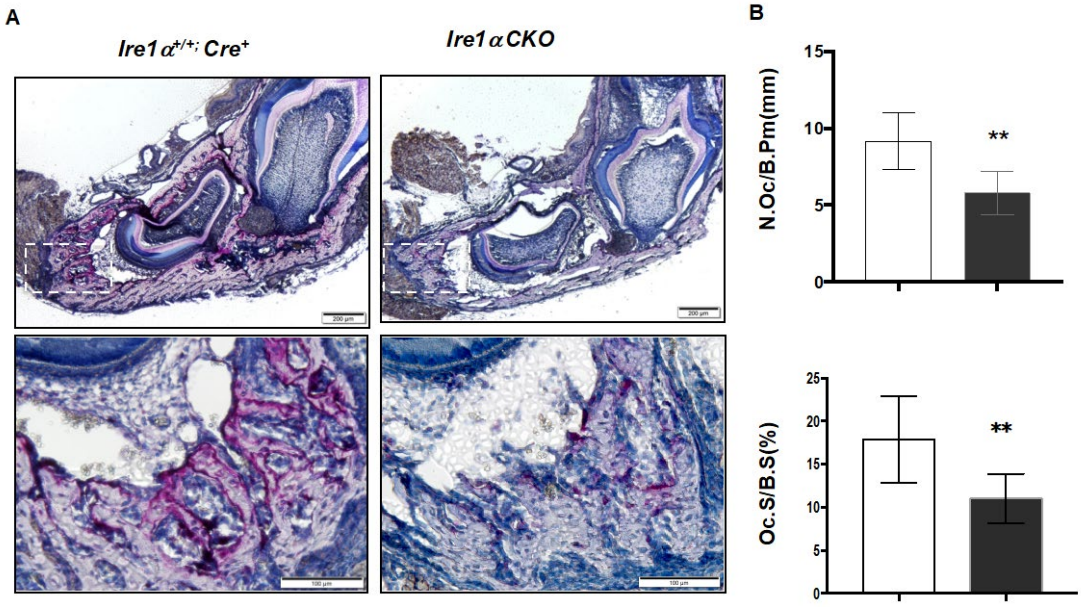

Figure 15. Osteoclastogenesis is compromised in Ire1α CKO mice mandibles.

(A) Representative images of paraffin-embedded sections of mandibles stained for TRAP activity. TRAP-positive cells representing active osteoclast are stained red. Enlargement of representative area of the alveolar bone in the mandible were shown in lower panel. Scale bars: upper panel (200μm); lower panel (100μm). (B) Number of TRAP-positive osteoclasts per millimeter bone parameter (N.Oc/B.Pm; number per millimeter) and the surface of osteoclasts relative to the bone surface (Oc.S/B.S; percentage) were

determined in the dental alveolar bone of TRAP-stained mandibles of 14-day-old *Ire1α*$^{+/+}$; *Cre*$^{+}$ and *Ire1α* CKO mice ($n = 3$; $^{**}P < 0.01$.) Error bars represent SE of the mean.

3.4 DISCUSSION

I demonstrated for the first time that ER stress transducer IRE1α is an essential regulator for tooth eruption during postnatal tooth development. in the *Ire1α* CKO mice, displayed low bone mineral density in their long bones compared with control littermates (Figure 13A and B). This observation prompted me to further investigated bone formation and bone resorption in bones formed via intramembranous ossification. Further, slow bone remodeling was found in in *Ire1α* CKO mice mandibular bones, evidenced by compromised bone formation (via calcein double labeling, and qRT-PCR analysis) and bone resorption (via TRAP staining), in *Ire1α* CKO mice skull and mandibular bones. Taken together, these results demonstrated that the osteopenia in *Ire1α* CKO mice is due to slow bone turnover and revealed the critical roles of osteoblast IRE1α in controlling both osteoblastogenesis and osteoclastogenesis. Thus the delayed tooth eruption of *Ire1α*CKO mice was due to defective metabolic process of the bone, where both bone formation and bone resorption were compromised.

The lack of an intact function of IRE1α/XBP1 signaling in osteoblast and dental mesenchyme leads to multiple pathological consequences involving both bone formation defects and delayed tooth eruption. It has been shown that osteoclast-mediated alveolar bone resorption is essential for timely tooth eruption (Okaji et al., 2003). The receptor activator of nuclear factor-kappa B ligand (RANKL) is an ultimate common regulator for osteoclast differentiation and

activity (Boyle et al., 2003). Dental follicle cells and osteoblasts are known local resources for RANKL during tooth eruption (Liu et al., 2005). β-catenin has been reported to repress postnatal bone remodeling via repressing RANKL gene expression. Despite the reduced protein expression of beta-catenin in the IRE1α-deficient mice, these mice nevertheless still experienced delayed tooth eruption. Thus, I suspected that there are additional molecular mechanisms downstream of IRE1α/XBP1s signaling underlying the delayed tooth eruption in the absence of IRE1α. Dr. Ouyang's lab previously reported that XBP1s controls RANKL gene and protein expression in human osteoblast lineage cells (Xu et al., 2012). Since Osx is expressed in odontoblasts, alveolar bone osteoblasts and dental follicle cells (Chen et al., 2009), it would be important to determine whether there exists biochemical and/or functional linkages between the IRE1α/XBP1s pathway and the RANKL signaling in regulating adequate tooth eruption. Such investigations could help to identify novel drug targets for managing deregulated tooth eruption in humans. Further investigation is needed to determine the molecular mechanisms by which the IRE1α/XBP1s pathway controls tooth eruption and bone formation.

3.5 CONCLUSION

The IRE1α /Xbp1s signaling axis is important for bone remodeling and tooth eruption. Thus the delayed tooth eruption of *Ire1α*CKO mice was due to defective metabolic process of the bone, where both bone formation and bone resorption are compromised.

3.6 ACKNOWLEDGEMENTS

This study was supported by NIH/NCI (RO1DE017439, RO1CA182418 and R21CA161150 to H.J.O.), start-up funds from the University of Pittsburgh School of Dental Medicine, School of Medicine, and the Office of Senior Vice Chancellor for the Health Sciences (H.J.O.). I am thankful for Lyudmila Lukashova for the Micro-CT scanning of femurs.

4.0 SPECIFIC AIM 3: THE ASSOCIATION BETWEEN *ERN1* AND *XBP1* POLYMORPHISMS AND TOOTH ERUPTION, CARIES AND BONE PHENOTYPES

4.1 INTRODUCTION

Our work in genetic knockout mice suggests that the IRE1α/XBP1 pathway is important for mineralized tissues formation, with roles in bone formation and remodeling and tooth eruption. Specifically, mice with the *Ern1* knocked out in *Osterix*-positive cells showed delayed tooth eruption, skeletal and dental morphological differences, and low bone mineral density (BMD). Given the biological functions of IRE1α/XBP1 in mineralized tissue development, I asked the question whether human genetic variants in *ERN1* and *XBP1* influence dental and bone phenotypes. Therefore, Chaters 4-7 are dedicated to testing the central hypothesis that **genetic variants at the *ERN1* and *XBP1* loci are associated tooth eruption (Chapter 5), dental caries (Chapter 6), and bone phenotypes (Chapter 7),** by employing an ***in silico* candidate gene approach**. In this chapter (Chapter 4) I provide general introductions of the aims, rationale and methods for the analyses. Descriptions of the study design, sample recruiting, genotyping and analysis methods common to all phenotypes are described in the Chapter 4 **Overview of Methods** section. Methods details and results that are specific to each phenotype are presented in the following chapters where tooth eruption, dental caries, and bone phenotypes are addressed, accordingly.

Chapters 5 and 6 focus on tooth eruption and caries phenotypes, respectively. The hypothesis is **that common and low-frequency variants at the *ERN1* and *XBP1* loci are associated with tooth eruption and caries phenotypes.** To address this hypothesis, three main

testing strategies were employed: (1) Investigating the association between ***common coding*** variants in *ERN1* and *XBP1* genes with tooth eruption and caries phenotypes (2) Examining the association between ***common variants within the genomic context*** (500kb up- and downstream) of *ERN1 and XBP1* with tooth eruption and caries phenotypes, and (3) Examining the association between ***low-frequency coding variants in aggregate*** in *ERN1* and *XBP1* gene and tooth eruption and caries phenotypes. In Chapter 7, I describe my investigation of the hypothesis that ***common variants*** at the *ERN1* and *XBP1* loci are associated with bone phenotypes, by examining common variants within the genomic context (500kb up- and downstream) of *ERN1 and XBP1.* Note: For Chapter 7, common and low-frequency coding variants were not tested for bone phenotypes due to lack of such genetic data (exome panel) in the only cohort with bone data.

Rationale for each strategy**:** *The first strategy* for testing genetic association with *ERN1* and *XBP1* candidate genes focused on common coding variants (MAF>0.01). These are variants which alter IRE1α and XBP1 protein. *The second strategy* examined common variants within the genomic context of *ERN1* and *XBP1*, including the 500kB flanking regions on either side of the genes because of the potential cis-acting regulatory role of variants in close physical proximity. This strategy allows me to identify possible causal variants in the genomic context of candidate gene, but does not tell me which SNP is causal. In *the third strategy* I interrogated low-frequency coding variants, which I defined as variants with MAF <0.01, under the hypothesis that these low-frequency coding variants, in aggregate, could explain additional trait variance in timing of tooth eruption/caries susceptibility seen in population.

Structure of testing strategies. Figure 16 depicts the testing strategies for each phenotype and which cohorts are included in the analysis. The presentation of the results for each

phenotype, in turn, will be similarly structured in the following Chapters, addressing the following testing strategies:

1. Common-coding variants in *ERN1* and *XBP1* (Tooth eruption, caries phenotypes)
2. Common variants in the genomic context of *ERN1* and *XBP1* (Tooth eruption, caries and bone phenotypes)
3. Low-frequency coding variants in *ERN1* and *XBP1* (Tooth eruption, caries phenotypes)

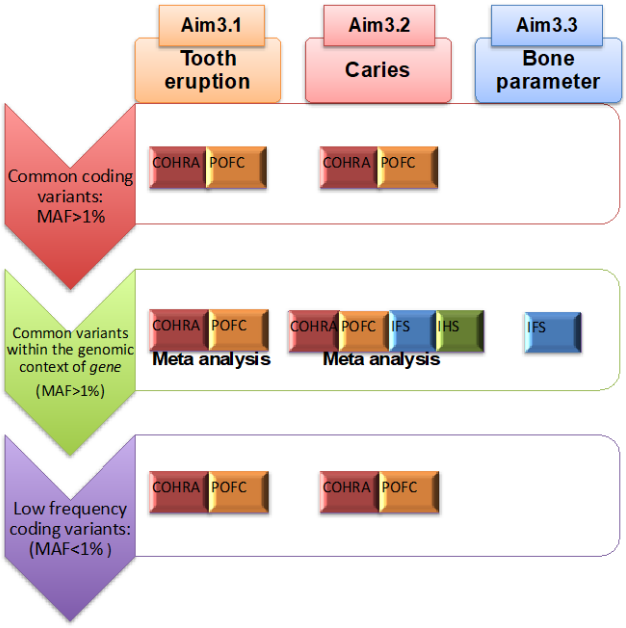

Figure 16. The testing strategies for each phenotype and cohorts included.

Up to three different testing strategies were employed to investigate each phenotype. For each analysis strategy, the cohorts included are listed in color-coded rectangles: COHRA (red), IFS (blue), IHS (green), POFC (orange). The details of the cohorts will be described below.

4.2 OVERVIEW OF METHODS

4.2.1 Study Cohorts

Participants from four cohorts were used to pursue candidate gene analyses: The Center for Oral Health Research in Appalachia (COHRA), The Pittsburgh Orofacial Clefting (POFC), The Iowa Fluoride Study (IFS) and Iowa Head Start (IHS) Study. To control for population stratification, analyses were limited to self-identified, non-Hispanic whites. The total sample size for each cohort may be different from the samples used in the analysis, because for each phenotype I used a subset of the total sample size. All study protocols were approved by the Institutional Review Boards of the pertinent Universities.

Center for Oral Health Research in Appalachia (COHRA) (N = 2304)

The Center for Oral Health Research in Appalachia (COHRA) cohort was a collaborative initiative between University of Pittsburgh, and West Virginia University to investigate factors (genetics, environmental, microbiological, and epidemiological) contributing to oral health disease and oral health disparities in Appalachia (Polk et al., 2008). Participants were recruited from rural and urban Appalachian communities in West Virginia and Western Pennsylvania using a household based recruitment protocol, which required a minimum of one biological parent-child pair. All adults gave written informed consent. Dental phenotypes (total teeth number, dental caries indices) were determined by intra-oral examination by licensed dentists and/or dental hygienists. DNA was extracted from blood, buccal swab, mouthwash, and saliva samples.

Iowa Head Start Study (IHS) (N = 162)

The Iowa Head Start (IHS) study, recruited participants from a federally funded child development program for low-income children aged 3 to 5 years old (Slayton et al., 2005) who were enrolled in Head Start. Dental examinations for each participant were conducted by licensed dentists. DNA was extracted via buccal or saliva samples taken in Oragene kits (DNA Genotek).

The Iowa Fluoride Study (IFS) (N = 399)

The Iowa Fluoride Study (IFS) is a longitudinal study of children designed to assess the relationship between fluoride exposures from both dietary and non-dietary sources and to associate longitudinal fluoride exposures with dental fluorosis and dental caries. IFS recruited new mothers and newborns from eight Iowa postpartum wards and followed their offspring from adult to childhood (Wang, Willing, et al., 2012). Dental assessments were performed for children between the ages of 4-6, during field examinations by trained dentists. DNA was extracted from blood, buccal swab, or saliva samples.

The Pittsburgh Orofacial Clefting (POFC) (N = 1960)

The Pittsburgh Orofacial Clefting (POFC) study was designed to identify genes involved in nonsyndromic orofacial clefts in a variety of populations worldwide (Weinberg et al., 2006). Participants in POFC included affected cleft cases, unaffected relatives of cases, and controls. The number of total primary/permanent teeth present and caries phenotypes were assessed by intra-oral examination. Informed consent was obtained from all participants, and Institutional Review Board approval was obtained locally and by the University of Pittsburgh and University of Iowa.

4.2.2 Genotyping

Genotyping for common variants. Genotyping for COHRA, IFS, IHS was performed as part of the GENEVA consortium by the Johns Hopkins University Center for Inherited Disease Research (CIDR) (www.cidr.jhmi.edu) using the Illumina Human610-Quadv1_B BeadChip (Illumina, San Diego, CA, USA) and the Illumina Infinium II assay protocol. Quality control procedures were performed as previously described (Laurie et al, 2010). Briefly, DNA samples with call rates < 85%, SNPs with more than 1 HapMap replicate error, more than a 2% (autosomal) or 10% (X) difference in call rate between genders, more than 1.8% male AB frequency (X), or more than a 7% (autosomal) or 5% (XY) difference in AB frequency were dropped. The GENEVA Coordinating Center performed genotype imputation with the HapMap Phase III reference panel using BEAGLE software (Browning and Browning, 2009). All participants provided verbal assent with parental written consent, and all study protocols were approved by the pertinent Institutional Review Boards at the University of Pittsburgh and West Virginia University.

Genotyping for the exome panel. Exome variants were genotyped on the exome chip of COHRA samples of European ancestry, as a follow-up to the GWAS genotyping. Briefly, samples were genotyped for 238,028 SNPs using the Infinium Exome-24 BeadChip, by the Center for Inherited Disease Research (CIDR). ***Quality control*** included CIDR technical filters and QC at the sample- and variant-level. Sample-level QC included interrogating samples for missing call rate (missing data per person), genetic sex, chromosomal anomalies, relatedness among participants and batch effects. Variant-level QC included Mendelian errors, missing call rate (missing data per SNP), and Hardy-Weinberg equilibrium.

Genotyping for POFC. Samples were genotyped for approximately 580,000 SNPs using an Illumina HumanCore+Exome array by the CIDR at Johns Hopkins University. Data quality assurance and data cleaning were implemented cooperatively with the CIDR Genetics Coordinating Center (GCC) at the University of Washington (Laurie et al., 2010). Imputation was performed using IMPUTE2 (Lambert et al., 2013) and phase 3 of the 1000 Genomes Project as the reference panel. Accuracy of imputation was determined by masked variant analysis, which revealed high-quality imputation; mean concordance was 0.960 for SNPs with MAF ≥ 0.05 and 0.995 for SNPs with MAF < 0.05. Only SNPs whose "most-likely" genotype probability was > 0.5 were included in statistical analysis. Imputed SNPs out of HWE in European controls were excluded from subsequent analyses.

4.2.3 Statistical analysis

Separate statistical analyses were used for the three strategies for testing genetic association: (1) examination of common coding variants (MAF>1%), (2) examination of common variants within the genomic context (500kb up and downstream) of *ERN1* and *XBP1*, and (3) examination of low-frequency coding variants are described as follows:

(1) **Common coding variants** were genotyped in COHRA and POFC as part of the Exome panel, as described above. Only coding variants with MAF > 1% were tested individually due to insufficient statistical power for testing rarer variants. Variance components modeling were implemented in RVTESTS (Zhan et al., 2016) while adjusting for pertinent covariates. I tested one missense SNP in *ERN1* and one in *XBP1*, respectively:

ERN1: : c.1421T>G (rs186305118) leading to p.Leu474Arg

XBP1: c.19G>A(rs5762809) leading to p.Ala7Thr

(2) **Common variants within the genomic context of ERN1 and XBP1**

All available common SNPs (MAF>1%) within the introns of the candidate genes in addition to 500kB flanking regions on either side of the genes were included because of their potential regulatory roles. Two main software programs, PLINK1.9 (Purcell et al., 2007) and EMMAX (Kang et al., 2010) were used to test the common variants. EMMAX implemented a variance components modeling framework to account for biological relationships among participants, as well as any population structure (Kang et al., 2010), and was used for COHRA and POFC cohorts, which include related individuals. For IFS and IHS cohorts, linear regression analysis was implemented in PLINK1.9, while adjusting for pertinent covariates and principal components (PCs) of ancestry. PCs ancestry were generated by principal components analysis using the R package SNPRelate following the approach introduced by Patterson et al (Patterson et al., 2006).

Multiple comparison adjustment. A total of 1503 and 1809 common SNPs (i.e., MAF > 1%) were tested for the *ERN1* and *XBP1* gene regions, respectively. To adjust for multiple comparisons, the Li and Ji (Li and Ji, 2005) method was used to determine the effective number of independent tests. I determine that the effective number of independent tests were 228 for *ERN1* and 292 for *XBP1*. A multiple testing–adjusted significance threshold was computed by setting α to 0.05 divided by the effective number of independent tests, thus, the locus-wise threshold for significance given the effective number of independent tests was p-value<0.00022 for *ERN1*, and P<0.00017 for *XBP1*.

Meta-analysis. Multiple cohorts with requisite data were available for investigating potential common regulatory variants near *ERN1* and *XBP1* with tooth eruption and dental caries phenotypes (Figure 16). In order to combine the evidence of genetic association across these cohorts, meta-analysis was performed using Stouffer's p-value-based method as implemented in METAL software (Willer et al., 2010). The benefits of meta-analysis compared to mega-analysis (i.e., combining the participant-level data across cohorts and analyzing altogether) is that meta-analysis has nearly as good statistical power, but is comparatively safer for guarding against spurious associations due to confounding by population structure or genotyping artifacts that differ across studies.

Results annotation. Results were visualized by utilizing LocusZoom66 (hg19), where association signals for candidate genes were plotted with 500kB flanking regions. Lead SNPs (i.e., the SNP with the smallest p value) in the candidate gene regions were queried using HaploReg for evidence of functional variation, including evidence of promoter and enhancer histone marks, DNAse hypersensitivity, and eQTL information. SNPs in high LD ($r^2 > 0.8$) with the lead SNPs were also queried in HaploReg. Literature searches were performed for lead SNPs and nearby genes for corroborating information about their biological roles in tooth and bone development.

(3) Low-frequency coding variants association analysis

Low-frequency coding variants genotyped by the Exome Chip with minor allele frequencies less than 1% were tested in a gene-based framework. The gene-based tests were implemented in RVTESTS (Zhan et al., 2016). The gene-based tests were developed because single SNP-based association analyses are underpowered for low-frequency variants, due to the low number of participants carrying the minor allele of a specific locus. Hence, statistical analysis methods have been developed that aggregate variants by taking the total number of minor alleles

per gene into account (Li and Leal, 2008; Wu et al., 2011). The gene-based analysis includes the Combined Multivariate and Collapsing (CMC) test and the Sequence Kernel Association Test (SKAT). The CMC method is a burden test that collapses variants across specific regions (e.g., each the candidate genes) into a single score. The CMC test makes the assumption that the region has a large fraction of causal rare variants with the same direction of effect , thus I also utilized a second test, the SKAT method which can detect sets of variants with opposite effects. The first 2 PCs of ancestry were included as covariates to protect against confounding due to population structure, in addition to pertinent covariates such as sex and age. Since I only tested *ERN1* and *XBP1* genes for genetic association with each phenotype, p values less than 0.05 were considered significant.

4.2.4 Implementing these strategies to test phenotypes

The next three chapters describe the application of these analysis strategies to detect genetic associations with different categories of genetic variants, (1) common coding variants, (2) common possible cis-acting regulatory variants and (3) low-frequency coding variants. Various cohorts were used to study tooth eruption, caries, and bone phenotypes, but not all of them have all the phenotypes available for testing, given differences in phenotype data collection and ages of the sample. Moreover, genetic data in each cohort were collected differently. Given the differences in what phenotype and genetic data were collected, only some cohorts and some analysis strategies were used to investigate the genetic architecture of each phenotype. All of these analyses/cohorts are intended to explore my over-reaching hypothesis that genetic variants at the *ERN1* and *XBP1* loci are associated tooth eruption (Chapter 5), dental caries (Chapter 6), and bone phenotypes (Chapter 7).

5.0 SPECIFIC AIM 3.1: THE ASSOCIATION BETWEEN *ERN1* AND *XBP1* POLYMORPHISMS AND TOOTH ERUPTION PHENOTYPES

5.1 INTRODUCTION

Our *in vivo* data demonstrated that mouse with the *ERN1* gene knocked out, and subsequent loss of function of the downstream target XBP1 in *Osterix*-positive cells, showed delayed tooth eruption. This observation led me to hypothesize that variants at these two genetic loci may influence tooth eruption phenotypes in humans.

Identifying genetic variants for tooth eurption is of clinical significance because proper timing and sequence of tooth eruption has implications for dental health. For example, timing of tooth eruption influences the colonizing of microbes on the tooth surface, and host response to the microbes, thus delayed/accelerated tooth eruption could predispose the host to periodontal disease and caries (Nibali, 2018). Sequential and timely eruption of teeth is also critical to the timing of orthodontic treatment and the selection of treatment modality (Suri et al., 2004).

In the human dentition, variation in the timing of tooth eruption has been found to be under strong genetic control (Townsend et al., 2012). GWAS studies have identified genetic variants influencing eruption of both primary and permanent teeth. Loci associated with the timing of primary tooth eruption have also been found to be associated with height and craniofacial distances (Fatemifar et al., 2013; Geller et al., 2011). Published GWAS on permanent tooth eruption have discovered four loci, two of which had previously been associated with primary tooth eruption, suggesting an overlap between the factors controlling primary and permanent teeth eruption (Geller et al., 2011). Variants in *ERN1* and *XBP1* have not been identified by these GWAS. This

is unsurprising since only one GWAS has been performed for primary and permanent tooth eruption, respectively. I expect that any particular GWAS study will identify only a fraction of the associated variants, and that many true associations will go undetected. *ERN1 and XBP1* could be among these loci.

In contrast to GWAS, a candidate gene approach tests only variants based on the hypothesized or known biological functions of genes chosen *a priori*, which is suitable for my study given the evidence from the mouse model. Integrating mouse and human genetics has been successful in discovering candidate genes for tooth development, regardless of the differences between mice and human dentition. For example, various tooth eruption genes that has been discovered through functional studies have been corroborated by GWAS results (Nibali, 2018), for instance, *BMP4, EDA* and *PTH1R* (Fatemifar et al., 2013; Ono et al.; Philbrick et al., 1998; Yamaguchi et al., 2011).

Guided by the delayed tooth eruption phenotypes of the mouse model, I hypothesize that common and/or low-frequency variants at *ERN1* and *XBP1* loci are associated with tooth eruption phenotype in humans. To address this hypothesis, I conducted analyses to explore three types of variants, common coding, cis-acting regulatory, and low-frequency coding variants at the *ERN1* and *XBP1* loci.

5.2 METHODS

5.2.1 Sample and study design

Participants were Caucasian, Non-Hispanic children aged 0-14.9 from 2 studies: the Center for

Oral Health Research in Appalachia (COHRA) and the Pittsburgh Orofacial Clefting (POFC) as described in Chapter 4. Samples sizes for three tooth eruption phenotypes in each cohorts are summarized in the Table1.

Table 1. Basic characteristics of the study populations

	COHRA1			POFC			Total
	N	Female sex(%)	Age range (years)	N	Female sex(%)	Age range (year)	N
Time of first tooth eruption (units)	421	48.7	0.8-10.9	-	-	-	421
Primary total tooth number	287	47.7	0.84-4	134	47.0	0-4	421
Permanent total tooth number	500	50.1	5.02-14.9	666	47.0	6-14	1166

5.2.2 Phenotype collection and variable generation

Two separate measures of primary tooth development were collected: (1) time to first tooth eruption and (2) number of primary teeth. Time to first tooth eruption was analyzed in COHRA1 children aged 0-11 years. This variable was derived by interviewing parents whose children were younger than 11 years of age, "At what age did your child first get a tooth?" Number of primary teeth was measured in children aged 0-4 years by counting the number of primary teeth present via intra-oral examination. Number of permenant teeth was determined in children aged 5-14 years by counting the number of permenant teeth present.

5.2.3 Statistical analysis

An overview of the three testing strategies, including SNPs tested, software, statistical methods, and p-value thresholds were described in Chapter 4 Methods section.

(1) Examination of common coding variants (MAF>1%)

I tested the association between SNPs in the coding regions of *ERN1* and *XBP1* with three tooth eruption phenotypes. **Common coding variants** were genotyped in COHRA and POFC as part of the Exome panel, as described above. The common (MAF**>1%)** coding SNPs from both COHRA and POFC exome panel were summarized in Table2.

Table 2. Common coding SNPs genotyped from the Exome panel

Gene	Function	SNP	Cohorts with genotyping available
ERN1	**Missense**	**rs186305118**	**COHRA, POFC**
	Synonymous	rs196912	POFC
	Synonymous	rs75995183	POFC
	Synonymous	rs55653398	POFC
XBP1	Synonymous	rs2228260	POFC
	Missense	**rs5762809**	**COHRA, POFC**

The scope of my study was to test coding variants that alter the protein, thus I focused on common **missense SNPs** in single gene test. Synonymous SNPs may be regulatory thus they were tested in the "genomic context" strategy which will be discussed later. I tested one missense SNP in *ERN1* and one in *XBP1*, respectively:

ERN1: : c.1421T>G (rs186305118) leading to p.Leu474Arg

XBP1: c.19G>A(rs5762809) leading to p.Ala7Thr

For the COHRA exome panel, single SNP-based association analyses were implemented in RVTESTS (Zhan et al., 2016) using variance components modeling while adjusting for covariates. For POFC, common coding variants in *ERN1* and *XBP1* were tested for genetic association using variance-components models as implemented by EMMAX (Kang et al., 2010). All analysis was adjusted for pertinent covariates (such as age, sex, cleft type) and kinship (i.e., both the biological relatedness and population structure in the sample). Given the limited scope of the analysis of common coding variants (up to two variants tested), p-values less than 0.05 considered statistically significant.

(2) Examination of common variants within the genomic context of *ERN1 and XBP1* loci.

Common variants 500kb up- and downstream of *ERN1* and *XBP1* were tested for genetic association using variance-components models as implemented by EMMAX (Kang et al., 2010) for COHRA1 and POFC cohorts while adjusting for pertinent covariates (age, sex) and kinship (i.e., both the biological relatedness and population structure in the sample). For IFS, which did not include related individuals, linear regression was used while adjusting for age, sex, and the first two PCs of ancestry via PLINK1.9. ***Meta-analysis.*** Meta-analysis was performed using Stouffer's p-value-based meta-analysis as implemented in METAL software (Willer et al., 2010). Meta-analysis included combining association results from COHRA and POFC for the number of permanent teeth, and the number of primary teeth.

(3) Examination of low-frequency variants:

Two statistical tests were implemented: Combined and Multivariate Collapsing (CMC) and Sequence Kernel Association Test (SKAT). The threshold for inclusion in the gene-based

analysis of low-free variants was 1%. The actual MAFs of SNPs meeting this criterion ranged from 0.03% -0.96% in POFC, and from 0.24%-0.28% in COHRA.

5.2.4 Sample distribution and covariates modeling

To describe the distribution of tooth eruption phenotypes and to test the effect of covariates, the potential demographic predictors of "number of teeth" and "time of first tooth eruption" were explored using the R statistical analysis environment (R Foundation for Statistical Computing, Vienna, Austria). Linear regression was used to determine the association between tooth eruption traits and covariates.

5.3 RESULTS

5.3.1 Trait distribution and covariates

Distributions of "number of teeth" phenotypes and "Time of first tooth eruption" are shown in Figure 17. Covariates included in each cohorts and their associations with trait outcomes are shown in Table 3.

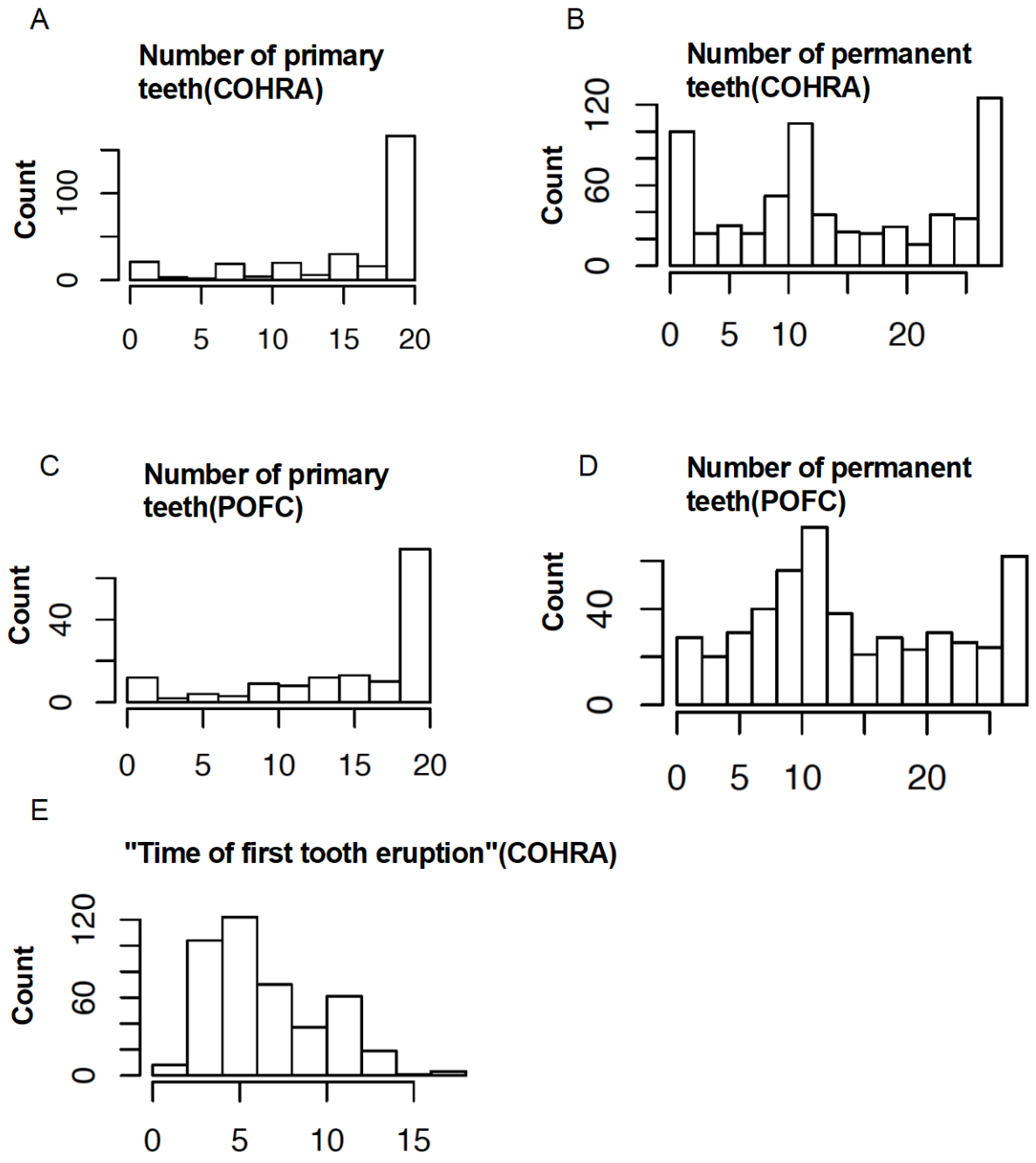

Figure 17. Distribution of "number of teeth" phenotypes and "Time of first tooth eruption" in COHRA and POFC cohorts

Covariates modeling. Regression beta coefficients (SE) and p-values for the tests of association between demographic and cleft history variables and tooth eruption traits are shown in Table 3. As expected, age was significantly associated with both "Number of Primary teeth" and "Number of Permanent teeth", in COHRA and POFC cohorts. Sex was significantly associated with Number of Primary teeth in COHRA, but not in POFC cohort. Because participants in POFC included affected cleft cases, unaffected relatives of cases, and controls, cleft status was included as covariate. Cleft status was significantly associated with "Number of Permanent teeth" but not "Number of Primary teeth" in POFC cohort. Sex was not associated with "Time of first tooth eruption"

Table 3. Association of Covariates with Tooth Eruption Traits in COHRA and POFC

Variable	POFC			COHRA		
	Beta	**SE**	**P**	**Beta**	**SE**	**P**
Number of Permanent teeth						
Age	2.660	0.070	3.0E-140	3.059	0.049	5.4E-278
Sex	0.550	0.380	1.4E-01	1.264	0.282	8.7E-06
Cleft status	-1.920	0.400	2.4E-06	NA[1]	NA[1]	NA[1]
Number of Primary teeth						
Age	3.203	0.301	9.9E-20	2.829	0.368	2.4E-13
Sex	-0.771	0.724	2.9E-01	0.444	0.653	5.0E-01
Cleft status	-0.562	0.730	4.4E-01	NA[1]	NA[1]	NA[1]
Time of first tooth eruption						
Sex	NA[2]	NA[2]	NA[2]	0.127	0.316	6.9E-01

[1] The phenotype (Cleft status) was not collected for COHRA, IFS and IHS;

[2] "Time of first tooth eruption" was not collected for POFC cohort.

5.3.2 Examination of common coding variants of ERN1 and XBP1

I did not detect associations between missense SNPs in *ERN1:* c.1421T>G, leading to p.Leu474Arg (rs186305118) and *XBP1*: c.19G>A(rs5762809) leading to p.Ala7Thr, and tooth eruption phenotypes assessed in the primary dentition (***"number of primary teeth", "time of first tooth eruption"),*** and permanent dentition ***("number of permanent teeth***"), in COHRA and POFC cohorts (p>0.05 for all). Note: not all variants were available for testing in both cohort because of the >1% MAF cut-off (Table 4).

Table 4. Common coding variants tested for "tooth eruption phenotypes"

Phenotypes	SNP	COHRA		POFC	
		N	MAF	N	MAF
Time of first tooth eruption	ERN1:rs186305118	321	0.016	NA[1]	NA[1]
	XBP1:rs5762809	321	0.168	NA[1]	NA[1]
Primary total tooth number	ERN1:rs186305118	NA[2]	NA[2]	NA[2]	NA[2]
	XBP1:rs5762809	181	0.141	130	0.134
Permanent total tooth number	ERN1:rs186305118	582	0.018	NA[2]	NA[2]
	XBP1:rs5762809	582	0.154	479	0.126

[1] "Timing of first tooth eruption" was not collected in the POFC cohort

[2] MAF for this variant is too low (<0.01) in this sample

5.3.3 Examination of common variants in the genomic context of ERN1 and XBP1.

Top hits for association analysis in this section are summarized in Table 5, followed by detailed results for each trait.

Table 5. Top hits for common variants in the genomic context of ERN1 and XBP1 and "tooth eruption phenotypes"

Phenotypes	SNP (minor allele)	COHRA N = 421			POFC N = 0 [1]			META N = 421
		MAF	beta	P	MAF	beta	P	P
Time of first tooth eruption	ERN1:rs11655332(T)	0.31	-0.96	0.0081	NA[1]	NA[1]	NA [1]	NA[1]
	XBP1:rs4547624(C)	0.093	0.93	0.0062	NA[1]	NA[1]	NA[1]	NA[1]
Phenotypes	**SNP (minor allele)**	**COHRA N = 287**			**POFC N = 134**			**META N = 421**
Number of primary teeth	ERN1:rs56325317(A) *	0.027	3.86	0.0045	0.041	4.66	0.0148	0.0002*
	XBP1:rs76891380(A) *	0.011	7.96	0.0006	0.012	3.78	0.0685	0.0001*
	XBP1:rs55962108(A) *	0.011	7.96	0.0007	0.012	3.75	0.0707	0.0001*
Phenotypes	**SNP (minor allele)**	**COHRA N = 500**			**POFC N = 666**			**META N = 1166**
Number of permanent teeth	ERN1:rs12449561(G)	0.477	0.05	0.8276	0.5	0.85	0.0008	0.014
	XBP1:rs55676901(A)	0.012	4.21	0	0.025	0.63	0.425	0.0009

*SNPs that reached locus-wide significant association

[1] "Timing of first tooth eruption" was not collected in the POFC cohort

"Number of primary teeth". Meta analysis combining COHRA and POFC cohorts revealed a locus-wide significant association for the *ERN1* region between a variant located in the *ICAM* gene, which is downstream of *ERN1*, and **number of primary teeth** (rs56325317, p = 0.0002)(Figure 18A, Table 5). The minor allele A for this SNP is associated with a higher number of erupted primary teeth (adjusted for age) in both COHRA (3.86 more teeth per A allele, p=0.0045) and POFC (4.66 more teeth per A allele, p=0.0148). The SNP showed promoter and enhancer chromatin marks in many different cell types, including in bone-forming osteoblast

lineage cells and CD14+ monocytes, which are cells important for the bone remodeling process involved in tooth (Fujikawa et al., 1996), and it is in moderate LD ($r^2 = 0.46$) with an intronic SNP in the *ERN1* gene.

Meta-analysis for the *XBP1* region yielded locus-wide significant associations between two SNPs upstream of the *XBP1* gene with **number of primary teeth**: rs76891380 (minor allele A; p=0.0006, beta=7.96 in COHRA; p=0.0685, beta= 3.78 in POFC; and rs55962108 (minor allele A; p=0.0006, beta=7.96 in COHRA; p=0.0707, beta= 3.75 in POFC). The two SNPs are in high LD with each other (r^2 =0.87)(Figure 18D). The SNP rs76891380 is physically located in the *ZNRF3* gene and is an exonic synonymous SNP exhibiting chromatin features of promoters and enhancers in many different cell types, and is in a DNAse I hypersensitivity site in multiple tissues. Therefore, the exonic synonymous SNP could potentially be regulatory. Furthermore, synonymous SNPs, which historically have been considered as silent, more recently have been shown to potentially affect protein conformation and function, leading to altered disease susceptibilities. The second suggestive SNP, rs55962108, also exhibits chromatin features characteristic of promoters and enhancers in many different cell types, including in bone-forming osteoblast lineage cells and CD14+ monocytes. These associations were mainly driven by COHRA, (rs76891380, p=0.0006, beta=7.96 in COHRA; rs55962108, p=0.0006, beta=7.96 in COHRA). These two top SNPs showed suggestive associations in the POFC cohort, with p values of 0.06 and 0.07, and the same direction of effect (beta =3.78 and 3.75), respectively.

"Time of first tooth eruption". I found suggestive associations (p-value = 0.008) between *ERN1* gene locus rs11655332 (Figure 18B) with *"time of first tooth eruption"*. This locus has been found to show evidence of histone marks indicative of enhancer in multiple tissues.

Suggestive association was detected for *XBP1* gene region, and the lead SNP is rs4547624 (p-value =0.006) located upstream *XBP1,* in the *EMID1* gene (Figure 18E). This locus is in strong LD with a variant in known enhancer regions in several tissue types.

"Number of permanent teeth ". For *ERN1* locus, meta-analysis revealed a suggestive association between rs12449561, downstream of *ERN1, and* located in *PRR29* (p= 0.014) (Figure 18C). This locus exhibits features of enhancers in many different cell types, including osteoclast precursor Monocytes-CD14+ cells. A variant upstream of the *XBP1* gene, rs55676901, located in *EMID1*, was suggestively associated with **"**number of permanent teeth**"**) (Figure 18F)**.** Meta analysis yielded a p value of 0.0009 for this a variant, which was mainly driven by the statistical evidence from COHRA1 (p=4.98e-06). This locus exhibits features of promoters and enhancers in many different cell types, including osteoclast precursor Monocytes-CD14+ cells, DNAse I hypersensitivity site in multiple tissues, and numerous transcription factor-binding sites.

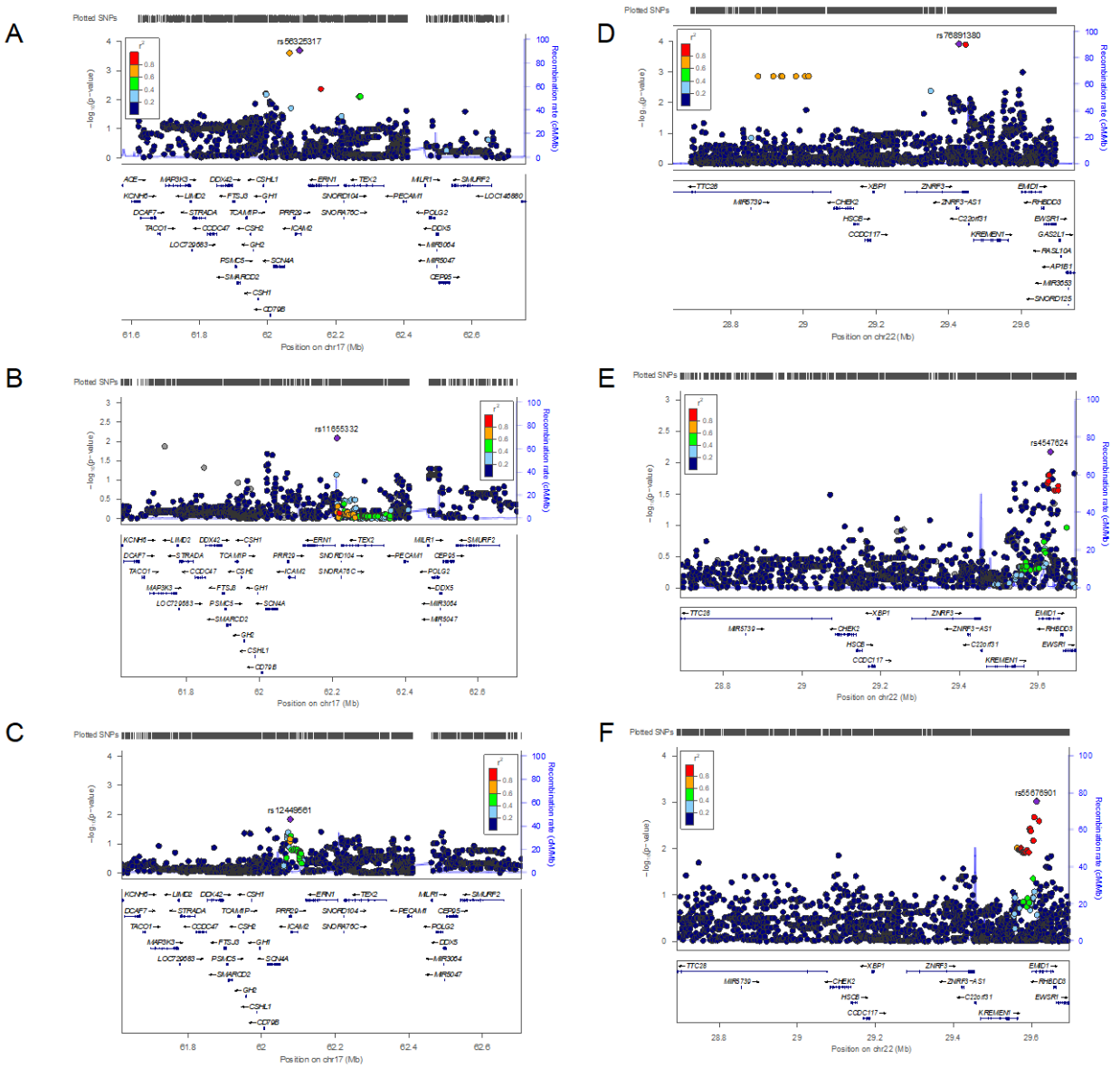

Figure 18. Plots of genetic association results for chr 17q23.3 near *ERN1* (A-C) and 22q12 near *XBP1* (D-F) associated with "number of primary teeth".

(A,D) and "number of permanent teeth" (C,F) in meta-analyses. B and E shows results for "first tooth eruption" in COHRA. Displayed are the recombination rates over the region and the association (left y-axis; log10-transformed p-values) for the analyzed SNPs. Positions of genes are shown below the plot.

5.3.4. Examination of low-frequency variants

I tested association for low-frequency variants in the *ERN1* loci, using two gene-based tests implemented in RVTESTS (Zhan et al., 2016). Both SKAT and CMC tests showed that low-frequency coding variants in the *ERN1* gene were not significantly associated with "number of primary teeth" (in both COHRA and POFC cohorts) nor "time of first tooth eruption" (in COHRA) (Table 6, $p>0.05$ for all). No significant association was found between low-frequency coding variants in *XBP1* and "Permanent total teeth number" in POFC cohort. Note: Less than two low-frequency coding variants were found in *XBP1* for "number of primary teeth" and "time of first tooth eruption", thus I couldn't perform aggregated test for them.

Table 6. Gene based association for tooth eruption phenotypes

Phenotypes	Gene	COHRA				POFC			
		Sample size	Number of variants	CMC *p*	SKAT Permutation *p*	Sample size	Number of variants	CMC *p*	SKAT Permutation *p*
Number of primary teeth	ERN1	181	3	0.712	0.773	130	4	0.388	0.621
	XBP1	NA	NA[1]	NA[1]	NA[1]	NA[1]	NA[1]	NA[1]	NA[1]
Number of permanent teeth	ERN1	582	3	0.571	0.293	479	9	0.637	0.477
	XBP1	NA	NA[1]	NA[1]	NA[1]	479	2	0.77	0.71
Time of first tooth eruption	ERN1	321	2	0.22	0.584	NA[2]	NA[2]	NA[2]	NA[2]
	XBP1	NA	NA[1]	NA[1]	NA[1]	NA[2]	NA[2]	NA[2]	NA[2]

[1]MAF for this variant is too low (<0.01) in these samples
[2] "Timing of first tooth eruption" was not collected in the POFC cohort

5.4 DISCUSSION

To address my hypothesis that variants in *ERN1* and *XBP1* are associated with tooth eruption phenotypes, I conducted analyses to explore three types of variants, (1) common coding variants in *ERN1* and *XBP1*, (2) common possible cis-acting regulatory variants near the candidate gene, and (3) low-frequency coding variants in *ERN1* and *XBP1*. Most of the associated SNPs identified were located in the regions nearby *ERN1* and *XBP1*, and are putative regulatory variants. The first mechanism to explain for these associations is that SNPs near *ERN1* and *XBP1* may regulate gene expression, and in turn impact the phenotypes. For example, the top hits associated with primary tooth number were rs76891380 (p=0.0001), an exonic synonymous SNP, and rs55962108 (p=0.0001; which is in high LD with rs76891380) located upstream of the *XBP1* gene, which exhibited features of promoters and enhancers in many different cell types, including in

bone-forming osteoblast lineage cells and CD14+ monocytes (cells important for tooth eruption).

Locus-wide significant association was revealed in meta-analysis for primary tooth number (rs56325317, p = 0.0002). The minor allele, A, for this SNP is associated with a higher number of erupted primary teeth in both COHRA and POFC (p=0.0045, beta=3.86 in COHRA, p=0.0148, beta= 4.66 in POFC). The variant is located in the *ICAM* gene and is in moderate LD (r^2=0.46) with a variant intronic to *ERN1*, rs76959113. One mechanism for association is that the SNP regulates *ERN1* gene expression, although this regulation was not tested in this study, and has not been reported in previous eQTL studies. Alternatively, the association may also be explained by another mechanism: instead of regulating *ERN1,* the variants may instead acting through other genes, e.g. the genes they are physically located in, *ICAM gene, which* encodes intercellular adhesion molecule-1, expressed in the junctional epithelium, a gingival tissue that is formed during tooth eruption, indicating its importance in tooth eruption. The associated SNPs (rs76891380 and rs55962108 for the *XBP1* region, and rs56325317 for *ERN1*) showed promoter and enhancer chromatin marks in many different cell types, including in bone-forming osteoblast lineage cells and CD14+ monocytes, which are cells important for the bone remodeling process involved in tooth.

Only suggestive associations were identified for "time of first tooth eruption". A limitation that may have reduced my ability to detect genetic associaiton was the fact that this phenotype was collected by interviewing the mothers whose children were less than 11 years old. This means that people with one phenotype (e.g., earlier tooth eruption or atypical tooth eruption) respond more accurately or systematically differently than people with a different phenotype. Thus the outcome of the phenotype may not be reflecting the true "age of first tooth eruption" for the children. This kind of noise of data (phenotype misclassification or measurement error) would bias the statistical

test toward the null hypothesis of no association. This would reduce statistical power to detect true associations leading to type II error, but would not lead to false positive results (type I error).

In summary, my study suggests an association between common possible cis-acting regulatory variants near the candidate gene of *ERN1* and *XBP1* and variation in the "time of tooth eruption" and "tooth number". Further investigations are needed to thoroughly understand how the variants nearby *ERN1* and *XBP1* regulate them. Taken together with my mice data, my findings demonstrated a possible role of IRE1α and XBP1 in regulating tooth eruption. This study provides insights into the genetic and molecular requirement for timely tooth eruption. Understanding the genetic contribution to normal variation of tooth eruption can facilitate understanding of pathological conditions with tooth eruption disturbances, such as delayed tooth eruption and tooth eruption failure, and in the long run, could help identify patient susceptibility to tooth eruption disturbances.

6.0 SPECIFIC AIM 3.2: ASSOCIATION BETWEEN COMMON AND LOW-FREQUENCY VARIANTS AT THE *ERN1* AND *XBP1* LOCI WITH DENTAL CARIES PHENOTYPES

6.1 INTRODUCTION

Dental caries is a multifactorial disease, and among the important factors influencing susceptibility to dental caries are the host genes that control enamel development (Opal et al., 2015; Shaffer et al., 2015) . ER stress genes have been found to be involved in the biological process of enamel secretion (Brookes et al., 2017). Enamel secreting cells, ameloblasts, are highly developed in ER and are potentially under ER stress during amelogenesis stage. The ER stress signaling pathway is activated during amelogenesis by increasing the volume of the ER to increase the handling capacity of the cell's secretory pathway. The IRE1/XBP1 pathway has been indicated to play a role in ameloblast development and enamel secretion, *in vitro*, in cell lines. IRE1 activation is important in secretory stage ameloblasts (Kubota et al., 2005), while *Xbp1* mRNA was expressed five times greater in secretory enamel organ cells compared to maturation stage enamel organ, indicating that IRE1/XBP1 activation and the triggering of ER stress response are important events in the secretory ameloblasts (Tsuchiya et al., 2008). Moreover, the activation of ER stress accompanied by an increase in ER stress markers, including *xbp1* has been implicated in Amelogensis Imperfecta, a genetic condition characterized by enamel biomineralization defects. (Brookes et al., 2017; Liu et al., 2015). *XBP1* is also involved in fluorosis, characterized by enamel hypomineralization (Brookes et al., 2017; Liu et al., 2015) .

I observed irregularity of the ameloblast cell layers, specifically, lacking of homogeneity and continuity among IRE1α *CKO mice* molars at D5 and D14. This preliminary observation in addition to the published evidence on the role of IRE1/XBP1 in amelogenesis led me to hypothesize that variants at the *ERN1* and *XBP1* loci may contribute to caries susceptibility. To address this hypothesis, I investigated the association between common and low-frequency coding variants in *ERN1* and *XBP1*, and potential cis-acting common regulatory variants in the genomic context (i.e., the 500kb flanking region) of *ERN1 and XBP1* with caries phenotypes.

6.2 METHODS

6.2.1 Sample and study design.

Participants for the analysis of dental caries in the primary dentition were Caucasian, Non-Hispanic children ages 1 to 12 years from four cohorts: COHRA1 (N=1037), IHS (N = 162), IFS (N = 399) and POFC (N=561). Participants for the analysis of dental caries in the permanent dentition (17 to 59 years) were available in two of the cohorts, COHRA1 (N = 1106) and POFC (N = 1418). The characteristics of study samples are summarized in Table 4. Details of the recruitment and data collection in COHRA1, POFC, IFS and IHS studies are described in Chapter 4.

Table 7. Basic characteristics of the study populations

	COHRA1			POFC			IFS			IHS			Total
Phenotype	N	Female sex(%)	Age range (years)	N	Female sex(%)	Age range (year)	N	Female sex(%)	Age range (year)	N	Female sex (%)	Age range (year)	N
dft	1037	49.1	1.01-12.99	561	45.3	2-12	399	51.1	4-6	162	48.2	3-5	2159
DMFT	1106	61.8	17.05-59.76	1418	59	18-59	-	-	-	-	-	-	2524

6.2.2 Phenotype collection and variable generation

Participants received comprehensive intraoral examinations by licensed dentists or research dental hygienists for COHRA, IHS and IFS. In the POFC cohort, dental caries status was assessed by intraoral photos or in-person dental examinations. Each tooth was identified as either permanent or primary and each surface on each tooth was scored for evidence of decay or restorations, from which traditional caries indices were generated. DMFT index of the permanent dentition was defined as the total number of teeth that were decayed (D), missing (M), or restored/filled (F), excluding the third molars. Note that POFC cohort does not have the (M) component as part of caries assessment, thus the permanent caries index in POFC is slightly different than DMFT in other cohorts. For convenience I would call the outcome "DMFT" in meta analysis results. Correspondingly, dft index was defined as the number of teeth that were decayed and filled in the primary dentition. All study procedures were approved by Institutional Review Boards at the participating universities.

6.2.3 Statistical Analysis

An overview of the three genetic association testing strategies, including SNPs tested, software, statistical methods, and p value thresholds, was described in the Chapter 4 Methods section.

(1) Examination of common coding variants in ERN1 and XBP1 gene (MAF>1%)

Briefly, variance components modeling was implemented to test the association between *ERN1 and XBP1* missense SNPs (rs186305118 in *ERN1* gene, and rs5762809 in *XBP1)*, and dental caries indices assessed in the primary dentition and permanent dentition, while adjusting for ancestry and pertinent covariates (age, sex for COHRA; age, sex and cleft sites for POFC).

(2) Examination of common variants within the genomic context (500kb up and downstream) of *ERN1* and *XBP1*

I tested for genetic association between common SNPs within the genomic context of *ERN1 and XBP1* loci, and caries indices while adjusting for ancestry and pertinent covariates, including age and sex, under an additive genetic model by linear regression in PLINK1.9 (for IFS and IHS cohorts) and variance-component modeling as implemented by EMMAX (for COHRA and POFC cohorts), respectively. **Meta analysis.** Meta-analysis was performed using Stouffer's p-value-based meta-analysis as implemented in METAL software. Meta-analysis included combining COHRA, POFC, IFS and IHS for **dft**, and combining COHRA and POFC for **DMFT**.

(3) Examination of low-frequency variants in *ERN1 and XBP1* gene.

Combined and Multivariate Collapsing (CMC) and Sequence Kernel Association Test (SKAT) using minor allele frequency cutoff of 1% in a gene-based framework, while adjusting for PCs of ancestry and pertinent covariates.

6.2.4 Sample distribution and covariates modeling

To describe the distribution of caries indices and determine which variables to control for in the association analysis, the demographic predictors of dft and DMFT were explored using the R statistical analysis environment (R Foundation for Statistical Computing, Vienna, Austria). Linear regression was used to determine the association between caries indices and pertinent covariates. For POFC cohorts, covariates included age, sex, and presence/absence of any type of orofacial cleft, and for COHRA, IFS and IHS, the covariates included age and sex.

6.3 RESULTS

6.3.1 Trait distributions.

Histograms showing the distributions of caries indices in primary and permanent dentition, of the four cohorts COHRA, OFC, IFS and IHS cohorts are shown in Figure19. Note: DMFT in permanent dentition is not available for IFS and IHS cohorts.

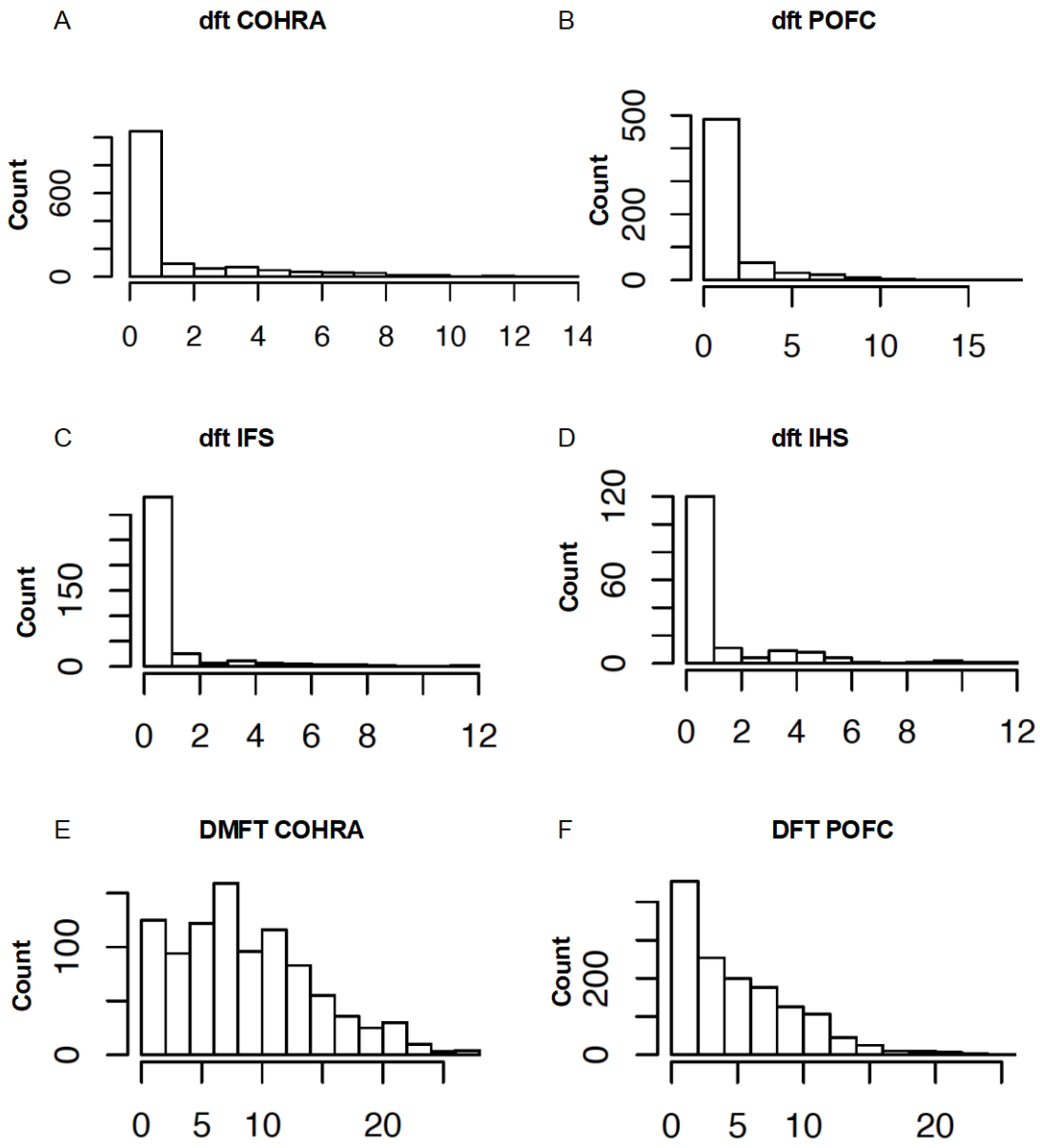

Figure 19. Histograms showing the distributions of caries indices in primary and permanent dentition in COHRA, OFC, IFS and IHS cohorts

Covariate modeling. Regression beta coefficients (SE) and p-values for the test of association between demographic variables and caries indices are shown in Table 8. As expected, in the COHRA sample, age was significantly associated with dft (beta=0.166 (SE=0.025), p =7.1E-12), and DMFT (beta=0.14 (SE = 0.02), p = 8.4E-12), indicating that caries index increases with age. Boys had significantly higher dft scores (about 0.3 more affected teeth) than girls in the primary dentition (p=0.016). Sex was not significantly associated with DMFT in the permanent dentition of adults. For POFC cohort, age was significantly associated with DFT (p=9.7E-25) but not dft. Cleft status was significantly associated with both dft (p=0.02) and DFT (p=7.0E-03) with cleft cases having approximately 0.5 and 1.4 more affected teeth in the primary and permanent dentitions, respectively. For IFS and IHS cohort, which were limited to narrow age ranges, neither age nor sex was associated caries indices.

Table 8. Association between caries indices and covariates

Phenotype	Variable	POFC			COHRA			IFS			IHS		
		Beta	SE	P	Beta	SE	P	Beta	SE	P	Beta	SE	P
dft	**Age**	-0.006	0.032	8.50E-01	0.166	0.024	7.10E-12	0.382	0.21	6.90E-02	0.374	0.242	1.20E-01
	Sex	0.056	0.192	7.70E-01	-0.303	0.126	1.60E-02	0.294	0.179	1.00E-01	-0.315	0.376	4.00E-01
	Cleft status	0.465	0.199	2.00E-02	NA[1]	NA[1]	NA[1]	NA[1]	NA[1]	NA[1]	NA[1]	NA[1]	NA[1]
DMFT	**Age**	0.135	0.013	9.70E-25	0.14	0.02	8.40E-12	NA[2]	NA[2]	NA[2]	NA[2]	NA[2]	NA[2]
	Sex	0.193	0.243	4.30E-01	0.373	0.378	3.20E-01	NA[2]	NA[2]	NA[2]	NA[2]	NA[2]	NA[2]
	Cleft status	1.366	0.506	7.00E-03	NA[1]	NA[1]	NA[1]	NA[1]	NA[1]	NA[1]	NA[1]	NA[1]	NA[1]

[1] The phenotype (Cleft status) was not collected for COHRA, IFS and IHS;

[2] "DMFT" was not collected for POFC cohort.

6.3.2 Examination of common coding variants

For the COHRA sample, significant association was detected between the **missense SNP**

rs186305118 in *ERN1* and **dft index in the primary dentition** in children (N=619, beta=1.577(SE0.089), p=0.0096), but not for DMFT in adults (N=868, beta=0.739(SE0.034), p=0.5885) (Table 9). The SNP investigated, rs186305118: ERN1: c.1421T>G , leading to p.Leu474Arg. The amino acid substitution caused by this variant has been predicted by SIFT(Adzhubei et al., 2010) and PolyPhen-2(Adzhubei et al., 2010) to be benign and tolerable, however, it has been indicated as a somatic mutation in a lung adenocarcinoma sample (Greenman et al., 2007). The same missense SNP was not replicated in POFC cohort (p>0.05).

I did not find any association between the missense SNP at the *XBP1* locus, c.19G>A rs576280) and dental caries of either primary or permanent dentition in both COHRA and POFC cohorts (Table 9).

Table 9. Common missense variant association with dft and DMFT in COHRA and POFC cohorts

Phenotypes	SNP	COHRA					POFC			
		N	MAF	beta	SE	p	N	MAF	beta	p
dft	ERN1:rs186305118	619	0.015	1.577	0.089	**0.009**	559	0.011	-0.072	0.917
	XBP1:rs5762809	619	0.151	0.353	0.033	0.118	559	0.037	0.911	0.18
DMFT	ERN1:rs186305118	868	0.013	0.739	0.034	0.589	1288	0.013	-0.543	0.617
	XBP1:rs5762809	868	0.139	-0.143	0.011	0.753	1288	0.127	0.135	0.538

Note: POFC doesn't have SE column because EMMAX output doesn't have SE

6.3.3Examination of common variants in the genomic context of ERN1 and XBP1

Top hits for common variants in the genomic context of *ERN1 and XBP1* and caries indices are summarized in Table 10.

Table 10. Top hits for caries indices

Phenotype	SNP (minor allele)	COHRA N = 1037			POFC N = 561			IFS N = 399			IHS N = 162			META N = 2159
		MAF	beta	P	MAF	beta	P	MAF	beta	P	MAF	beta	P	P
dft	ERN1: rs11655332 (T)*	0.02	-2.19	**0.0001**	0.03	-1.02	**0.0128**	0.017	-0.43	0.342	0.021	0.24	0.684	**0.00004**
	XBP1: rs62235748 (G)	0.064	-0.81	0.0045	0.109	-0.24	0.311	0.066	-0.33	0.366	0.086	0.71	0.135	0.004
Phenotype	**SNP (minor allele)**	**COHRA N = 1106**			**POFC N = 1418**			**IFS**			**IHS**			**META N = 2524**
DMFT	ERN1: rs17562856 (A)	0.084	0.87	0.0769	0.079	1.06	0.0113	NA	NA	NA	NA	NA	NA	0.002
	XBP1: rs134618 (A)	0.466	-0.18	0.573	0.466	-0.86	0.0003	NA	NA	NA	NA	NA	NA	0.0036

NA: Phenotype (DMFT) was not collected for IFS and HIS

*SNP that reached locus-wide significant association

dft in the primary dentition. Meta-analysis of four (COHRA1, POFC, IFS, IHS) cohorts revealed locus-wide significance between SNP rs113715096, located at 3kb 5' of *ERN1* and dft (p=4.629e-05) (Figure 18A, Table10). The association was mainly driven by COHRA (beta=-2.19 p=0.00013) and POFC cohorts (beta=-1.02, $p<0.05$) (Table10). The beta coefficient for the association indicated that that carriers of the minor allele (T) had lower caries experience in the primary dentition. The association was not significant ($p>0.05$) for IFS or IHS cohorts. This SNP exhibits chromatin features of enhancers in many different cell types, including osteoblasts, osteoclast precursors, DNAse I hypersensitivity in multiple tissues, and transcription factor-binding site for many transcription factors. This SNP is in high LD ($r^2=0.88$) with SNP rs75995183, which is a synonymous variant in *ERN1*.

For the *XBP1* region, the top SNP for **"dft in the primary dentition"** via meta-analysis was rs62235748 (p=0.004), a variant upstream of *XBP1*, and intronic to the *ZNRF3* gene (Figure 18C).

DMFT in the permanent dentition. Meta anlaysis of two cohorts (COHRA and POFC) yielded a suggestive association between DMFT and rs17562856 160kb upstream of *ERN1* and located in the *TEX2* (testis expressed 2) gene (p=0.002) (Figure 20B). This locus exhibits chromatin features of enhancers in many different cell types, including osteoblasts, osteoclast precursors, DNAse I hypersensitivity site in multiple tissues, and numerous transcription factor-binding sites. The top associated SNP for the *XBP1* region was rs134618, 108 kb upstream of *XBP1* (p=0.0036) (Figure 20D), which is a known eQTL for the nearby *KREMEN1* gene, but has not been documented to infleunce expression of *XBP1*.

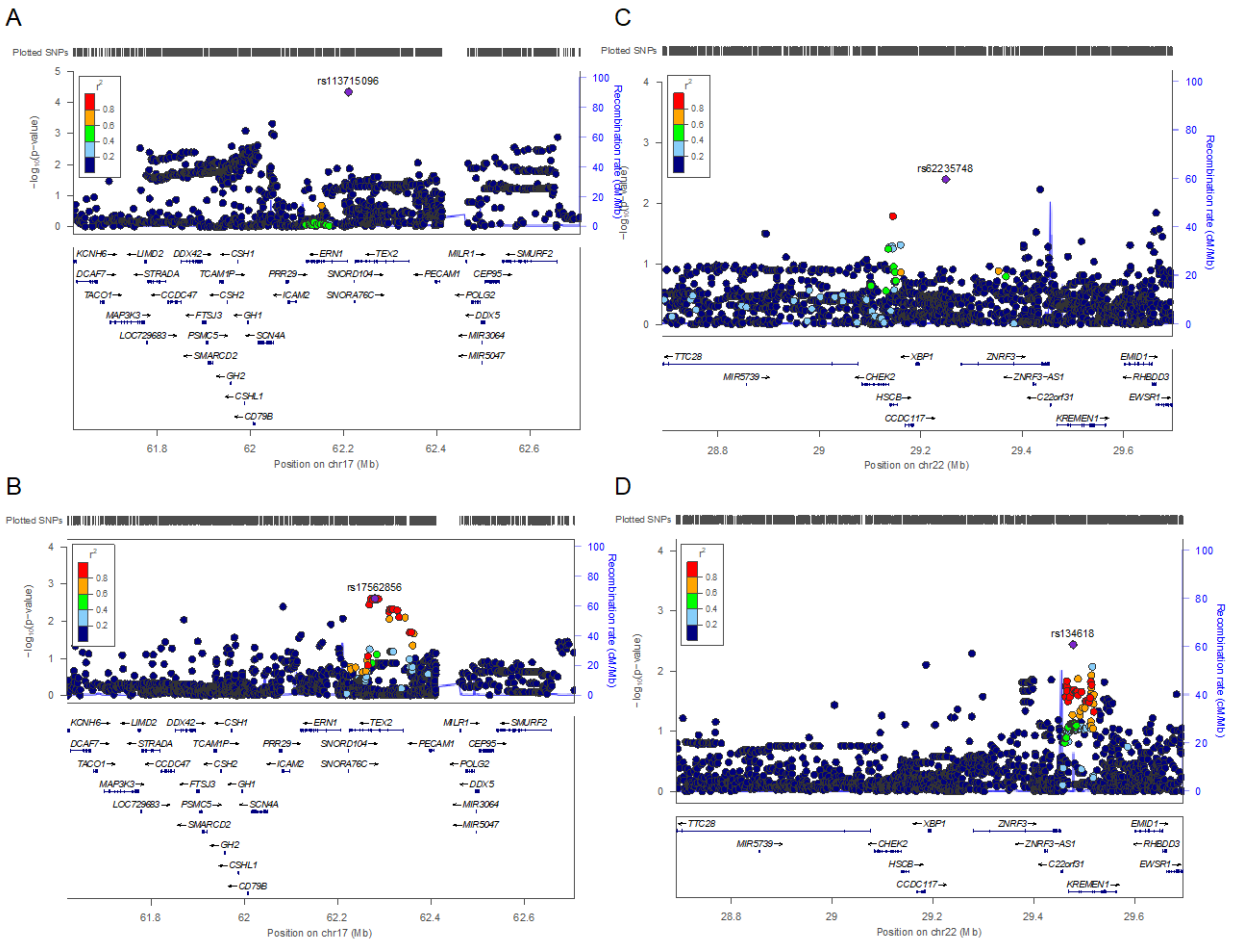

Figure 20. Regional association plots of ERN1 (A, B) and XBP1(C, D) associated with "dft"(A, C) and "DMFT" (B, D) in meta analysis.

The figure shows chromosome 17q23.3 **(A, B),** and chromosome 22q12**(C, D)** (generated with LocusZoom). Displayed are the recombination rates over the region and the association (left y-axis; log10-transformed p-values) for the analyzed SNPs. Positions of genes are shown below the plot.

6.3.4 Examination of low-frequency variants analysis

Gene-based association for low-frequency variants in the *ERN1* gene revealed no significant association for dft in both COHRA (p^{SKAT}=0.76, p^{CMC}=0.92) and POFC (p^{SKAT}=0.79, p^{CMC}=0.51) cohorts (Table 11). Significant association was found between low-frequency coding variants in *ERN1* and DMFT in the CMC test (p^{CMC}=0.034), but not in the SKAT test (p^{SKAT}= 0.11) . Low-frequency coding variants in *XBP1* were significantly associated with dft (p^{CMC}= 0.0006, p^{SKAT}= 0.005) in the POFC cohort.

Table 11. Gene based association for caries indices

Phenotypes	Gene	COHRA				POFC			
		Sample size	Number of variants	CMC *p*	SKAT Permutation *p*	Sample size	Number of variants	CMC *p*	SKAT Permutation *p*
dft	*ERN1*	619	2	0.76	0.92	559	8	0.51	0.79
	XBP1	NA[1]	NA[1]	NA[1]	NA[1]	559	2	**0.0006**	**0.005**
DMFT	*ERN1*	868	2	**0.034**	0.11	1288	15	0.95	0.63
	XBP1	NA[1]	NA[1]	NA[1]	NA[1]	1288	3	0.98	0.99

Highlighted: significant association (p<0.05) ;

[1] MAF for this variant is too low (<0.01) in this sample

6.4 DISCUSSION

I conducted three different analyses to detect genetic association with three different categories of

genetic variants. Strategy one and three focused on variants with roles in protein coding for IRE1 and XBP1, while strategy two focused on common possible cis-acting regulatory variants in the genomic context of *ERN1 and XBP1*. Common coding variants were tested via single gene based test, while low-frequency coding variants were tested in aggregate. All three tests yielded interesting results, as discussed below.

I discovered that a common missense variant in *ERN1,* rs186305118, was associated with dft (beta=1.577 (SE = 0.089), p=0.009) in the COHRA cohort (N=619). The identified mutation causes the substitution of a non-polar hydrophobic amino acid, leucine, for the basic amino acid, arginine. The mutation led to a higher dft score (beta=1.577 (SE = 0.089)). The variant is indicated as a somatic mutation in a lung adenocarcinoma sample (Greenman et al., 2007). Although predicted to be benign and tolerable by SIFT and PolyPhen-2, the missense variant was predicted to be damaging (scaled C-score >15) by CADD prediction software (Kircher et al., 2014), indicating it was a potentially deleterious variant. The CADD C-score is a combined score generated by 63 distinct annotation tools including SIFT and PolyPhen, thus is more comprehensive than individual annotation tools. For the POFC cohort, the same missense SNP was not associated with dft (p=0.97, N=559). One explanation for the different results across cohorts may be differences in environmental exposures associated with caries indices. Another possible reason is that the results could be spurious.

Gene-based association for low-frequency coding variants revealed significant association between low-frequency coding variants in *ERN1* and DMFT in the CMC test (p^{CMC}=0.034). The SKAT test did not reveal significant association for *ERN1*. This is not surprising since the two tests have different assumptions and statistical power. Notably, low-frequency coding variants in

the *XBP1* locus were significantly associated with dft in POFC cohort (p^{CMC}= 0.0006, p^{SKAT}= 0.005). The association was mainly driven by a variant that causes frameshift mutation in exon 1 of *XBP1* (c.14_15insGCCG), and is predicted to result in the production of a truncated nonfunctional protein via PROVEAN (Protein Variation Effect Analyzer))(Choi et al., 2012). The association between low-frequency coding variants in *XBP1* and caries indices indicate a possible role for XBP1 in caries etiology. Evidence of XBP1 in enamel development and pathogenesis (e.g., Amelogensis Imperfecta, fluorosis) has been indicated by functional studies (Brookes et al., 2017; Liu et al., 2015) .

Common possible cis-acting regulatory variants in the genomic context of *ERN1* were found to be significantly associated with dft in the primary dentition. Meta-analysis of the three cohorts revealed a locus-wide significant association (p=0.00013) for dft and SNP rs113715096, which is located 3kb 5' of *ERN1*. The association was mainly driven by COHRA (beta=-2.19 p=0.00013) and POFC (beta=-1.02, p<0.05) cohorts. Carriers of the minor allele (T) had lower caries experience in the primary dentition. This SNP is in high LD (r^2=0.88) with SNP rs75995183, which is a synonymous variant in *ERN1*. Synonymous SNPs might affect protein conformation and function, leading to altered disease susceptibilities. Supporting my observation, a recent candidate gene study reported found nominal associations between *ERN1 and XBP1* regulatory variants and dental caries (children and adults combined) (Bezamat et al., 2019). More work is needed to confirm the association and determine the mechanism through which are acts on caries risk

In conclusion, I found that (i) a missense SNP in the *ERN1* gene was significantly associated with increased susceptibility to dental caries in the primary dentition in the COHRA cohort, but not in POFC cohort, (ii) a common variant 3kb 5' of *ERN1* was significantly associated

with dental caries in the primary dentition in meta analysis of four cohorts, and (iii) the burden of low-frequency variants in *ERN1* was associated with dental caries in the permanent dentition, while the burden of low-frequency variants in *XBP1* was associated with dental caries in both the primary and permanent dentitions. Our findings are corroborated by my mice study, demonstrating that IRE1/XBP1 loss of function disrupted ameloblast morphology in young mice. Genetic polymorphisms in the *ERN1* and *XBP1* gene may influence the quality of dental tissues and ability to resist carious attacks. This effect may be dentition-specific, as I observe different SNPs and different levels of significance (yes and no) for association between caries of primary and permanent dentition. One possible explanation is that enamel rod sheaths structure and enamel contents are different in primary and permanent teeth. Thus the gene may exert their effects differentially on caries development across the life course (i.e. some gene might have stronger effect on caries of the primary dentition). Alternatively, there may be two different sets of genes affecting caries of the primary and permanent dentition. Consistent with my finding, genetic association studies (Shaffer et al., 2013) and genetic correlations (Wang et al., 2010) suggest their may be partly different risk variants for caries in primary and permanent dentitions.

The strength of the work is that I tested my over-reaching hypothesis with three comprehensive strategies. I tested both common coding variants and common variants of in the genomic context of the gene that are putatively regulatory. Furthermore, I tested low-frequency coding variants in aggregate. For low-frequency variant testing, I performed two tests, benefiting from the high power of burden tests (CMC) and allowing for different directions of effect by applying SKAT tests. Lastly, I included two exome panels from COHRA (N=619) and POFC (N=559) cohorts, respectively to increase sample size for coding variants testing.

Limitations for this work exist. Firstly, I found significant association between a missense variant in *ERN1* and dft in COHRA cohort, but the association was not significant in the POFC cohort. This may be due to lack of statistical power or different environmental exposure in different cohorts. Further investigation could benefit from additional cohorts with available data on coding variants of *ERN1* and *XBP1* genes.

7.0 SPECIFIC AIM 3.3: THE ASSOCIATION BETWEEN *ERN1* AND *XBP1* POLYMORPHISMS AND BONE PHENOTYPES

7.1 INTRODUCTION

Our preliminary work in knockout mice suggests that mice with *ERN1* knocked out in Osterix positive cells, and subsequent loss of function IRE1α/XBP1 signaling pathway, showed skeletal morphological differences, and low bone mineral density (BMD). Supporting my observation, published functional studies indicate IRE1α/XBP1 play a role in osteoblast differentiation, osteoclast formation, and chondrogenesis (Cameron et al., 2015a; Tohmonda et al., 2011; Tohmonda et al., 2013; Tohmonda et al., 2015a). According to the International Mouse Phenotyping Consortium, *XBP1* knockout mice (heterozygous) displayed bone mineralization defects, and vertebral fusion (the union of one or more vertebrae into a single structure) (Muñoz-Fuentes et al., 2018). Whether human genetic variants within *ERN1* and *XBP1* genes influence bone phenotypes remains unknown. Of the three ER stress signaling branches (ATF6, PERK/eIF2α and IRE1α/XBP1s), the deletion of *ATF6* does not cause skeletal anomalies (Wu et al., 2007), while mutations in the human *PERK* gene cause Wolcott-Rallison syndrome (WRS), a genetic disorder featuring skeletal dysplasia and osteopenia (Delepine et al., 2000). Thus, it is evident that adequate capacity to sense and respond to ER stress is essential for proper bone development. Therefore, I hypothesize that common genetic variants in the genomic context of *ERN1* and *XBP1* are associated with bone phenotypes in human. To test this hypothesis, I investigated the association between common variants at the *ERN1* and *XBP1* loci with bone mineral density (BMD) and bone mineral content (BMC) phenotypes.

7.2 METHODS

7.2.1 Sample and study design

Subjects were Caucasian, Non-Hispanic children, recruited for Iowa Fluoride Study (IFS n=296) with mean age of 5.28(SD 0.45), and 53% of the samples are female.

7.2.2 Phenotype collection and variable generation

Participants received dual-energy x-ray aborptiometry (DXA) scans as previously described (Levy et al., 2014). The following bone parameters were obtained from the scan: Bone mineral content (BMC, g) for left proximal femur (hip), and anteroposterior lumbar spine, and bone mineral density (BMD, g/cm^2) for the left hip and anteroposterior lumbar spine.

7.2.3 Covariates modeling

To describe the distribution of BMD and BMC and determine which variables to control for in the association analysis, the demographic predictors of BMD and BMC were explored using the R statistical analysis environment (R Foundation for Statistical Computing, Vienna, Austria). Linear regression was used to determine the association between BMD and BMC, age, sex, height and weight.

7.2.4 Correlation across the bone traits

The correlation between bone traits of spine and hip was evaluated by Pearson's correlation in R statistical analysis environment (R Foundation for Statistical Computing, Vienna, Austria). Pearson correlation coefficient (r) and significance of the correlation (p) are indicated for each pair. A p-value of less than or equal to 0.05 was considered to be statistically significant

7.2.5 Association between common variants in genomic context of ERN1 and XBP1

Association analysis was performed as described in the Chapter 4 methods section. Briefly, common SNPs in the candidate genes plus 500kB up- and downstream flanking regions were tested for genetic association with DXA-derived spine and hip BMD and BMC while adjusting for ancestry and pertinent covariates. Linear regression was used to test for genetic association under the additive genetic model using the genetic software PLINK1.9. Bone phenotypes were adjusted for sex, age, height, weight and PCs of ancestry.

7.3 RESULTS

7.3.1 Distributions of bone phenotypes

The distribution of bone phenotypes is normally distributed, as shown in Figure 21.

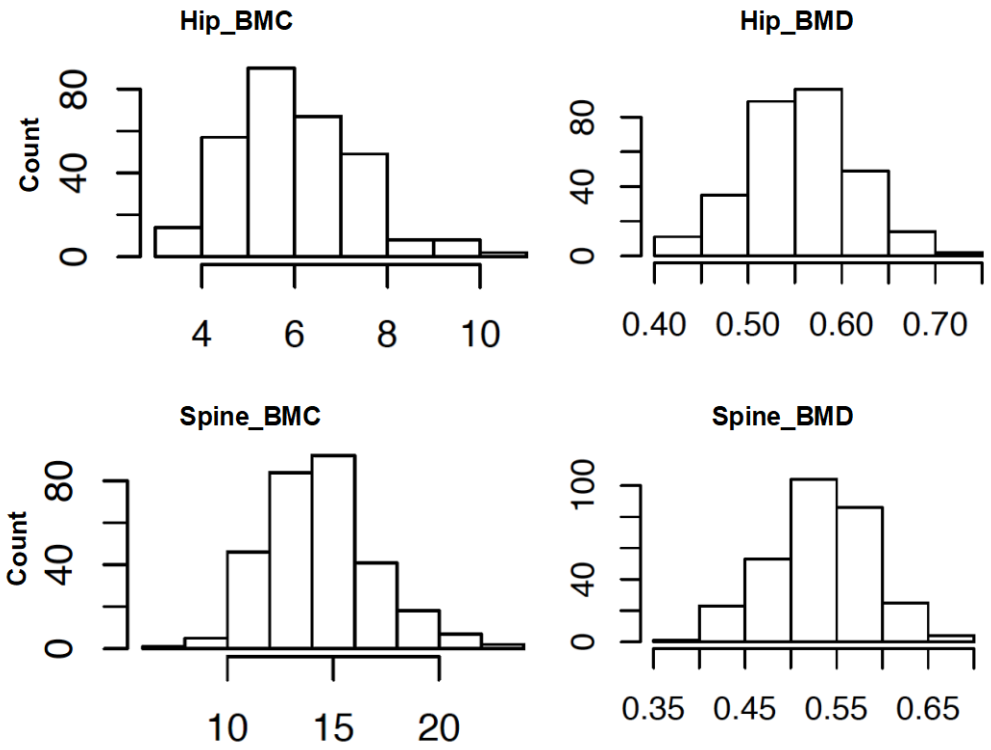

Figure 21. Histograms showing the distributions of BMC and BMD of different sites.

Correlation of bone traits of different sites. BMD and BMC of two different sites (spine and hip) showed significantly ($p < 5E-33$) high ($r=0.62-0.82$) correlation with each other (Table 12).

Table 12. Correlation coefficients (r values) of the BMD and BMC of the two different skeletal sites (Hip and Spine)

	Spine BMD	Spine BMC	Hip BMC	Hip BMD
Spine BMD	-	0.78*	0.64*	0.62*
Spine BMC	0.78*	-	0.82*	0.63*
Hip BMC	0.64*	0.82*	-	0.71*
Hip BMD	0.62*	0.63*	0.71*	-

*All r values are statistically significant ($p < 5E-33$)

Effects of covariates. As shown in Table 13, height and weight are positively associated with bone mineral content for all bone traits but Hip BMD (Weight, but not height was positively associated with Hip BMD). Sex was significantly associated with BMD, but not BMC. Females had significantly lower hip BMD than males (beta=-0.034, p=5.0E-09), but higher spine BMD than males (beta=0.014, p=0.012). Bone traits in my study were not associated with age. This is expected because I have a relatively narrow age range (age 4-6).

Table 13. Association of Covariates with bone traits

Variable	Spine BMD			Spine BMC			Hip BMD			Hip BMC		
	Beta	SE	P	Beta	SE	P	Beta	SE	P	Beta	SE	P
Age	-0.005	0.007	5.1E-01	-0.307	0.274	2.6E-01	0.009	0.007	2.1E-01	0.004	0.135	9.8E-01
Sex	0.014	0.006	**1.2E-02**	-0.300	0.212	1.6E-01	-0.034	0.006	**5.0E-09**	0.132	0.104	2.1E-01
Weight	0.004	0.001	**3.9E-05**	0.145	0.037	**1.4E-04**	0.004	0.001	**6.7E-05**	0.117	0.018	**9.3E-10**
Height	0.002	0.001	**3.2E-03**	0.258	0.031	**1.8E-15**	0.001	0.001	3.1E-01	0.126	0.015	**2.9E-15**

Highlighted: Significant association with p value <0.05

7.3.2 Genetic association

I observed locus-wide significant associations with bone phenotypes for common variants in the genomic regions flanking both *ERN1* and *XBP1*. For the *ERN1* region (Figure 22A), SNP rs71376922 located 5.8kb 5' of *ERN1* was associated with hip BMD (P=2.5E-5) . The minor allele of rs71376922 (C) was associated with higher levels of bone mineral density in the hip area (beta=0.061 (SE=0.014)) . This SNP is in strong LD with a variant in known promoter and

enhancer regions in osteoblasts (i.e., bone forming cells). I did not observe locus-wide significant association for other BMD and BMC phenotypes for the *ERN1* locus.

For the *XBP1* region (Figure 22B), I detected a locus-wide significant association of rs5752758, located downstream of XBP1, with spine BMC (P=2E-6). The minor allele A is associated with lower levels of bone mineral content in the spine area (beta= -1.20 (SE=0.238)) . This SNP showed suggestive evidence of association for all other bone phenotypes (hip BMD (beta=-0.025 (SE=0.007), P=0.0007), hip BMC (beta=-0.469 (SE 0.137) , P=0.0009), spine BMD (beta= -0.024 (SE 0.006), P=0.0007)).

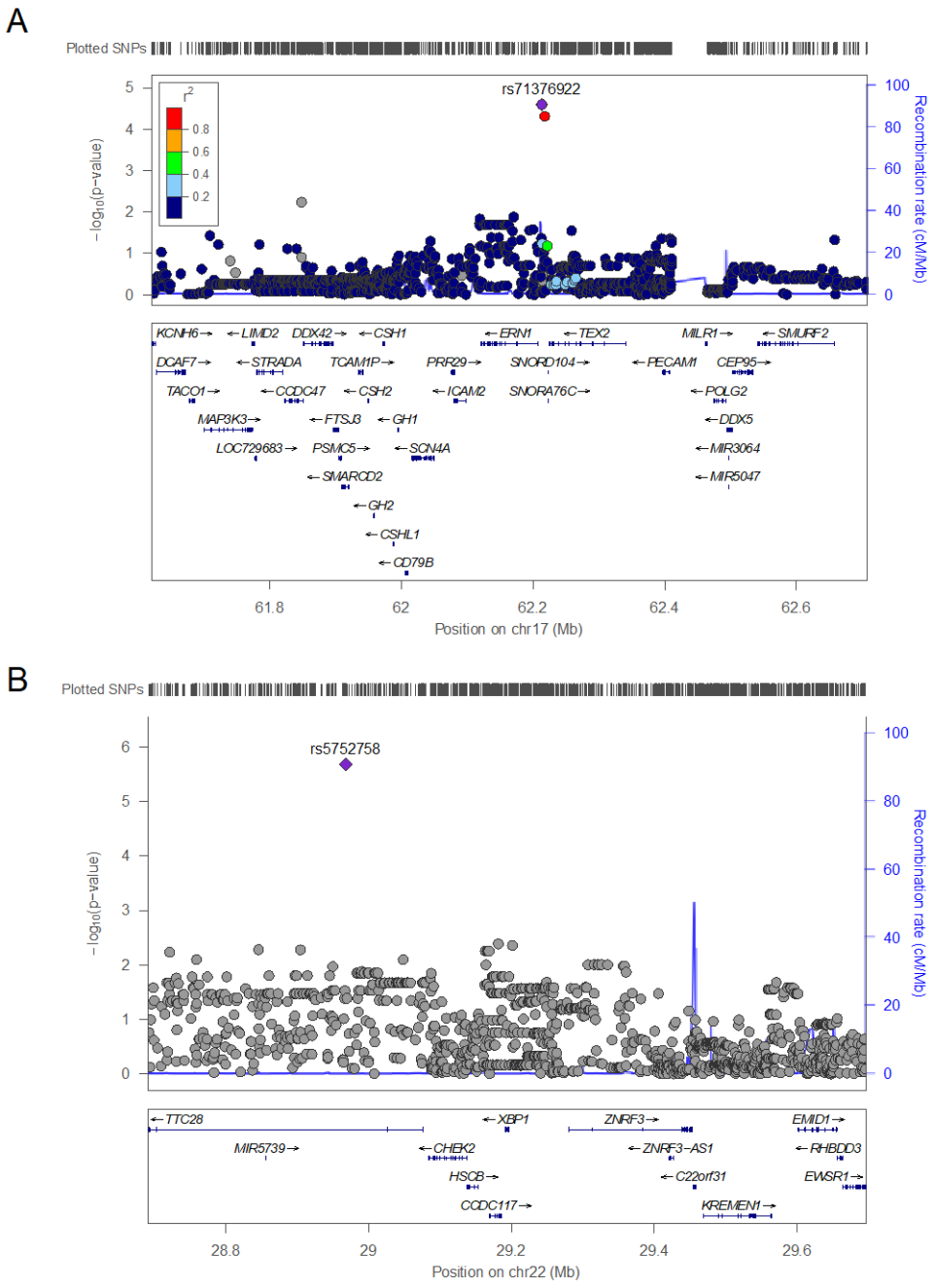

Figure 22. Plots of genetic regions near ERN1 associated with Femur (Hip area) BMD (A) and XBP1 associated Spine BMC (B).

The figure shows chromosome 17q23.3 (A), and chromosome 22q12(B) (generated with LocusZoom). Displayed are the recombination rates over the region and the association (left y-axis; log10-transformed p-values) for the analyzed SNPs. Positions of genes are shown below the plot.

7.4 DISCUSSION

I found locus-wide significant associations between variant in the genomic context of *ERN1* gene and *XBP1* loci and BMD/BMC, echoing the mouse genetic evidence indicating that loss of IRE1a leads to reduce bone mass, shown by Dr. Hongjiao Ouyang's lab (Revu et al., 2014).

The present study also showed a significantly high correlation of BMD and BMC of hip and spine (Table 12), which is consistent with other studies (Namwongprom et al., 2011). The lead variant for the *XBP1* region, rs5752758, located downstream of *XBP1*, was consistently associated with BMD and BMC of most sites (spine BMC P=2E-6, hip BMD P=0.0007, hip BMC P=0.0009, spine BMD P=0.0007). This SNP is located in the nearby *TTC28* gene, the deletion of which result in craniofacial dimorphism and cleft palate phenotype (Breckpot et al., 2016).

At the *ERN1* locus, the lead SNP for hip BMD, rs71376922, located 5.8kb 5' of *ERN1* gene (P=2.5E-5), is in strong LD with a variant (rs117162915, r^2 = 0.82) in known promoter and enhancer regions in osteoblasts. However, I failed to see locus-wide significant association for other BMD and BMC parameters for the *ERN1* loci. This may be due to differences in bone properties of the different sites (Xiao et al., 2011).

A recent candidate gene study found significant association between human osteoporosis/osteopenia and variants within *ERN1*, rs11655020 and rs16947425 (Bezamat et al., 2019). Allele A (the minor allele) of *ERN1* SNP rs16947425 increased the risk of osteoporosis/osteopenia almost 3-fold in the studied cohort [OR=2.71 (95% C.I. 1.37-5.35); p= 5.0E-5]. The authors investigated twenty-two cases of osteoporosis/osteopenia (mean age of 62 years), and 553 unaffected individuals (mean age of 68 years) as controls. Given the small sample size of cases and correspondingly wide confidence intervals in their study, it is difficult to estimate the true OR. The two significant SNPs they found did not exhibit association with BMD and BMC

phenotypes in my study (e.g. hip BMC: rs16947425, beta =0.1774, p=0.4121; rs11655020, beta=-0.12, p=0.75). There are several explanations for this; first is the phenotype difference. I used BMD/BMC collected via DXA scan, while their study used self-reported osteoporosis/osteopenia. Secondly, their study population has a mean age of over 60, while my study was focused on children aged 5. A reason that I selected younger age is because the bone phenotypes in the mouse model were most drastic at a young age (D14-D30), and the skeletal differences in CKO mice went away with age (around 6 month of age). Thus, their study is more about age-related bone loss while mine are focused on bone formation and mineralization in children.

XBP1 is located at chromosome 22q12.1-12.2, a region critical for craniofacial and palate development. Our top SNP for spine BMC (rs5752758, P=2E-6), located downstream of *XBP1* is also in this region. A possible mechanism for the association is that this variant may regulate *XBP1,* and in turn impact the bone phenotypes. The second possibility is the variant is instead acting through the gene it is physically located in, *TTC28*. Copy number variants in *TTC28* have been found to be associated with orofacial development (Xiao et al., 2011). Likewise, a microdeletion in the same genetic region has been found in children with craniofacial dysmorphism and cleft palate (Breckpot et al., 2016; Davidson et al., 2012). Moreover, *TTC28* knockout mice showed decreased bone mineral density, bone mineral content, short tibia and craniofacial abnormalities (International Mouse Phenotyping Consortium (IMPC)), further suggesting the potential for this gene to impact bone mineral density and morphology. The result is not due to cleft status since IFS cohort (unlike the POCF cohort used elsewhere in this dissertation) is not a cleft cohort.

Taken together with my mice data, my findings demonstrated a role of IRE1α and XBP1 in regulating bone mass, and could potentially serve as biomarkers defining patient susceptibility to low bone density in the future.

Several limitations exist for this chapter: Firstly, I have a relatively small sample size (n=296), and did not have replication cohorts available for testing my top variants. To confirm the association, replication in larger cohorts and meta-analysis are warranted. Second, I did not test the effects of coding variants on BMD and BMC, because exome chip data were not available in the cohort that had bone phenotype data. Further, mechanism for association would need to be clarified, for example, by evaluating the effect of associated variants on expression of *ERN1 and XBP1* through additional eQTL analysis.

Future perspective: IRE1α/XBP1 has already become a promising drug target for diseases such as rheumatoid arthritis (Rahmati et al., 2018), multiple myeloma (Mimura et al., 2012) and pathological bone resorption (Tohmonda et al., 2015b). Genetic studies such as mine have potential to provide biological knowledge that might ultimately guide the development of therapeutic measures for diseases with low bone density. Future functional analysis will be needed to determine the mechanisms of IRE1α/XBP1 regulation of bone, and the down-stream targets of IRE1α/XBP1 that could serve as drug targets for treating osteopenia/osteoporosis.

8.0 SUMMARY OF THESIS WORK

8.1 SUMMARY OF MAJOR FINDINGS

The overall goal of this thesis was to elucidate the biological role of IRE1α in regulating postnatal tooth development. Our primary hypothesis was that IRE1α/XBP1 signaling pathway is an essential physiological regulator for postnatal tooth development. I designed three aims to test this overall hypothesis and work towards meeting my primary objective. In Chapter 2 (Aim 1), I confirmed my hypothesis that the IRE1α /Xbp1 signaling axis in odontoblasts is important for dentinogenesis, with roles in regulating odontoblast proliferation and differentiation. With the deletion of IRE1α in odontoblast lineage cells, molecular changes were observed in dental mesenchyme including 1) loss of function of XBP1s signaling, 2) heightened ER stress level and compensatory activation of p-PERK/p-eIF2a, and 3) compromised Wnt/β-catenin signaling, a key signaling transduction pathway that promotes odontoblast differentiation and proliferation. The last of these findings is consistent with previous studies reporting that an intact IRE1α function is required for maintaining the steady-state protein expression of β-catenin in osteoblasts (Revu et al., 2014). At the tissue level, odontoblast deficiency of IRE1α leads to compromised dentinogenesis, as evident by the reduced matrix deposition observed by calcein double labeling and the delayed dentin matrix biomineralization observed by HE staining and micro-CT. At the cellular level, I observed that IRE1α-deficiency resulted in decreased odontoblast differentiation markers and reduction in Brdu-positive cells in dental papilla. These results, taken together, suggest a role of IRE1α in regulating odontoblast differentiation and proliferation. In Chapter 3 (Aim 2), I confirmed my hypothesis that the IRE1α /Xbp1 signaling axis regulates tooth eruption,

and this regulation is, at least, partially through regulating bone remodeling (bone formation and resorption).

Aim 3 is addressed in Chapters 4-7. I observed evidence in support of my hypotheses that genetic variants at the *ERN1* and *XBP1* loci are associated tooth eruption (Chapter 5), dental caries (Chapter 6), and bone phenotypes (Chapter 7). I used three analysis strategies to detect genetic association with different categories of genetic variants, (1) common coding variants, (2) common possible cis-acting regulatory variants and (3) low-frequency coding variants.

In Chapter 5 I revealed locus-wide significant associations between common possible cis-acting regulatory variants near *ERN1* (rs56325317) and *XBP1 (* rs76891380 and rs55962108) and " number of primary tooth number" (meta-analysis p value< 0.0002). The SNPs were located in the regions upstream of *ERN1 and XBP1*, and are putative regulatory variants. For coding variants, I observed significant association between low-frequency coding variants as a group in *ERN1* and "number of permanent teeth" (p^{CMC}=0.038) in the COHRA cohort. I not only found a possible role of genetic variants in *ERN1* and *XBP1* in regulating tooth eruption, but also observe a role of genetic variation nearby these genes affecting tooth eruption.

In Chapter 6, I found that a missense SNP in the *ERN1* gene, rs186305118, was associated with dft (beta=1.577(SE 0.089), p=0.009) in the COHRA cohort (N=619). The minor allele C was significantly associated with increased susceptibility to dental caries in the primary dentition in the COHRA cohort. I also found that a common variant 3kb 5' of *ERN1* (rs113715096) was significantly associated with dental caries in the primary dentition in the meta-analysis of four cohorts (p=0.00013). Carriers of the minor allele (T) had lower caries experience in the primary dentition (beta = -2.19, p=0.00013 in COHRA and beta= -1.02, p<0.05 in POFC). This SNP is in high LD (r^2=0.88) with rs75995183, which is a synonymous variant in *ERN1*. I also showed that

the burden of low-frequency variants in *ERN1* is associated with dental caries in the permanent dentition ($p^{CMC}<0.05$); Moreover, the burden of low-frequency variants in *XBP1* is associated with dental caries in both the primary and permanent dentitions ($p^{CMC}<0.05$). These findings, coupled with the observation from my mouse study showing that IRE1α/XBP1 deficiency disrupted ameloblast morphology, indicates that genetic polymorphisms in *ERN1* and *XBP1* may influence the quality of dental tissues and ability to resist carious attacks.

Last, in Chapter 7 I observed locus-wide significant associations with bone phenotypes for common variants in the genomic regions flanking both *ERN1* and *XBP1*. rs71376922, a variant located 5.8kb 5' of *ERN1* was associated with hip BMD (P=2.5E-5). The minor allele of rs71376922 (C) was associated with higher levels of bone mineral density in the hip area (beta=0.061 (SE 0.014)). This SNP is in strong LD with a variant in known promoter and enhancer regions in osteoblasts. For the *XBP1* region, I detected a locus-wide significant association of rs5752758, located downstream of *XBP1*, with spine BMC (P=2E-6). The minor allele A is associated with lower levels of bone mineral content in the spine area (beta= -1.20 (SE 0.238)). This SNP showed suggestive evidence of association for all other bone phenotypes (hip BMD (beta=-0.025 (SE=0.007), P=0.0007), hip BMC (beta=-0.469 (SE 0.137), P=0.0009), spine BMD (beta= -0.024 (SE 0.006), P=0.0007)). A possible mechanism for the association is that the associated variant may regulate *XBP1,* and in turn impact the bone phenotypes. A second possibility is that the variant may instead act through the gene it is physically located in, *TTC28*, a gene critical for bone and orofacial development.

Scientific context. Because of the possible biological connections in the dental phenotypes tested, for example, tooth eruption in the primary dentition may influence that of the permanent dentition, it is reasonable to assume that the top SNPs identified for tooth eruption in one dentition

would be identified for another. However, this is not the case. For example, the top SNPs for "number of primary teeth" were not significantly associated with "number of permanent teeth", or "Time of first tooth eruption" (P>0.05). One possible explanation for this is that there may be a set of SNPs relevant for both primary and permanent tooth eruption, while some other SNPs exert their effects differentially across different periods, thus they would be associated for one phenotpye, but not the other. Alternatively, there may be different sets of SNPs driving tooth eruption in the primary and permanent dentition. Likewise, when I compared lead SNPs between tooth eruption and caries phenotype, there were few overlapping.

8.2 STRENGTHS AND LIMITATIONS

Overall, the strength of the work is that my approach is a combination of novel *in vivo* loss-of-function mouse model with *in silico* human genetics study. Mouse functional studies at the tissue, cellular and molecular levels, coupled with human candidate gene association studies offers robust and multidisciplinary investigation of the IRE1α/XBP1 signaling transduction pathway in regulating postnatal tooth and bone phenotypes.

8.2.1 Strengths and limitations in the mouse functional study

An innovation and strength of the mouse functional work is that I employed a novel genetically engineered mouse model with heightened ER stress pathway in bone/dentin producing cells. Global deletion of Ire1α or Xbp1 is E12 embryonic lethal in mice. Thus the tissue-specific physiological role of Ire1α in postnatal tooth and bone development remain elusive. I bred

homozygous mice having loxP site-flanked Ire1□ alleles (Ire1□F/F) onto transgenic mice expressing Cre recombinase under an Osterix promoter. Such strategy allowed me to characterize the consequence of tissue specific deletion of Ire1α, specifically in bone and dental tissues. The mouse model offer me a unique *in vivo* model for studying inherited genetic diseases displaying both tooth and bone phenotypes that may have a broader application. Crossing IRE1αCKO mice with other mouse disease model will potentially benefit the investigation of mineralized tissue defects accompanied by heightened ER stress, such as amelogenesis imperfecta and dentinogenesis imperfecta.

Several limitations of the mouse genetic studies warrant discussions. First, it is not known whether the dental phenotypes evidenced with Ire1α deletion differs from that due to Xbp1 deletion, as Ire1α has another downstream target other than Xbp1 splicing (known as regulated IRE1- dependent decay, or RIDD). Although I showed a down-regulation of Xbp1 upon Ire1α deletion, my hypothesis that a role for Xbp1 is relevant here is not supported. This would require future work where I compare phenotypes of mice with *Osterix*-specific Ire1α and that of Xbp1 deletion. Results of the comparison would support the current hypothesis if the same phenotypes are observed. Secondly, the observation of ameoloblast morphological changes in IRE1α CKO mice suggested a trend for poor enamel formation upon IRE1α deficiency, however, I did not characterize the actual enamel structural changes, thus the observation is very preliminary. Further analysis are needed to confirm enamel structural changes, e.g., mechanical testing of the enamel and transmission electron microscopy. In addition, the mechanisms proposed in Chapter 2 are incomplete. It is unclear why beta-catenin was downregulated. I speculated that increased p-PERK levels via eIF2 alpha led to inhibition of the translation of beta-catenin mRNAs in odontoblasts, as we observed in osteoblasts (Revu et al., 2014), however this needs further investigation.

8.2.2 Strengths and limitations in the human genetics work

A strength of the *in silico* human genetics study is that I comprehensively tested the over-reaching hypothesis with three complementary analysis strategies. I tested common variants that alter protein structure , and also tested for common variants in the genomic context of the candidate genes, for their possible cis-regulatory role. Each category of variants tested may help explain a portion of the variation in the phenotypes seen in population. In addition, I tested low-frequency coding variants, in aggregate, which could explain additional trait variance.

Another strength of this study is the combination of the human genetic evidence with functional studies (conditionally knockout-mice) . This study not only established statistical associations between genetic variants in *ERN1 and XBP1* and traits important for tooth development, but also the biological effect of the genes in regulating the same processes.

Several limitations exist for the human genetic study: Firstly, I have relatively small sample size for bone traits (n=296) and did not have replication cohorts available for testing my top variants. To further confirm the association, replication in larger cohorts, and meta-analysis are warranted. Second, I did not test the effects of coding variants on BMD and BMC, because genotype data from the exome chip was not available in the cohort that had bone data. Further, the mechanisms for association need to be clarified, for example, by evaluating the effects of associated variants on expression of *ERN1* and *XBP1* through additional eQTL analysis. Secondly, in this work, various levels of significance were derived for the purpose of controlling for multiple testing. I was careful to control for locus-wide multiple testing for 1503 and 1809 common SNPs for *ERN1* and *XBP1* gene regions, respectively, in strategy #2. In strategy #1 and #3 I did not adjust for multiple testing because there were few individual tests performed. I did

not attempt to control for multiple testing across the two loci (*ERN1* and *XBP1)* at the same time, and I did not attempt to control for the multiple phenotypes. Therefore, while type I error was reasonably controlled within each analysis, type I error was not necessarily controlled across the dissertation as whole, meaning some (but likely not all) of the significant statistical results could be spurious.

8.3 SIGNIFICANCE AND FUTURE DIRECTIONS

This work elucidated the role of IRE1α/XBP1 in regulating postnatal tooth and bone development, and advanced the field of mineralized tissue development and provided insights in the genetic and molecular requirement for timely tooth eruption, proper dentin/enamel formation and bone development. In the long run, my findings could facilitate the development of biomarkers for identifying patient susceptibility to diseases such as dental caries, tooth eruption disturbances, and bone disease, such as osteoporosis. Additionally, as the therapeutic approach targeting ER stress signaling pathway moves forward, better understanding of how IRE1α/XBP1 regulates postnatal tooth and bone development are required.

For the mouse functional study, further investigation is needed to determine the molecular mechanisms by which the IRE1α/XBP1 pathway controls dentin formation and tooth eruption and to elucidate the broader biological functions of this pathway in regulating the development, homeostasis and regeneration of other mineralized tissues of tooth, such as enamel and cementum.

For the human genetics study, additional research including analysis in larger cohorts is warranted to further assess the effect of these variants. For example, I plan to investigate tooth eruption and caries phenotypes in additional cohorts, including the COHRA2 Study, which has

recruited women from West Virginia and southwest Pennsylvania who were in their first and second trimesters of pregnancy, and followed them and their offspring until the children reached age six.

8.4 CONCLUDING REMARKS

Pathological level of ER stress has been implicated in multiple pathological conditions involving tooth and bone. A profound understanding of how ER stress molecules regulate ER stress during postnatal tooth development is necessary for the development of targeted interventions aiming at rescuing dental phenotypes by relieving ER stress. Our study, for the first time, provided both genetic and *in vivo* mouse functional evidence for the role of IRE1α/XBP1 in regulating dentinogenesis , tooth eruption and bone mass during postnatal tooth development, and that the lack of IRE1α/XBP1 leads to multiple pathological consequences involving both transcriptional and translational mechanisms. Further, I identified significant association between genetic variants in (or nearby) *ERN1* and *XBP1* and all three phenotypes tested. This work advanced the field of mineralized tissue development in terms of genetic and molecule requirement needed for proper dentinogenesis, tooth eruption and bone formation. Studies such as mine have potential to provide biological knowledge that might ultimately guide the development of therapeutic measures for diseases such as tooth eruption disturbances, dental caries and low bone density.

BIBLIOGRAPHY

Adzhubei IA, Schmidt S, Peshkin L, Ramensky VE, Gerasimova A, Bork P *et al.* (2010). A method and server for predicting damaging missense mutations. *Nature methods* 7(4)*:*248.

Bertolotti A, Zhang Y, Hendershot LM, Harding HP, Ron D (2000). Dynamic interaction of BiP and ER stress transducers in the unfolded-protein response. *Nature cell biology* 2(6)*:*326-332.

Bezamat M, Deeley K, Khaliq S, Letra A, Scariot R, Silva RM *et al.* (2019). Are mTOR and Endoplasmic Reticulum Stress Pathway Genes Associated with Oral and Bone Diseases? *Caries research* 53(3)*:*235-241.

Boyle WJ, Simonet WS, Lacey DL (2003). Osteoclast differentiation and activation. *Nature* 423(6937)*:*337-342.

Breckpot J, Anderlid B-M, Alanay Y, Blyth M, Brahimi A, Duban-Bedu B *et al.* (2016). Chromosome 22q12. 1 microdeletions: confirmation of the MN1 gene as a candidate gene for cleft palate. *European Journal of Human Genetics* 24(1)*:*51.

Brookes SJ, Barron MJ, Boot-Handford R, Kirkham J, Dixon MJ (2013). Endoplasmic reticulum stress in amelogenesis imperfecta and phenotypic rescue using 4-phenylbutyrate. *Human molecular genetics* 23(9)*:*2468-2480.

Brookes SJ, Barron MJ, Dixon MJ, Kirkham J (2017). The Unfolded Protein Response in Amelogenesis and Enamel Pathologies. *Frontiers in physiology* 8(653.

Browning BL, Browning SR (2009). A unified approach to genotype imputation and haplotype-phase inference for large data sets of trios and unrelated individuals. *The American Journal of Human Genetics* 84(2)*:*210-223.

Cameron TL, Gresshoff IL, Bell KM, Pirog KA, Sampurno L, Hartley CL *et al.* (2015a). Cartilage-specific ablation of XBP1 signaling in mouse results in a chondrodysplasia characterized by reduced chondrocyte proliferation and delayed cartilage maturation and mineralization. *Osteoarthritis and cartilage* 23(4)*:*661-670.

Cameron TL, Gresshoff IL, Bell KM, Piróg KA, Sampurno L, Hartley CL *et al.* (2015b). Cartilage-specific ablation of XBP1 signaling in mouse results in a chondrodysplasia characterized by reduced chondrocyte proliferation and delayed cartilage maturation and mineralization. *Osteoarthritis and Cartilage* 23(4)*:*661-670.

Chen Q, Liu K, Robinson AR, Clauson CL, Blair HC, Robbins PD *et al.* (2013). DNA damage drives accelerated bone aging via an NF‐κB‐dependent mechanism. *Journal of Bone and Mineral Research* 28(5)*:*1214-1228.

Chen S, Gluhak-Heinrich J, Wang YH, Wu YM, Chuang HH, Chen L *et al.* (2009). Runx2, osx, and dspp in tooth development. *Journal of dental research* 88(10)*:*904-909.

Choi Y, Sims GE, Murphy S, Miller JR, Chan AP (2012). Predicting the functional effect of amino acid substitutions and indels. *PloS one* 7(10)*:*e46688.

Davidson TB, Sanchez-Lara PA, Randolph LM, Krieger MD, Wu S-Q, Panigrahy A *et al.* (2012). Microdeletion del (22)(q12. 2) encompassing the facial development-associated gene, MN1 (meningioma 1) in a child with Pierre-Robin sequence (including cleft palate) and neurofibromatosis 2 (NF2): a case report and review of the literature. *BMC medical genetics* 13(1)*:*19.

Delepine M, Nicolino M, Barrett T, Golamaully M, Lathrop GM, Julier C (2000). EIF2AK3, encoding translation initiation factor 2-alpha kinase 3, is mutated in patients with Wolcott-Rallison syndrome. *Nat Genet* 25(4)*:*406-409.

Fatemifar G, Hoggart CJ, Paternoster L, Kemp JP, Prokopenko I, Horikoshi M *et al.* (2013). Genome-wide association study of primary tooth eruption identifies pleiotropic loci associated with height and craniofacial distances. *Human molecular genetics* 22(18)*:*3807-3817.

Fujikawa Y, Quinn JM, Sabokbar A, McGee JO, Athanasou NA (1996). The human osteoclast precursor circulates in the monocyte fraction. *Endocrinology* 137(9)*:*4058-4060.

Geller F, Feenstra B, Zhang H, Shaffer JR, Hansen T, Esserlind A-L *et al.* (2011). Genome-wide association study identifies four loci associated with eruption of permanent teeth. *PLoS genetics* 7(9)*:*e1002275.

Greenman C, Stephens P, Smith R, Dalgliesh GL, Hunter C, Bignell G *et al.* (2007). Patterns of somatic mutation in human cancer genomes. *Nature* 446(7132)*:*153.

Han N, Zheng Y, Li R, Li X, Zhou M, Niu Y *et al.* (2014). β-catenin enhances odontoblastic differentiation of dental pulp cells through activation of Runx2. *PloS one* 9(2)*:*e88890.

Heinrich J, Bsoul S, Barnes J, Woodruff K, Abboud S (2005). CSF-1, RANKL and OPG regulate osteoclastogenesis during murine tooth eruption. *Archives of oral biology* 50(10)*:*897-908.

Hetz C (2012). The unfolded protein response: controlling cell fate decisions under ER stress and beyond. *Nature reviews Molecular cell biology* 13(2)*:*89-102.

Kang HM, Sul JH, Service SK, Zaitlen NA, Kong S-y, Freimer NB *et al.* (2010). Variance component model to account for sample structure in genome-wide association studies. *Nature genetics* 42(4)*:*348.

Kim JW, Choi H, Jeong BC, Oh SH, Hur SW, Lee BN *et al.* (2014). Transcriptional factor ATF6 is involved in odontoblastic differentiation. *Journal of dental research:*0022034514525199.

Kim TH, Bae CH, Lee JC, Ko SO, Yang X, Jiang R *et al.* (2013). β-catenin is required in odontoblasts for tooth root formation. *Journal of dental research* 92(3)*:*215-221.

Kircher M, Witten DM, Jain P, O'Roak BJ, Cooper GM, Shendure J (2014). A general framework for estimating the relative pathogenicity of human genetic variants. *Nature genetics* 46(3)*:*310.

Lambert J-C, Ibrahim-Verbaas CA, Harold D, Naj AC, Sims R, Bellenguez C *et al.* (2013). Meta-analysis of 74,046 individuals identifies 11 new susceptibility loci for Alzheimer's disease. *Nature genetics* 45(12)*:*1452.

Laurie CC, Doheny KF, Mirel DB, Pugh EW, Bierut LJ, Bhangale T *et al.* (2010). Quality control and quality assurance in genotypic data for genome ‐ wide association studies. *Genetic epidemiology* 34(6)*:*591-602.

Levy SM, Warren JJ, Phipps K, Letuchy E, Broffitt B, Eichenberger-Gilmore J *et al.* (2014). Effects of life-long fluoride intake on bone measures of adolescents: a prospective cohort study. *Journal of dental research* 93(4)*:*353-359.

Li B, Leal SM (2008). Methods for detecting associations with rare variants for common diseases: application to analysis of sequence data. *The American Journal of Human Genetics* 83(3)*:*311-321.

Li J, Ji L (2005). Adjusting multiple testing in multilocus analyses using the eigenvalues of a correlation matrix. *Heredity* 95(3)*:*221.

Liu D, Yao S, Pan F, Wise GE (2005). Chronology and regulation of gene expression of RANKL in the rat dental follicle. *European journal of oral sciences* 113(5)*:*404-409.

Liu F, Chu EY, Watt B, Zhang Y, Gallant NM, Andl T *et al.* (2008). Wnt/β-catenin signaling directs multiple stages of tooth morphogenesis. *Developmental biology* 313(1)*:*210-224.

Liu L, Zhang Y, Gu H, Zhang K, Ma L (2015). Fluorosis induces endoplasmic reticulum stress and apoptosis in osteoblasts in vivo. *Biological trace element research* 164(1)*:*64-71.

Luzzi V, Consoli G, Daryanani V, Santoro G, Sfasciotti GL, Polimeni A (2006). Malignant infantile osteopetrosis: dental effects in paediatric patients. Case reports. *Eur J Paediatr Dent* 7(1)*:*39-44.

Magne D, Bluteau G, Lopez-Cazaux S, Weiss P, Pilet P, Ritchie HH *et al.* (2004). Development of an odontoblast in vitro model to study dentin mineralization. *Connective tissue research* 45(2)*:*101-108.

Marks SC, Cahill DR (1984). Experimental study in the dog of the non-active role of the tooth in the eruptive process. *Archives of Oral Biology* 29(4)*:*311-322.

Mimura N, Fulciniti M, Gorgun G, Tai Y-T, Cirstea D, Santo L *et al.* (2012). Blockade of XBP1 splicing by inhibition of IRE1α is a promising therapeutic option in multiple myeloma. *Blood:*blood-2011-2007-366633.

Muñoz-Fuentes V, Cacheiro P, Meehan TF, Aguilar-Pimentel JA, Brown SDM, Flenniken AM *et al.* (2018). The International Mouse Phenotyping Consortium (IMPC): a functional catalogue of the mammalian genome that informs conservation. *Conservation Genetics* 19(4)*:*995-1005.

Namwongprom S, Ekmahachai M, Vilasdechanon N, Klaipetch A, Wongboontan C, Boonyaprapa S (2011). Bone mineral density: correlation between the lumbar spine, proximal femur and Radius in northern Thai women. *Journal of the Medical Association of Thailand* 94(6)*:*725.

Nibali L (2018). Development of the gingival sulcus at the time of tooth eruption and the influence of genetic factors. *Periodontology 2000* 76(1)*:*35-42.

Okaji M, Sakai H, Sakai E, Shibata M, Hashimoto F, Kobayashi Y *et al.* (2003). The regulation of bone resorption in tooth formation and eruption processes in mouse alveolar crest devoid of cathepsin k. *Journal of pharmacological sciences* 91(4)*:*285-294.

Ono W, Sakagami N, Nishimori S, Ono N, Kronenberg HM Parathyroid hormone receptor signalling in osterix-expressing mesenchymal progenitors is essential for tooth root formation. *Nature* 7(11277)*:*1.

Opal S, Garg S, Jain J, Walia I (2015). Genetic factors affecting dental caries risk. *Australian dental journal* 60(1)*:*2-11.

Patterson N, Price AL, Reich D (2006). Population structure and eigenanalysis. *PLoS genetics* 2(12)*:*e190.

Philbrick WM, Dreyer BE, Nakchbandi IA, Karaplis AC (1998). Parathyroid hormone-related protein is required for tooth eruption. *Proceedings of the National Academy of Sciences* 95(20)*:*11846-11851.

Polk DE, Weyant RJ, Crout RJ, McNeil DW, Tarter RE, Thomas JG *et al.* (2008). Study protocol of the Center for Oral Health Research in Appalachia (COHRA) etiology study. *BMC Oral Health* 8(1)*:*18.

Purcell S, Neale B, Todd-Brown K, Thomas L, Ferreira MAR, Bender D *et al.* (2007). PLINK: a tool set for whole-genome association and population-based linkage analyses. *The American Journal of Human Genetics* 81(3)*:*559-575.

Rahmati M, Moosavi MA, McDermott MF (2018). ER Stress: A Therapeutic Target in Rheumatoid Arthritis? *Trends in pharmacological sciences*.

Reimold AM, Etkin A, Clauss I, Perkins A, Friend DS, Zhang J *et al.* (2000). An essential role in liver development for transcription factor XBP-1. *Genes Dev* 14(2)*:*152-157.

Revu S, Liu K, Wang F, Verdelis K, Bezamat M, Vieira A *et al.* ER Stress Signaling Molecule IRE1 alpha Regulates Bone Develpment and Confers Genetic Risk for Human Osteoporosis. Journal of bone and mineral research2014: WILEY-BLACKWELL 111 RIVER ST, HOBOKEN 07030-5774, NJ USA.

Rutkowski DT, Kaufman RJ (2004). A trip to the ER: coping with stress. *Trends Cell Biol* 14(1)*:*20-28.

Shaffer JR, Feingold E, Wang X, Lee M, Tcuenco K, Weeks DE *et al.* (2013). GWAS of dental caries patterns in the permanent dentition. *Journal of dental research* 92(1)*:*38-44.

Shaffer JR, Wang X, McNeil DW, Weyant RJ, Crout R, Marazita ML (2015). Genetic susceptibility to dental caries differs between the sexes: a family-based study. *Caries research* 49(2)*:*133-140.

Suri L, Gagari E, Vastardis H (2004). Delayed tooth eruption: pathogenesis, diagnosis, and treatment. A literature review. *American Journal of Orthodontics and Dentofacial Orthopedics* 126(4)*:*432-445.

Tohmonda T, Miyauchi Y, Ghosh R, Yoda M, Uchikawa S, Takito J *et al.* (2011). The IRE1α–XBP1 pathway is essential for osteoblast differentiation through promoting transcription of Osterix. *EMBO reports* 12(5)*:*451-457.

Tohmonda T, Yoda M, Mizuochi H, Morioka H, Matsumoto M, Urano F *et al.* (2013). The IRE1α-XBP1 pathway positively regulates parathyroid hormone (PTH)/PTH-related peptide receptor expression and is involved in pth-induced osteoclastogenesis. *Journal of Biological Chemistry* 288(3)*:*1691-1695.

Tohmonda T, Yoda M, Iwawaki T, Matsumoto M, Nakamura M, Mikoshiba K *et al.* (2015a). IRE1α/XBP1-mediated branch of the unfolded protein response regulates osteoclastogenesis. *The Journal of clinical investigation* 125(8)*:*3269.

Tohmonda T, Yoda M, Iwawaki T, Matsumoto M, Nakamura M, Mikoshiba K *et al.* (2015b). IRE1α/XBP1-mediated branch of the unfolded protein response regulates osteoclastogenesis. *The Journal of clinical investigation* 125(8)*:*3269-3279.

Townsend G, Bockmann M, Hughes T, Brook A (2012). Genetic, environmental and epigenetic influences on variation in human tooth number, size and shape. *Odontology* 100(1)*:*1-9.

Verdelis K, Lukashova L, Atti E, Mayer-Kuckuk P, Peterson MGE, Tetradis S *et al.* (2011). MicroCT morphometry analysis of mouse cancellous bone: intra-and inter-system reproducibility. *Bone* 49(3)*:*580-587.

von Marschall Z, Mok S, Phillips MD, McKnight DA, Fisher LW (2012). Rough endoplasmic reticulum trafficking errors by different classes of mutant dentin sialophosphoprotein (DSPP)

cause dominant negative effects in both dentinogenesis imperfecta and dentin dysplasia by entrapping normal DSPP. *Journal of Bone and Mineral Research* 27(6)*:*1309-1321.

Wang S, Chen Z, Lam V, Han J, Hassler J, Finck Brian N *et al.* (2012). IRE1α-XBP1s Induces PDI Expression to Increase MTP Activity for Hepatic VLDL Assembly and Lipid Homeostasis. *Cell Metabolism* 16(4)*:*473-486.

Wang X, Shaffer JR, Weyant RJ, Cuenco KT, DeSensi RS, Crout R *et al.* (2010). Genes and their effects on dental caries may differ between primary and permanent dentitions. *Caries Research* 44(3)*:*277-284.

Weinberg SM, Neiswanger K, Martin RA, Mooney MP, Kane AA, Wenger SL *et al.* (2006). The Pittsburgh Oral-Facial Cleft study: expanding the cleft phenotype. Background and justification. *The Cleft palate-craniofacial journal* 43(1)*:*7-20.

Willer CJ, Li Y, Abecasis GR (2010). METAL: fast and efficient meta-analysis of genomewide association scans. *Bioinformatics* 26(17)*:*2190-2191.

Wise GE, King GJ (2008). Mechanisms of tooth eruption and orthodontic tooth movement. *Journal of dental research* 87(5)*:*414-434.

Wu J, Rutkowski DT, Dubois M, Swathirajan J, Saunders T, Wang J *et al.* (2007). ATF6α optimizes long-term endoplasmic reticulum function to protect cells from chronic stress. *Developmental cell* 13(3)*:*351-364.

Wu MC, Lee S, Cai T, Li Y, Boehnke M, Lin X (2011). Rare-variant association testing for sequencing data with the sequence kernel association test. *The American Journal of Human Genetics* 89(1)*:*82-93.

Xiao S-M, Kung AWC, Gao Y, Lau K-S, Ma A, Zhang Z-L *et al.* (2011). Post-genome wide association studies and functional analyses identify association of MPP7 gene variants with site-specific bone mineral density. *Human molecular genetics* 21(7)*:*1648-1657.

Xu G, Liu K, Anderson J, Patrene K, Lentzsch S, Roodman GD *et al.* (2012). Expression of XBP1s in bone marrow stromal cells is critical for myeloma cell growth and osteoclast formation. *Blood* 119(18)*:*4205-4214.

Yamaguchi T, Hosomichi K, Narita A, Shirota T, Tomoyasu Y, Maki K *et al.* (2011). Exome resequencing combined with linkage analysis identifies novel PTH1R variants in primary failure of tooth eruption in Japanese. *Journal of Bone and Mineral Research* 26(7)*:*1655-1661.

Yoshida H, Matsui T, Yamamoto A, Okada T, Mori K (2001). XBP1 mRNA is induced by ATF6 and spliced by IRE1 in response to ER stress to produce a highly active transcription factor. *Cell* 107(7)*:*881-891.

Zhan X, Hu Y, Li B, Abecasis GR, Liu DJ (2016). RVTESTS: an efficient and comprehensive tool for rare variant association analysis using sequence data. *Bioinformatics* 32(9)*:*1423-1426.

Zhang K, Wong HN, Song B, Miller CN, Scheuner D, Kaufman RJ (2005). The unfolded protein response sensor IRE1alpha is required at 2 distinct steps in B cell lymphopoiesis. *J Clin Invest* 115(2)*:*268-281.

Zhang K, Wang S, Malhotra J, Hassler JR, Back SH, Wang G *et al.* (2011). The unfolded protein response transducer IRE1α prevents ER stress‐induced hepatic steatosis. *The EMBO journal* 30(7)*:*1357-1375.

Zhang R, Yang G, Wu X, Xie J, Yang X, Li T (2013). Disruption of Wnt/beta-catenin signaling in odontoblasts and cementoblasts arrests tooth root development in postnatal mouse teeth. *Int J Biol Sci* 9(3)*:*228-236.